

Initiation and regulation of cytosolic innate immunity during sepsis

Dissertation

in partial fulfilment of the requirements for the degree of doctor rerum naturalium (Dr. rer. nat.)

**Submitted to the
Faculty of Medicine,
Friedrich Schiller University,
Jena.**

by

M.Sc., Shivalee Nilesh Duduskar

born on 04.05.1992 in Buldhana, Maharashtra, India.

October 2020

Gutachter:

1. Prof. Dr. Dr. Bernd Nürnberg
Institute Für Experimentelle und Klinische
Pharmakologie und Pharmakogenomik
Tubingen, Germany

2. Prof. Dr. Hortense Slevogt
Host septomics
Universitätsklinikum Jena, Germany

3. PD Dr. med. Sebastian Weis
Leiter AG Damage Control
Jena, Germany

Tag der öffentlichen Verteidigung: 19.10.2021

TABLE OF CONTENT

List of Tables.....	I
List of Figures	II
List of Abbreviations.....	III
List of Units.....	V
SUMMARY	VI
ZUSAMMENFASSUNG	VII
1. INTRODUCTION	1
1.1 Immune system	1
1.1.1 PAMPs and DAMPs	2
1.2 Pattern recognition receptors.....	2
1.2.1 Toll like receptors	3
1.2.1 C-type lectin receptors	4
1.2.2 RIG-I-like receptors	5
1.2.3 cGAS-STING pathway	5
1.2.4 AIM2- and NOD-like receptors	7
1.3 Inflammasome assembly	7
1.3.1 NLRP1 inflammasome.....	8
1.3.2 NLRC4 inflammasome	8
1.3.3 AIM2 inflammasome	9
1.3.4 NLRP3 inflammasome.....	9
1.3.5 Non.canonical inflammasome.....	11
1.4 Effector functions of inflammasome activation.....	12
1.4.1 Pyroptosis.....	12
1.4.2 Cytokine maturation and release	12
1.4.3 Unconventional protein secretion.....	13
1.5 Gram positive pathogens.....	15
1.5.1 <i>Staphylococcus aureus</i>	15
1.5.2 Staphyloxanthin	17
1.5.3 Accessory Gene Regulator system.....	18
1.5.4 Regulatory RNA	20
1.5.5 RNAlII	21
1.6 Extracellular vesicles	22
1.7 Lipoproteins	23
2. STATE OF THE ART	25
AIM	27

3. MATERIALS AND METHODS	28
3.1 MATERIALS	28
3.2 METHODS	35
3.2.1 Isolation and characterization of MLBs and MVs	35
3.2.1.1 Isolation	35
3.2.1.2 Characterization	36
3.2.2 Isolation of staphyloxanthin and its precursor from <i>S. aureus</i>	37
3.2.3 Molecular biology	37
3.2.3.1 RNA extraction	37
3.2.3.2 RNA sequencing	38
3.2.3.3 RNAIII cloning	39
3.2.3.4 In-vitro-transcription.....	40
3.2.3.5 Binding assay for μ RNA and CDN.....	41
3.2.4 LC-MS for binding of μ RNA and CDN	42
3.2.5 Spinach fluorescence assay	42
3.2.6 Cell Culture	43
3.2.6.1 Maintenance of THP1 wild type and knockout cell line	43
3.2.6.2 Cell Storage.....	43
3.2.6.3 Isolation of human blood derived primary macrophages.....	44
3.2.6.4 Cell Stimulations.....	44
3.2.7 LDH Assay.....	46
3.2.8 Cytokine and alarmin analysis by enzyme-linked immunosorbent assay (ELISA)	46
3.2.9 Protein biochemistry	47
3.2.9.1 Protein isolation from supernatants.....	47
3.2.9.2 Protein extraction from cultured cells	47
3.2.9.3 SDS-PAGE and Western Blotting	47
3.2.10 Immunocytochemistry.....	48
3.2.10.1 STING and LAMP1 co-staining	48
3.2.11 Infection model	48
3.2.11.1 Infection of <i>Galleria mellonella</i>	48
3.2.11.2 Monitoring of <i>Galleria mellonella</i> larvae.....	48
3.2.12 Generation of the Lgt knockout strain.....	49
3.2.13 Patient Samples	51
3.2.14 Statistics	51
4. RESULTS	52
4.1 Gram-positive bacteria exhibit active production of multilamellar lipid bodies (MLBs) and unilamellar membrane vesicles (MVs)	52
4.2 CRISPR macrophages demonstrated canonical and non-canonical inflammasome pathway.....	54
4.3 Gram-positive bacterial RNA is a potent agonist for inflammasome activation.....	55
4.4 <i>S. aureus</i> MLBs accumulates different species of small RNA	57
4.5 RNA aptamers present in MLBs activate the canonical inflammasome pathway via STING.....	59

4.6 Gram-positive bacteria and its vesicles activate inflammasome for the release of IL-1 β and progranulin	61
4.7 Gram-positive bacteria mediates canonical inflammasome via STING	61
4.8 Gram-positive bacterial MLBs activate canonical inflammasome pathway via STING	63
4.9 Accessory gene regulator system of <i>S. aureus</i> locus is engaged in RNA aptamer mediated inflammasome activation	65
4.10 <i>S. aureus</i> RNAIII activates inflammasome pathway for the release of IL-1 β	67
4.11 A unique fragment of RNAIII with A, 7, 8, 9, A hairpins present in SA-MLBs activate the inflammasome pathway	68
4.12 Staphyloxanthin type of lipids targets RNA PAMPs to mediate inflammasome activation	71
4.13 Gram-positive bacteria and its vesicles activates non-canonical pathway for the release of progranulin	73
4.14 Gram-positive bacterial lipoproteins mediate progranulin release via caspase-5 yet bypassing TLR2	75
4.15 Membrane vesicles enriched with lipoproteins show protective effect in <i>Galleria mellonella</i> via progranulin	77
4.16 Inflammasome activation associated with organ damage during sepsis	79
5. DISCUSSION	83
5.1 Gram-positive bacteria secrete multilamellar lipid bodies and membrane vesicles.....	83
5.2 Bacterial small RNAs are enclosed in <i>S. aureus</i> shed MLBs	86
5.3 Bacterial μ RNA is a potent activator of the canonical inflammasome via STING.....	87
5.4 RNAIII of <i>S. aureus</i> activates the canonical inflammasome pathway via STING	89
5.5 Staphyloxanthin type of lipids in <i>S. aureus</i> target RNA PAMPs for the activation of inflammasome	90
5.6 Gram-positive bacteria activates the non-canonical inflammasome pathway for the release of progranulin	91
5.7 Cytoplasmic delivery of lipoproteins induces TLR2 independent caspase-5 dependent secretion of progranulin.....	92
5.8 Inflammasome activation and sepsis.....	94
6. CONCLUSIONS.....	96
7. PROSPECTIVE	98
8. REFERENCES.....	102
9. APPENDIX	118
Curriculum vitae.....	127
Acknowledgement.....	129
Ehrenwörtliche Erklärung	130

List of Tables

Title	Pg.no
Table 1: Consumables for isolation of MLBs and MVs	28
Table 2: Consumables for the characterization of MLBs	28
Table 3: Constituents for LC-MS and isolation of staphyloxanthin	28
Table 4: RNA extraction constituents	29
Table 5: RNA sequencing kit	29
Table 6: Primers used in the study	29
Table 7: Constituents for RNAIII Cloning	29
Table 8: Constituents for <i>in-vitro</i> transcription	31
Table 9: Constituents for CDN binding assay and Spinach fluorescence assay	31
Table 10: Media and consumables for cell culture	31
Table 11: Cell lines used in the study	31
Table 12: Ligand and inhibitors	32
Table 13: Kits (ELISA and LDH)	32
Table 14: Buffers for western blot	32
Table 15: Consumables for western blot	32
Table 16: Primary and secondary antibodies for western blot	33
Table 17: Constituents for Immunofluorescence	33
Table 18: Constituents for infection model	33
Table 19: Constituents for the generation of Lgt knockout	33
Table 20: List of software's used for the study	33
Table 21: Characteristics of <i>S. aureus</i> infected patients screened for inflammasome activation	125
Table 22: Characteristics of sepsis patients screened for galectin-1 release	125
Table 23: Characteristics of sepsis patients screened for PGRN release	126

List of Figures

Title	Pg.no
Figure 1: Toll-like receptor signaling pathway	3
Figure 2: cGAS STING signaling pathway	6
Figure 3: The formation of inflammasome complex	7
Figure 4: Signaling pathway activated by different type of inflammasome	8
Figure 5: Signaling pathway showing canonical inflammasome activation	9
Figure 6: Signaling pathway showing non-canonical inflammasome activation	11
Figure 7: Staphyloxanthin biosynthetic pathway in <i>S. aureus</i>	17
Figure 8: AGR (accessory gene regulator) quorum sensing system in <i>S. aureus</i>	19
Figure 9: Diagrammatic representation of isolation of MLBs and MVs	35
Figure 10: Diagrammatic representation of isolation of μ RNA and BRNA from Gram-positive bacteria	37
Figure 11: Procedure for the binding assay of RNA and CDN	41
Figure 12: Schematic representation of Spinach fluorescence assay	42
Figure 13: <i>S. aureus</i> and GBS secrete multilamellar lipid bodies and membrane vesicles	53
Figure 14: CRISPR macrophages demonstrated canonical and non-canonical inflammasome pathway	55
Figure 15: Gram-positive bacterial RNA is a potent agonist for inflammasome activation	56
Figure 16: <i>S. aureus</i> MLBs accumulates different species of small RNA	58
Figure 17: RNA aptamers present in MLBs activate the canonical inflammasome pathway	60
Figure 18: Gram positive bacteria and its vesicles activate the inflammasome for the release of IL-1 β and PGRN	61
Figure 19: Gram-positive bacteria mediates canonical inflammasome via STING	63
Figure 20: Gram positive bacterial MLBs activate canonical inflammasome pathway via STING	64
Figure 21: Accessory gene regulator system of <i>S. aureus</i> locus is engaged in RNA aptamer mediated inflammasome activation	66
Figure 22: <i>S. aureus</i> RNAIII activates inflammasome pathway for the release of IL-1 β	67
Figure 23: A unique fragment of RNAIII with A, 7, 8, 9, A hairpins present in SA-MLBs activate the inflammasome pathway	70
Figure 24: Staphyloxanthin type of lipids targets RNA PAMPs to mediate inflammasome activation	72
Figure 25: Gram-positive bacteria and its vesicles activates non-canonical pathway for the release of progranulin	74
Figure 26: Gram-positive bacterial lipoproteins mediated progranulin via caspase-5 yet bypassing TLR2	77
Figure 27: Membrane vesicles enriched with lipoproteins show protective effect in <i>Galleria mellonella</i> via progranulin	79
Figure 28: Inflammasome activation associated with organ damage during sepsis	80
Figure 29: Biogenesis of multi lamellar lipid bodies (MLBs)	85
Figure 30: Diagrammatic representation of the overview of the pathways activated by MLBs and MVs	96
Figure 31: Figure illustrating the interplay of toxins and virulence factors activating the inflammasome pathway for production of cytokines and alarmins	98
Figure 32: RAMAN spectroscopy data obtained for the study	119
Figure 33: LC-MS analysis for the detection of staphyloxanthin	123
Figure 34: RNA seq data obtained from μ RNA of SA, Δ agr and SA-MLB	124
Figure 35: Characteristics of <i>S. aureus</i> patient isolates :site of infection, referral department	125

List of Abbreviations

μRNA	Small RNA (<200 nucleotides)	LPS	Lipopolysaccharides
Agr	Accessory Gene Regulator	LRR	Leucine rich repeats
AIM2	Absent in melanoma 2	Lsp	Lipoprotein signal peptidase
AIP	Auto inducing peptide	LTA	lipoteichoic acid
ASC	Apoptosis-associated speck-like protein containing a CARD	MAVS	Mitochondrial antiviral signaling protein
BMDCs	Bone marrow-derived dendritic cells	MDA5	melanoma differentiation-associated gene 5
BMDM	Bone-marrow-derived macrophage	MLBs	multilamellar lipid bodies
CARD	Caspase activation and recruitment domain	MOI	multiplicity of infection
CDNs	cyclic-dinucleotides	MVs	Membrane vesicles
cGAMP	Cyclic guanosine monophosphate–adenosine monophosphate	MYD88	Myeloid differentiation primary response protein
cGAS	cyclic GMP-AMP synthase	NaCl	Sodium chloride
CLRs	C-type lectin receptors	NADPH	Nicotinamide adenine dinucleotide phosphate hydrogen
CNPY3	Canopy FGF Signaling Regulator 3	NAIP	NLR family apoptosis inhibitory proteins
CRISPR/Cas9	clustered regularly interspaced short palindromic repeats and CRISPR-associated protein 9	NF-κB	Nuclear factor 'kappa-light-chain-enhancer' of activated B-cells
CTLD	C-type lectin-like domain	NLRP1	NACHT, LRR, FIIND, CARD domain and PYD domains-containing protein 1
DAMPs	Damage associated molecular patterns	NLRP3	NLR family pyrin domain containing 3
DFHB1	3,5-Difluoro-4-hydroxybenzylidene	NMR	Nuclear magnetic resonance
DLS	Dynamic light scattering	NOB	nucleotide-binding domain
DMEM	Dulbecco's Modified Eagle Medium	NOD	nucleotide-binding and oligomerization domain
DMSO	Dimethyl sulfoxide	ORF	Open Reading Frame
DNA	Deoxyribonucleic acid	OxPAPC	oxidized phospholipid 1-palmitoyl-2-arachidonoyl-sn-glycerol-3-phosphorylcholine
ELISA	Enzyme-linked immunosorbent assay	PAMPs	Pathogen associated molecular patterns
ER	Endoplasmic Reticulum	PBS	Phosphate saline buffer
EVs	Extracellular vesicles	PGRN	Progranulin
FSL	S-(2,3-bispalmitoyloxypropyl)-CGDPKHSPKSF	PMA	Phorbol 12-myristate 13-acetate
GAPDH	Glyceraldehyde 3-phosphate dehydrogenase	PRR	Pattern Recognition Receptors
GBPs	guanylate-binding proteins	PTMs	post-translation modifications
GBS	Group B Streptococcus	PYD	Pyridin Domain
GSDMD	Gasdermin -D	RIG-I	retinoic acid-inducible gene I
HEPES	(4-(2-hydroxyethyl)-1-piperazineethanesulfonic acid)	RLRs	RIG-I-like receptors
Hld	δ-hemolysin peptide	RNA	Ribonucleic acid

HIN200	Hematopoietic interferon-inducible nuclear protein with 200-amino acid repeat	ROS	Reactive Oxygen species
HMGB1	High Mobility Group Box 1	S100A8	S100 calcium-binding protein A8
HPK	Histidine Protein kinase	SA	<i>Staphylococcus aureus</i>
HPLC	High Performance Liquid Chromatography	Sae	<i>S. aureus</i> exoprotein expression
HRP	Horse Raddish Peroxidase	SarA	Staphylococcal accessory regulator A
ICU	Intensive Care Unit	SD	Shine–Dalgarno
IFN	Human type I interferons	SDS-PAGE	sodium dodecyl sulfate polyacrylamide gel electrophoresis
IL-18	Interleukin-18	SigB	Sigma B
IL-1Ra	The interleukin-1 receptor antagonist	SIRS	Systemic inflammatory response syndrome
IL-1 β	Interleukin-1Beta	SOFA	sequential organ failure score of sepsis
IRAK	IL-1R-associated kinases	sRNA	Small RNA
IRF	interferon regulatory factors	STING	Stimulator of interferon genes
ITAM	Immune receptor tyrosine-based activation motifs	TBK-1	TANK-binding kinase 1
KCl	Potassium chloride	TBS-T	Tris-buffered saline-Tween 20
LAMP1	Lysosomal-associated membrane protein 1	TDP43	TAR DNA binding protein 43
LDH	Lactate Dehydrogenase	TIR	Toll-IL-1-resistance
LGP2	laboratory of genetics and physiology 2	TLR	Toll-like receptor
Lgt	phosphatidylglycerol-pro-LPP diacylglyceryltransferase	TSB	Trptic Soya Broth
Lnt	N-acyltransferase	UHPLC-MS	UltraHigh Performance Liquid Chromatography-Mass spectroscopy

List of Units

%	percent
°C	degree Celsius
Å	Ångström
cm ²	square centimeter
g	gram
h	hour
kDa	kilodalton
kg	kilogram
L	litre
M	molar
<i>m/z</i>	Mass to charge ratio
mg	milligram
min	minute
mL	millilitre
mM	millimolar
mm	millimeter
ms	Milli second
nm	nanometer
V	Volume
v/v	Volume to volume
µg	microgram
µL	microlitre
µM	micromolar

SUMMARY

The innate immune system recognizes pathogen-associated molecular patterns (PAMPs) and damage-associated molecular patterns (DAMPs) through a set of germline-encoded proteins called pattern recognition receptors (PRRs). Depending on the ligand, inflammasome activation can occur through either canonical or non-canonical inflammasome activation pathways. Gram-positive bacteria such as *Staphylococcus aureus* (SA) and Group B streptococcus (GBS) are the primary causal organisms of adult and neonatal sepsis. Molecular mechanisms through which these bacteria activate the inflammasome pathways are poorly understood. The principal aim of this thesis was to investigate the molecular mechanisms involved in the activation of inflammasome pathways induced by SA and GBS.

In human macrophages, Gram-positive bacteria activate the canonical inflammasome pathway via an upstream pathway involving stimulator of interferon genes (STING) but independent of the DNA sensor cyclic GMP-AMP synthase (cGAS). Small RNA aptamers are being delivered through multilamellar lipid bodies (MLBs) secreted by Gram-positive bacteria in turn activating STING. The expression of the CDN binding small regulatory RNAs is dependent on the accessory gene regulatory (AGR) system of SA. Moreover, we report that staphyloxanthin types of lipids are present in the multilamellar lipid bodies of SA that target the microbial RNA for the cytosolic activation of the inflammasome.

Another part of the thesis is dedicated to studying the mechanism through which Gram-positive bacteria secrete the unconventional secretory protein, progranulin. The involvement of non-canonical inflammatory caspases, mainly caspase-5, was demonstrated for the Gram-positive bacteria-induced progranulin release. Membranes vesicles enrich with lipoproteins were secreted by SA and GBS. These lipoproteins delivered in the cytoplasm induced TLR2 independent Caspase-5 dependent progranulin release.

Collectively, this work outlines the mechanism involved in Gram-positive bacteria mediated inflammasome activation for the release of IL-1 β and progranulin. Gram-positive sepsis patients demonstrated RNA mediated inflammasome activation and substantial accumulation of progranulin and caspase-5 mediation inflammasome activation. Thus, these findings contribute to a new panorama for the pathogenicity of Gram-positive sepsis in man.

Keywords: Gram-positive bacteria, MVs, MLBs, RNA, Canonical inflammasome, non-canonical inflammasome, progranulin.

ZUSAMMENFASSUNG

Das angeborene Immunsystem identifiziert pathogen-assoziierte molekulare Muster (PAMPs) und schadensassoziierte molekulare Muster (DAMPs) durch eine Reihe von in der Keimbahn kodierten Proteinen, die Mustererkennungsrezeptoren (PRRs) genannt werden. Eine breite Palette mikrobieller Liganden wie Lipide und Nukleinsäuren initiiert die zytosolische Inflammasom-Signalkaskade. Je nach Ligand kann die Inflammasomenaktivierung entweder über kanonische oder nicht-kanonische Inflammasomenaktivierungswege erfolgen. Gram-positive Bakterien wie *Staphylococcus aureus* (SA) und Streptokokken der Gruppe B (GBS) sind die primären Erreger der Sepsis bei Erwachsenen und Neugeborenen. Die molekularen Mechanismen, durch die diese Bakterien die inflammasomalen Wege aktivieren, sind nur unzureichend verstanden. Das Hauptziel dieser Arbeit war die Untersuchung der molekularen Mechanismen, die an der Aktivierung der durch SA und GBS induzierten inflammasomalen Wege beteiligt sind.

Für die Aktivierung der Inflammasome wurden die Gram-positiven Bakterien von menschlichen Makrophagen über den kanonischen Weg für die Freisetzung von IL-1 β erkannt. Der Stromaufwärtspfad für die Freisetzung von IL-1 β beinhaltete den Stimulator der Interferon-Gene (STING), während er unabhängig von der zyklischen GMP-AMP-Synthase (cGAS) des DNA-Sensors war. Kleine RNA-Aptamere werden durch multilamellare Lipidkörper (MLBs) abgegeben, die von grampositiven Bakterien abgesondert werden, um STING zu aktivieren. Die Expression der CDN-bindenden kleinen regulatorischen RNAs ist abhängig vom akzessorischen Genregulationssystem (AGR) von *S. aureus*. Darüber hinaus berichten wir, dass in den multilamellaren Lipidkörpern von *S. aureus* Staphyloxanthin-Typen von Lipiden vorhanden sind, die auf die mikrobielle RNA für die zytosolische Aktivierung des Inflammasoms zielen.

Ein weiterer Teil der Arbeit ist der Untersuchung des Mechanismus gewidmet, durch den grampositive Bakterien das unkonventionelle sekretorische Protein Progranulin absondern. Für die durch Gram-positive Bakterien induzierte Progranulinausschüttung wurde die Beteiligung von nicht-kanonischen Entzündungs-Caspasen, hauptsächlich Caspase-5, nachgewiesen. Membranvesikel, die mit Lipoproteinen angereichert sind, wurden von SA und GBS sezerniert. Diese im Zytoplasma abgegebenen Lipoproteine induzierten CASP5-abhängige Progranulinfreisetzung.

Zusammengefasst umreißt diese Arbeit den Mechanismus, der bei der durch grampositive Bakterien vermittelten inflammasomalen Aktivierung für die Freisetzung von IL-1 β und Progranulin eine Rolle spielt. Die in der Dissertation nachgewiesene RNA-vermittelte Inflammasomenaktivierung zeigte sich bei den grampositiven Sepsispatienten als charakteristisch. Darüber hinaus wurde bei Sepsis-Patienten auch eine erhebliche Anhäufung von Progranulin und caspase-5-vermittelter Inflammasomen-Aktivierung beobachtet. Somit tragen diese Befunde zu einem neuen Panorama für die Pathogenität der grampositiven Sepsis beim Menschen bei.

Schlüsselwörter: Gram-positive Bakterien, MVs, MLBs, RNA, Kanonisches Inflammasom, nicht-kanonisches Inflammasom, Progranulin.

1. INTRODUCTION

1.1 Immune system

Mammals are regularly exposed to a plethora of microorganisms from the environment. These microorganisms, in some circumstances, can be pathogenic, provoking multi-cellular organisms to develop different immunological strategies. Immunology is a branch of biology that concerns the study of the immune system in all organisms. In the late nineteenth century, immunologist divided the human immune system into two main branches based on the characteristic responses; the innate immune system, and the adaptive immune system. Both these systems play a role in the host defense against infection and are interlinked to each other.

The innate immune system is one such mechanism that shares some standard key features between plants, vertebrates, and mammals¹. Vertebrates are the only phylum that, together with the innate immune system, develops an adaptive immune response. The innate immune system senses the microbial ligands while the adaptive immune system develops immunological memory of the invading pathogens. The innate immune system constitutes the first line of defense in mammals comprising virtually all tissues, particularly surface barriers such as skin or mucosal surfaces of the respiratory and gastrointestinal tract whereas, adaptive immunity is characterized by antigen specificity. Activation of the innate immune system is represented by macrophages, dendritic cells, and NK-cells resulting in the production of pro-inflammatory cytokines, chemokines, alarmins, and interferon's that recruit and activate the B and T cells of the adaptive immune system^{2,3}. Hence, the presence and activation of the innate immune system are crucial for adaptive immune responses.

Imbalance in the innate immune system results in higher susceptibility to bacterial and viral infections. Hence, not only a deep understanding of the precise mechanisms of the innate immune system but also the bacterial pathogenesis is necessary for developing new therapeutic drugs against a broad range of bacterial and viral infections. In the current thesis, the introduction will be divided into two parts, first explaining the known innate immune pathways in the host, and the second part will focus on the mechanism of Gram-positive bacterial pathogenesis.

1.1.1 PAMPs and DAMPs

Serving as a sensor for invading pathogens, the innate immune system detects the extracellular and intracellular microbial ligands through pathogen-associated molecular patterns (PAMPs) and damage-associated molecular patterns (DAMPs)⁴. PAMPs and DAMPs play a crucial role in the activation of the innate immune system for inflammatory immune responses. PAMPs are small molecular motifs conserved within a class of microbes, which are recognized as non-self by the immune cells. DAMPs, on the other hand, are endogenous molecules released in response to a homeostatic disruption, resulting in cellular or subcellular injury. PAMPs and DAMPs such as lipopolysaccharide, flagellin, lipopeptides, nucleic acids, cyclic-dinucleotides (CDNs) activate the various pattern recognition receptors. These molecules are produced by bacteria, viruses, or damaged cells and are important for their viability⁴.

1.2 Pattern recognition receptors

The sensory systems detect the PAMPs and DAMPs, consisting of diverse families of receptors called pattern recognition receptors (PRRs). During the activation of the immune system, the host uses a variety of evolutionarily conserved receptors known as pattern recognition receptors expressed on the cell surface, intracellular compartments, or secreted into the bloodstream and tissue fluids⁵. The primary function of these PRRs includes opsonization, activation of complement and coagulation cascades, phagocytosis, and activation of pro-inflammatory signaling pathways and induction of apoptosis.

To date, major PRR families have identified Toll-like receptors to recognize a broad range of bacterial and fungal structures, C-type lectin receptors (CLRs) to sense mannose, and glucan carbohydrate structures present in the bacterial cell walls. Absent in melanoma 2 (AIM2)-like and nucleotide-binding and oligomerization domain (NOD)-like receptors are classified under PRR, which are involved in the formation of inflammasome and caspase-1 activation. Apart from these, retinoic acid-inducible gene I (RIG-I)-like receptors (RLRs) sense various cytosolic RNA species, whereas cytosolic DNA is being sensed by cGAS-STING pathway. Pattern recognition receptors are located in different compartments of the cell, Toll-like receptors and C-type lectin receptors are membrane-bound and localized in the cell or endosomal membrane while RLRs, ALRs, NLRs, and cGAS are cytosolic PRRs. Some PRRs such as mannose-binding protein or C reactive protein are secreted into the bloodstream at the site of microbial infection to perform opsonization, activation of the complement system,

inflammation, and phagocytosis⁶. Activation of various PRRs leads to activation of various signaling transduction through different adaptor proteins resulting in activation of various transcription factors such as NF- κ B, interferon regulatory factors (IRF). Out of all the PRRs, ALRs and NLRs are known to form inflammasome complex and activate caspase-1 leading to IL-1 β and IL-18 maturation and release^{7,8}. Even though the primary function of PRRs is inducing inflammation, their activation can lead to multiple cell deaths for the elimination of the pathogens and to trigger a potent immune response.

1.2.1 Toll like receptors

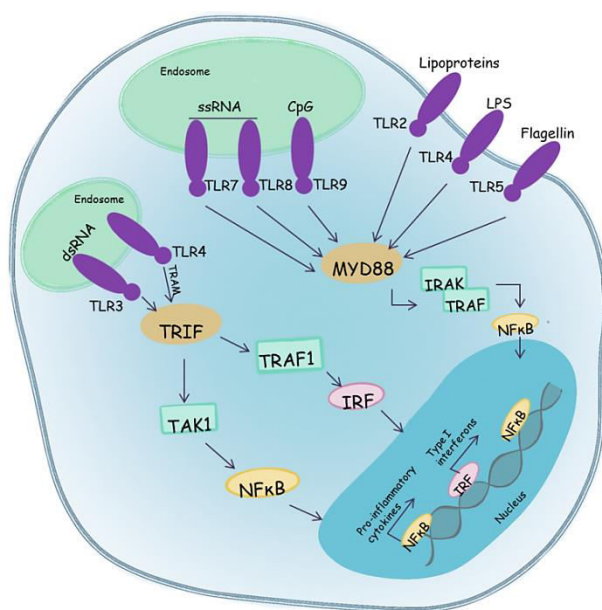


Figure 1: Toll-like receptor signaling pathway: Upon ligand binding (LPS, lipoproteins, flagellin, and nucleic acids), TLRs form homo or heterodimer and recruit adaptors MYD88 or TRIF for downstream signaling resulting in pro-inflammatory or cytokine production. (Figure adopted from reference 19,20,21,22)

Toll-like receptors are first described evolutionally conserved pattern recognition receptors, which are widely studied. They were first described in *Drosophila*, finding it crucial for dorsal-ventral polarity establishment in embryogenesis⁹. Apart from the function of development, toll-like receptors were also found important for *Drosophila's* defense against fungal infection¹⁰. Soon after this discovery, homologous proteins were found in

vertebrates corresponding to one of the largest families of pattern recognition receptors. Toll-like receptors represent a common structure containing the Toll-IL-

1-resistance (TIR) domain important for signal transduction, a transmembrane domain, and an ectodomain containing leucine-rich repeats (LRR) forms a horseshoe-shaped structure. An ectodomain is mainly responsible for ligand specificity and binding¹¹.

Toll-like receptors are expressed in various types of cells, such as epithelial cells, fibroblasts, and immune cells such as macrophages, dendritic cells, B- and T- cells¹². The TLR family comprises ten members in human and 12 members in the mouse. Structural components of bacteria such as lipoproteins, peptidoglycans, lipopolysaccharide, and flagellins are detected by extracellular TLRs 1, 2, 4, 5, and 6, respectively (**Fig. 1**). The presence of foreign nucleic acids is being monitored by the TLRs present in the lumen of the lysosomes. TLR3 is activated upon the binding of synthetic and viral dsRNA, while TLR7 and 8 are responsible

for GU-rich ssRNA secreted from viruses and bacteria^{13,14,15}. The unmethylated CpG motifs of bacterial and viral DNA are recognized by TLR 9¹⁶. Some of the TLRs absent in the humans were recently discovered in the mice. Mouse TLR13 also absent in humans specifically senses bacterial 23s RNA of Gram-positive and Gram-negative bacteria¹⁷. Upon the viral or microbial ligand binding, TLRs form homo or heterodimer that lead to adaptor recruitment and TIR conformational changes. The well-known example is the TLR2 of Gram-positive bacteria that form a heterodimer with TLR6 or TLR1 by recognizing peptidoglycan and di- or tri acyloptides, respectively¹⁸. Apart from this, TLR3, 4, 5, and 9 are also known to form homodimers^{19,20,21,22}. Such interlinked and cooperative interactions between the TLRs enhances the recognition of pathogens by combining the wide range of PAMP recognition and is also important for the regulation of TLRs.

After the ligand binding, TLRs recruit adaptor proteins myeloid differentiation primary-response protein 88 (MYD88) or TIR domain-containing adaptor protein inducing IFN β (TRIF) that lead to nuclear factor kappa light chain enhancer of activated B cells (NF- κ B) activation and pro-inflammatory cytokine production or type I IFN response respectively (**Fig. 1**). Most of the TLRs use MYD88, which forms a complex with IL-1R-associated kinases (IRAKs) via the death domain, forming a complex known as Myddosome²³. Myddosome initiates a kinase cascade leading to phosphorylation of NF- κ B inhibitory protein and translocation into the nucleus²⁴. TLR7 and TLR9 induce the type I IFN production in MYD88 dependent manner by phosphorylating transcription factors IRF1 or IRF7 that lead to IFN- β production. In contrast to other TLRs, TLR3 (and internalized TLR4), a sensor of endosomal dsRNA, binds adaptor TRIF that associates with kinases. TANK-binding kinase 1 (TBK1) and IKK-i which in turn phosphorylate and activate transcription factor IRF3 and IRF7 resulting in IFN- β induction and expression of IFN inducible genes^{25,26}.

1.2.1 C-type lectin receptors

C-type lectin receptors are transmembrane receptors that are part of a superfamily of metazoan proteins containing C-type lectin-like domains (CTLD). The CTLD is a double loop domain capable of recognizing Ca²⁺ dependent carbohydrates on fungi, viruses, and bacteria. The prominent members of the CLR family include dectin-1, dectin-2, and Mincle. CLRs stimulate the pro-inflammatory cytokines directly or through modulation of TLR signaling. They mainly detect carbohydrate structures such as mannose, fructose, and glucans. CLRs can stimulate the signal through the signaling motifs in the cytoplasmic domains or through association with immune receptor tyrosine-based activation motifs (ITAM) containing adaptor

proteins. Dectin-1 and dectin-2 are responsible for detecting β -glucans from fungi through ITAM. Similar to TLRs, CLRs upon recognition of PAMPs are able to activate dendritic cells and help to direct CD4⁺ activation²⁷.

1.2.2 RIG-I-like receptors

RIG-I like receptors are specialized in recognition of foreign RNA and consist of three receptors; retinoic acid-inducible gene I (RIG-I), melanoma differentiation-associated gene 5 (MDA5), and laboratory of genetics and physiology 2 (LGP2)^{28,29}. RLRs are located in the cytoplasm and composed of two N-terminal caspase recruitment domains (CARDs), a central dead box helicase or ATP domain, and a C-terminal regulatory domain. RLRs activate the innate immune system through the detection of various RNA viruses such as influenza A virus, Newcastle disease virus, Sendai virus, hepatitis C virus by recognizing their genome and replication products³⁰. Production of Type I interferon is the result of the activation of RLRs through RNA viruses. To differentiate the self from viral RNA, RIG-I recognize motifs and features specific to the viral genome. dsRNA greater than 19 bp with 5'-tri or di-phosphates is being specifically recognized by RIG-I^{31,32}. MDA5 recognizes long >1 kbp dsRNA, poly (I:C), and AU rich viral mRNA originating from measles viruses³³. LGP2 is the only RLR that lacks the downstream signaling domains, binds to dsRNA, and is the negative regulator of RIG-I and MDA5 signaling by sequestering³⁴. Upon detection of short dsRNA with 5'triphosphate ends by RIG-I and long dsRNA by MDA5 in the cytoplasm, RIG-I and MDA5 bind to mitochondrial antiviral signaling protein (MAVS). They activate the MAVS via the CARD-CARD interaction for further downstream signaling³⁵. Further MAVS undergo CARD mediated self-polymerization leading to the requirement of ubiquitin ligase TRAF -2, -5 and -6 required for the activation of Tank binding kinase I (TBKI) and the inhibitor of κ B kinase (IKK) which promote the expression of Type I interferon³⁶. Simultaneously, MAVS signaling induces nuclear translocation of NF- κ B via TRADD, FADD, and caspase-8/10 leading to the production of pro-inflammatory cytokines.

1.2.3 cGAS-STING pathway

DNA secreted by pathogens or damaged cells is a potent ligand to activate the innate immune system. The mammalian CDNs synthase cGAS (cyclic GMP-AMP synthase) and the stimulator of interferon genes (STING) is so far known mechanism to sense cytosolic DNA and promote downstream signaling^{37,38,39,40,41}. STING is a transmembrane dimeric protein residing on the endoplasmic reticulum. It acts as a receptor and adaptor with the N-terminal

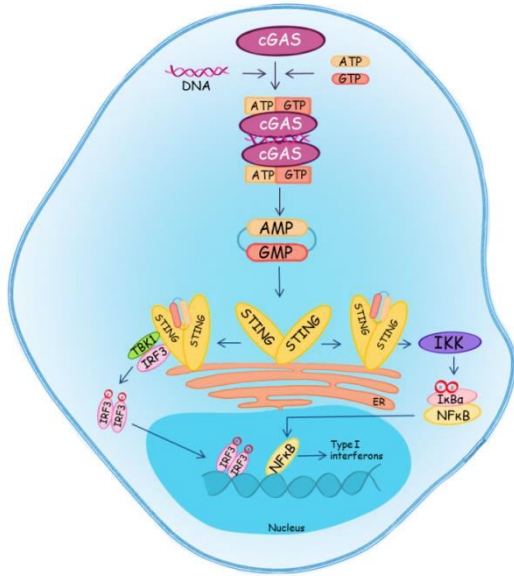


Figure 2: cGAS-STING signaling pathway: The cytosolic DNA activates cGAS forming cGAS-DNA complex which synthesizes 2'3'-cGAMP from ATP and GTP. 2'3'-cGAMP shows high affinity towards STING and in turns activates STING with several conformational changes. Activated STING then recruits TBK1 to phosphorylate IRF3 and activate IKK to phosphorylate IκBα, leading to IκBα degradation. IRF3 then dimerizes and translocated to nucleus along with NF-κB to induce the production of type I IFN and other cytokines. (Figure adopted from reference 38,45)

cytosolic domain and a flexible C-terminal tail responsible for signal transduction^{42,43}. STING is mainly responsible for the interferon induction upon infection with cytosolic bacteria as it is activated by cyclic dinucleotides (CDNs).

Cyclic GMP-AMP is a cytosolic nucleotidyltransferase dsDNA sensor binding to various DNA species despite the sequence un-specificity. Upon binding of the dsDNA with the active site of cGAS introduces a conformational change generating a second messenger cyclic GMP-AMP (cGAMP) from ATP and GTP. cGAS catalyzes the formation of an uncanonical 2'-5' linkage between 2' OH of GMP and 5' phosphate of AMP^{40,43}.

Second messenger cGAMP binds between the monomeric parts of the STING and introduces an active closed STING conformation^{42,44}. STING is translocated to the perinuclear region and recruits the TANK-binding kinase (TBK 1) responsible for the phosphorylation of the C-terminal domain. Phosphorylated STING builds a complex with TBK 1 and interferon regulatory factor 3 (IRF3) resulting in IRF 3 phosphorylation, dimerization and translocation into the nucleus where it initiates the expression of type I IFNs (**Fig. 2**)^{38,45}. Apart from the interferon production, STING was also reported to recruit transcription factor STAT6 in a TBK-1-dependent manner leading to chemokine production⁴⁶. Surprisingly, cGAS and STING are both IFN-stimulated genes, and their expression is enhanced by type 1 IFNs, creating a positive feedback loop⁴⁷.

STING is not only identified as a downstream adaptor of cGAS but also as a direct sensor of bacterial CDNs. Though 2'3'-cGAMP is reported most of the time as STING ligand, the type 1 IFN signaling pathway is triggered in response to c-di-AMP produced by such bacteria as Group B streptococci, *L. monocytogenes*, *M. tuberculosis*, and *C. trachomatis*^{48,49,50,51,52,53}.

1.2.4 AIM2- and NOD-like receptors

Among the conserved evolutionary PRRs, a broad range of PAMPs is being sensed by the absence of melanoma 2 (AIM2)-like receptors and nucleotide oligomerization domain (NOD)-like receptors (NLRs)⁵⁴. NLRs, ALRs, and recently discovered pyrin assemble into a multimeric protein complex called the inflammasome. They activate the downstream caspases leading to the IL-1 β , IL-18 secretion and cell death.

NLR family of proteins consists of the nucleotide-binding domain (NOB), C-terminal leucine-rich repeats (LRR), and variable N-terminal domain. The presence of N-terminal pyrin (PYD) or caspase activation and requirement domain (CARD) subdivides the NLR family into NLRP or NLRC. Members of the NLR family, including NLRP1, NLRP3, and NLRC4, have been well established to form inflammasome in response to various stimuli.

On the other hand, the ALR family is characterized by the presence of the N-terminal PYD domain and a C-terminal hematopoietic interferon-inducible nuclear protein with 200-amino acid repeat (HIN200) domain⁵⁵. The expression of ALR is conserved only in mammals.

1.3 Inflammasome assembly

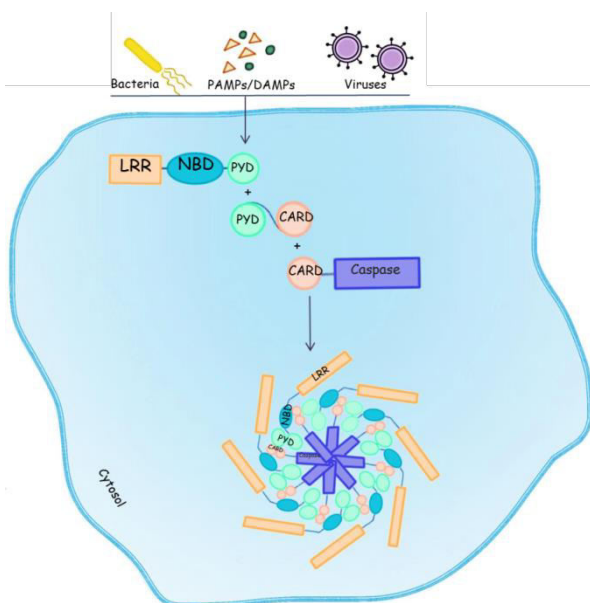


Figure 3: The formation of inflammasome complex: When the microbial ligand is detected the homotypic interaction of the PYD or CARD-CARD domain and the CARD PYD domain induce oligomerization which leads to inflammasome assembly. (NBD- nucleotide oligomerization domain, PYD- N-terminal pyrin domain). (Figure adopted from 57, 58).

A high molecular weight complex formed in the cytosol of the stimulated immune cells was described as an inflammasome by Tschopp and coworkers in 2002. Inflammasome mediates and regulates the activation of inflammatory caspases⁵⁶ and maturation of pro-inflammatory cytokines such as IL-1 β and IL-18. The homotypic interactions of the PYD-PYD or CARD-CARD domain and the CARD and PYD domain induced oligomerization is the basis of inflammasome assembly (**Fig. 3**)^{57,58}. Upon the detection of specific ligand activates the sensor to oligomerize ASC through the PYD interactions. The formed

ASC speck recruits caspase-1 through CARD interactions to form a multimeric

inflammasome complex. This complex ultimately contains the sensor, the adaptor, and the enzyme⁵⁸.

From the known inflammasomes, the assembly of NLRP3, AIM2, and pyrin inflammasomes is strictly dependent on ASC while NLRP1 and NLRC4 can recruit caspase-1 directly^{59,60,61}.

1.3.1 NLRP1 inflammasome

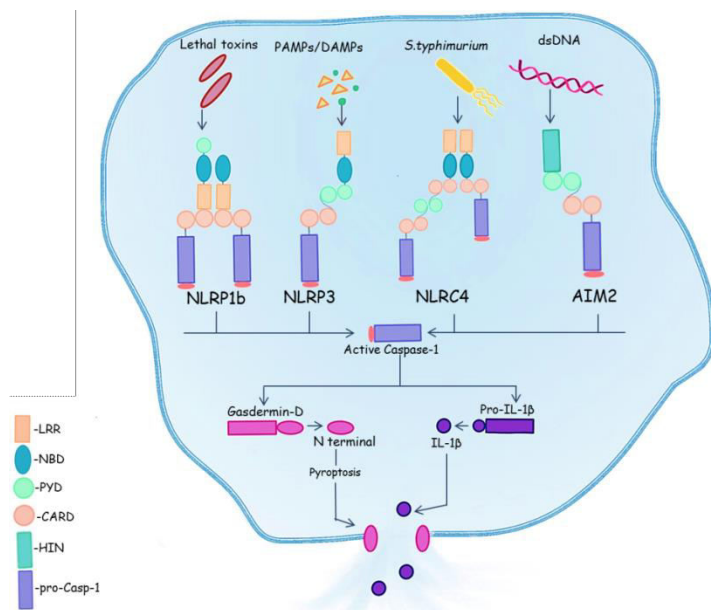


Figure 4: Signaling pathway activated by different types of inflammasome: NLRP1b, NLRP3, NLRC4 and AIM2 are capable of forming inflammasome through the detection of lethal toxins, PAMPs/DAMPs, *S. typhimurium* and dsDNA respectively. The formed inflammasome in turn activates caspase-1 and GSDMD for the release of IL-1 β . (Figure adopted from reference 62,67,72,75)

The first identified cytosolic receptor capable of recruiting caspase-1 in the absence of adaptor protein ASC was NLRP1⁵⁶. The Human NLRP1 protein consists of canonical PYD, NBD, and LRR domains in addition to function to find domain (FIIND) and C-terminal CARD (**Fig. 4**). However, there are three paralogs in mouse NLRP1 (a-c), which lacks the PYD. Mouse NLRP1b is known to be activated by the lethal factor, a component produced by *Bacillus anthrax*, which cleaves the N-terminal and FIIND

domains^{62,63}. However, the only known ligand for human NLRP1 is microbial cell wall component, muramyl dipeptide⁶⁴. NLRP1 is genetically associated with human diseases such as Addison's disease, autoimmune thyroid disease, and type I diabetes^{65,66}.

1.3.2 NLRC4 inflammasome

NLRP4 is another characterized NLR that is capable of binding and activating procaspase-1 through its CARD domain to induce cell death⁶⁷. It is shown that the NLRP4 inflammasome complex is activated in response to bacterial flagellin (**Fig. 4**)⁶⁸ and components of bacterial type III secretion systems^{69,70}. However, NLRC4 is not the direct receptor to these ligands; instead, NAIP (NLR family apoptosis inhibitory proteins) family of receptors acts as a sensor for NLRC4 inflammasome. In mice, bacterial needle and inner rod proteins are being recognized by NAIP1 and NAIP2 respectively, whereas NAIP5 and NAIP6 bind to the

flagellins^{70,71}. Humans have been detected with one NAIP, which can sense both the flagellins and the needle proteins.

1.3.3 AIM2 inflammasome

AIM2 is a cytosolic sensor of double-stranded (ds) DNA of the highly conserved ALR family. It forms the inflammasome complex via caspase-1 activation, dependent on ASC but independent of NLRP3 and TLRs^{72,73}. The HIN200 domain of the AIM2 mediates the dsDNA recognition, which is independent of sequence but requires a certain length (about 80 bp) (Fig. 4)⁵⁹. AIM2 is present in the cytoplasm in an auto-inhibitory form, with the HIN200 domain bound to PYD. Detection of dsDNA by HIN200 relieves the autoinhibition allowing the PYD domain to interact with ASC^{59,74}. Thus, AIM2 inflammasome is induced through cytosolic dsDNA from various infections such as *Francisella tularensis*, vaccinia virus, and several autoimmune diseases.

1.3.4 NLRP3 inflammasome

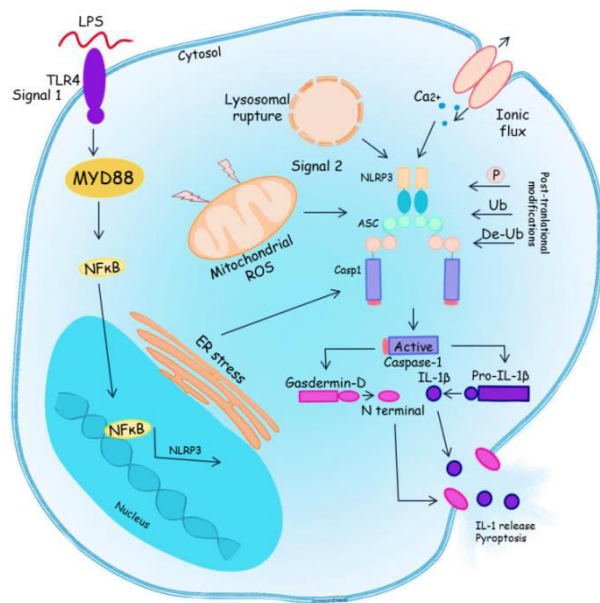


Figure 5: Signaling pathway showing canonical inflammasome activation: Canonical inflammasome pathway initiates with signal 1 by detection of LPS through TLR4 which activates NF-κB signaling pathway. This in turn upregulates transcription of the inactive pro-IL-1β and pro-caspase-1. The second inflammatory signal is been detected through PAMPs, DAMPs, lysosomal rupture, mitochondrial ROS or ionic efflux triggering the formation of inflammasome complex. This initiates the cleavage and activation of pro-caspase-1, pro-IL-1β allowing the secretion of IL-1β from the cell. (Figure adopted from reference 81, 85-89)

The NLRP3 (which encodes NOD-, LRR- and pyrin domain-containing protein 3) inflammasome is also known as a cryopyrin due to the gain of function mutations caused autoimmune disease known as a cryopyrin-associated periodic syndrome (CAPS)⁷⁵. For the function of the NLRP3 inflammasome, it consists of a sensor (NLRP3), an adaptor (ASC), and an effector (caspase-1). NLRP3 is a tripartite protein that comprises an amino-terminal pyrin domain (PYD), a central NACHT domain, and a carboxy-terminal leucine-rich repeat domain (LRR). ASC, which acts as an adaptor protein, has two protein interaction domains, an amino-terminal PYD and a carboxy-terminal caspase recruitment domain (CARD). Full-length caspase-1 has an amino-terminal CARD, central catalytic domain (p20), and a carboxy-terminal small catalytic subunit (p10).

In canonical inflammasome, PRRs recognize the microbial ligands or other signals which alter the homeostasis of the cytosol^{76,77}. Upon activation, receptors oligomerize and recruit the adaptor protein ASC (Apoptosis-associated speck-like protein containing a CARD), forming a large oligomeric structure called “ASC speck”^{78,79}. ASC is an adaptor protein that bridges the receptor to pro-caspase-1, and the formation of the ASC speck is a signaling mechanism to enhance caspase-1 (**Fig. 5**) activation⁸⁰. Recruitment of the pro-caspase-1 leads to the autoproteolytic cleavage and activation of caspases. Caspase-1, which is cysteine-specific aspartate directed protease, then induces two main signaling pathways; first the proteolytic cleavage, maturation, and release of pro-inflammatory cytokines like IL-1 β and IL-18 and second the cleavage and activation of gasdermin D (GSDMD)^{81,82}. This enables the permeabilization of the cellular membranes to form pores leading to a pro-inflammatory, lytic form of cell death called pyroptosis^{83,84}.

Inflammasome activation is a two-step process; first, the priming and then the activation. The priming involves the recognition of various PAMPs and DAMPs that engage the pattern recognition receptors. Priming serves for at least two main functions, first to upregulate the expression of the inflammasome components NLRP3, caspase-1, and pro-IL-1 β . The second function of priming is the induction of post-translation modifications (PTMs) of NLRP3, which stabilize NLRP3. Multiple PTMs have been described for NLRP3, such as ubiquitination, phosphorylation, and sumoylation, which can occur at the priming and activation phases. The priming step of the inflammasome activation alerts the cell while the second step recognizes the NLRP3 activator and induces the formation of the inflammasome. Apart from the bacterial, viral, fungal infections and various DAMPs, NLRP3 is activated through various upstream signals such as efflux of potassium ions (K⁺) or chloride ions (Cl⁻), a flux of calcium ions (Ca²⁺), lysosomal rupture, mitochondrial dysfunction, metabolic changes and trans-Golgi disassembly^{85,86,87,88,89}.

1.3.5 Non-canonical inflammasome

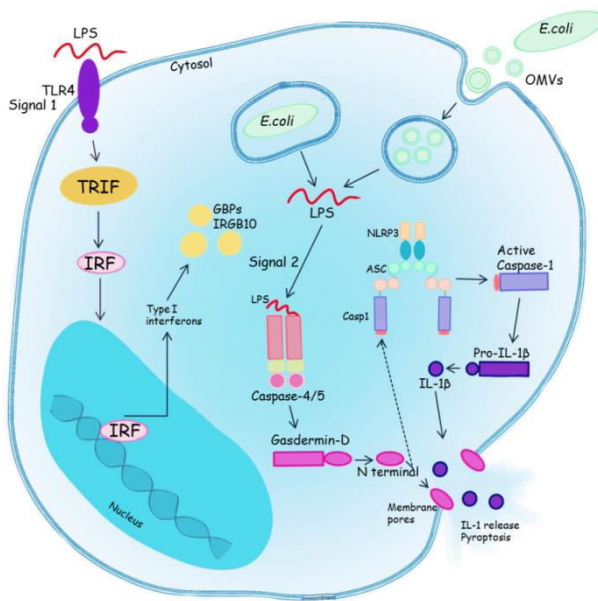


Figure 6: Signaling pathway showing non-canonical inflammasome pathway: LPS acts as a first signal through TLR4 and promotes vacuolar lysis through GBPs which enables entry of LPS into the cytosol of the cell. Pro-caspase-4/5 detects LPS initiating the formation of inflammasome as well as pyroptosis. Formation of NLRP3 inflammasome also leads to the release of cytokines similarly through canonical inflammasome. (figure adopted from reference 90,100).

for non-canonical activation includes priming of TLR4 via LPS for the induction of interferon, this induced interferon together with complement C3-C5aR axis upregulates the expression of caspase-11⁹². Recently discovered small clusters of GTPases and guanylate-binding proteins (GBPs), and their phylogenetic relative IRGB10 induces type I interferons (**Fig. 6**). GBPs and IRGB10 recruit the intracellular bacteria where they lyse and liberate the LPS into the cytosol^{93,94}. Caspase-11 detects LPS directly and triggers its oligomerization and activation by the auto-proteolytic cleavage^{95,96}. In due course, gasdermin D is cleaved by activated caspase-11, which eventually induces pyroptosis (**Fig. 6**). IRGB10 induces type I interferons (**Fig. 6**)^{81,91}. Pyroptosis causes the K⁺ efflux, which activates the NLRP3-caspase 1-dependent IL-1 β secretion. The oxidized phospholipid 1-palmitoyl-2-arachidonoyl-sn-glycerol-3-phosphorylcholine (oxPAPC) generated by the oxidation of plasma membrane phospholipids accumulate in the cell, which binds to caspase-11 to activates the non-canonical pathway⁹⁷.

Cytosolic LPS from the Gram-negative bacteria is sensed by human caspase-4 and caspase-5 (Mouse caspase-11) to induce a non-canonical inflammasome pathway^{91,98}. Contrasting to caspase-11, which is an inducible protein, caspase-4 is constitutively expressed in human cells

Apart from the canonical pathway, in the non-canonical inflammasome activation, the inflammatory protease caspase-11 closely related to caspase-1 acts as a receptor for intracellular LPS. It has been discovered in murine BMDMs infected with Gram-negative bacteria that resulted in pyroptotic cell death dependent on caspase-11^{90,91}. In this pathway, caspase-11 has an affinity towards the lipid A moiety of LPS, the same structural component that activates TLR4 via its CARD domain⁹¹. For the optimal activation of caspase-11 hexa-acylated lipid A structure of LPS is required, none the less Penta-acylated can weakly induce caspase-11. The mechanism

while caspase-5 expression in inducible^{91,99}. Similar to caspase-11, caspase-4 and caspase-5 bind to Hexa-acylated lipid A of LPS to undergo activation⁹¹. Several studies, such as siRNA knockdown and CRISPR/Cas9-deletion of caspase-4 in HeLa and THP-1 cells, show the requirement of caspase-4 for pyroptosis and IL-1 β responses to transfected LPS^{100,101,102}. Caspase-5 is essential during actual infections and is minimally required when LPS is transfected into the cytosol, although the exact contribution is yet to be wholly understood¹⁰².

Recently it was shown in human monocytes that LPS activates the alternative inflammasome pathway¹⁰³. For the activation of the monocyte-specific alternative pathway, TLR-4-TRIF-RIPK1-FADD-CASP8 signaling along with canonical inflammasome, is active while it is caspase-4/5 independent. The unique feature of the alternative pathway is that it does not trigger pyroptosis while it is independent of the potassium efflux (K⁺) and pyroptosome formation.

1.4 Effector functions of inflammasome activation

1.4.1 Pyroptosis

Activation of inflammasome leads to programmed cell death called pyroptosis, mediated by inflammatory caspases including caspase-11, caspase-4/5 and is characterized by plasma membrane perforation, cell swelling, the release of cytosolic contents to the extracellular milieu, and osmotic lysis^{90,91,104}. Recent studies have identified the critical mediator of pyroptosis, gasdermin D (GSDMD), which consists of an amino-terminal cell death domain (GSDMD^{Nterminal}), a central short linker region and a carboxy-terminal autoinhibition domain. Inflammatory caspases activating canonical and non-canonical signaling pathways cleaves GSDMD removing its carboxy-terminal and releasing it from intramolecular inhibition^{81,95,105}. Further, the cleaved GSDMD^{Nterminal} binds to the phosphatidylinositol phosphates and phosphatidylserine in the cell membrane inner leaflet forming 10-14 nm pore containing 16 symmetrical promoters, thus causing cell death¹⁰⁶. Following the inflammasome activations, cells deficient in gasdermin D are protected from cell death or pyroptosis. Gasdermin D also demonstrates bactericidal activity as it binds to cardiolipin, which is present in the bacterial membranes⁸³.

1.4.2 Cytokine maturation and release

The second foremost function of inflammasome activation is the release of cytokines, which are soluble immune-modulating proteins expressed on the plasma membrane. IL-1 α and IL-1 β

are potent proinflammatory cytokines produced during infections¹⁰⁷. The IL-1 (IL-1 α/β) family of cytokines includes IL-1 receptor antagonist (IL-1Ra), IL-18, IL-33, IL-36Ra, IL-36 α , IL-37, and IL-38¹⁰⁸. These cytokines possess a variety of functions, some act as proinflammatory (e.g. IL-1 α and IL-1 β), while some as an anti-inflammatory (e.g., IL-37, IL-38, and IL-1Ra). Few of the cytokines can be both anti as well as proinflammatory (e.g., IL-18). Some of the cytokines of the IL-1 family reside in the cytosol as primitive forms that require cleavage by the inflammatory caspases for the secretion in the active forms¹⁰⁹. IL-1 β , IL-18, and IL-37 are the cytokines that require maturation and secretion mediated by inflammatory caspases¹⁰⁹.

IL-1 β and IL-18 are expressed in the cytosol as inactive precursors (pro-IL-1 β and pro-IL-18) and require specific sites for their active secretion¹¹⁰. Canonical inflammasome activates caspase-1, which in turn, processes pro-IL-1 β at two sites D26 and D116, to produce a 26-kDa product and mature 17-kDa product⁷⁸. Similarly, caspase-1 also cleaves pro-IL-18 at residue D36 to convert inactive 23-kD precursor into active 18-kDa cytokine¹¹¹. Contrasting to the canonical inflammasome, non-canonical caspase-4/5 indirectly mediates the maturation of pro-IL-1 β . On the other hand, IL-18 is constitutively expressed in the cells and is directly cleaved by caspase-4 in response to enteric pathogens such as *Salmonella enterica* and *Shigella flexneri*^{112,113}.

1.4.3 Unconventional protein secretion

In addition to the release of mature cytokines, inflammasome activation involves the secretion of unconventional proteins into the extracellular space¹¹⁴. Generally, for the secretion of proteins, they follow a well-known secretory pathway from the endoplasmic reticulum (ER) to the Golgi apparatus and finally to the plasma membrane. This secretory pathway requires a signal peptide sequence, which leads them to the endoplasmic reticulum¹¹⁵. Nevertheless, there is a group of proteins that are secreted without the signal peptide, but their route of secretions needs to be characterized. These proteins are thought to be released following inflammasome activation through the pores formed by gasdermin D⁹¹. They follow an unconventional secretory route for the secretion, which is yet to be discovered. Besides, multivesicular bodies, secretory lysosomes, exosomes, microvesicles, and autophagy also contribute to the secretion of such proteins¹⁰⁹. Several secretory proteins such as IL-1 α , HMGB1, and S100A8 act as alarmins or DAMPs, for the regulation of inflammasome activation. The original release of these endogenous molecules is triggered by cytosolic LPS sensing and mediated by the activation of caspase-11 but caspase-1 independent⁹⁸. Alarmins

are released in the course of various host defense mechanisms and involved in diseases such as sepsis and cancer¹¹⁵. Galectin-1 and progranulin are recently studied unconventional proteins which act as anti-inflammatory molecules in immune system regulation and host pathogen interaction^{116,122}.

A proto-type member of lectin family, galectin-1 has the ability to recognize N-acetyllactosamine (LacNAc) residues present in *N*- and *O*-glycans¹⁷⁷. Galectin-1 plays differential role based on the relative concentration and the subcellular compartmentalization. Intracellular gal-1 is crucial for controlling the signaling pathways through protein-protein or protein-glycan interaction, while the extracellular gal-1 is involved in cell aggregation, cell adhesion to the extracellular matrix and regulation of cell survival, immunity and inflammation^{118,119}. Although galectin-1 is synthesized and secreted from wide range of immune cells such as T and B cells, macrophages the literature lacks the exact molecular mechanism of its secretion^{120,121}. On the other hand, progranulin (PGRN), mainly known as the granulin epithelial precursor, pro-epitheline, and acrogranin, is an evolutionarily conserved glycoprotein. Forming the unique bead on the string structure, PGRN has seven repeats of vibrant cysteine motifs^{122,123}. It is highly expressed in various cells, including immune cells, epithelial cells, and neuronal cells, as well as HeLa cells and H4 neuroglioma. This cell expresses the high PGRN levels in the cytoplasm. PGRN is widely involved in the pathogenesis of various diseases such as autoimmune disorders, atherosclerosis, and neurodegenerative diseases^{124,125}. PGRN plays a critical role in these diseases by wound healing and host defense mechanisms¹²⁶. It has been widely studied that the mutations in the PGRN gene, which result in null alleles and decreased protein expression, are responsible for frontotemporal lobar degeneration with ubiquitin-positive inclusions¹²⁵. In this subsequent study, TAR DNA binding protein-43 (TDP-43), a protein involved in alternative exon splicing, is cleaved by caspase-3 and caspase-7¹²⁷. It also demonstrated that staurosporin, a potent inducer of caspase-3 activation and apoptosis, cleaves TDP-43. Apart from neurodegenerative diseases, the importance of progranulin is highlighted in acute and chronic inflammation. The levels of inflammatory cytokines and interleukin-10 were significantly lowered in the macrophages of PGRN deficient mice compared to the wild type mice¹²⁸. Infection with *Listeria monocytogenes* was also less quickly cleared in PGRN deficient mice than the wild type mice and demonstrated the vital role of PGRN as a cytokine¹²⁹. Furthermore, PGRN has been extensively studied in sepsis, and studies show that septic patients have elevated levels of progranulin when compared to the healthy controls¹³⁰. In

experimental sepsis, PGRN levels were also increased, and mice deficient in PGRN showed increased susceptibility to septic shock as well as mortality.

1.5 Gram positive pathogens

Gram-positive bacterial infection leads to a major health burden till date, even after the clinical use of penicillin and other anti-bacterial agents. *Staphylococcus aureus* (SA) and Group B streptococcus (GBS) are the major Gram-positive pathogens that present global resistance challenges causing public health concerns.

Streptococcus agalactiae, commonly referred to as GBS, constitutes a normal flora of the intestinal and represents 20-40 % of vaginal flora in healthy women. So far, GBS is the leading cause of invasive infections such as pneumonia, septicemia, and meningitis in neonatal and adult sepsis. During the last decade, number of crucial virulence factors involved in survival, spread and persistence of GBS within the host have been identified such as: I) Degradation of the host tissue, hemolysin, II) Escaping or resistance to phagocytosis by the host (capsular polysaccharide, C5a peptidase, lipoteichoic acid (LTA)) and III) promote adherence and colonization; such as C5a peptidase, laminin-binding protein¹³¹.

On the other hand, *Staphylococcus aureus* (SA) is a widespread commensal human pathogen that causes community and hospital-acquired infections¹³². SA colonizes asymptotically in nostrils of about one in three healthy individuals without causing any associated disease. Additionally, SA has an ability to grow in any part of the body, causing infections in a broad range of body sites: such as skin, bloodstream, respiratory tract, heart, and skeleton system as well as the tissues surrounding implanted medical devices.

The deep-seated SA causes life-threatening infections such as pneumonia, endocarditis, osteomyelitis, urinary tract infections, bacteremia, and sepsis¹³³. These infections are threat because of multiple antimicrobial resistances such as methicillin resistance. SA mainly causes infections through mechanisms such as; Invasion of skin and tissue, causing inflammation, Production of the vast arsenal of virulence factors and biofilm formation. In the current thesis we will focus on SA and its virulence factors affecting the innate immune system.

1.5.1 *Staphylococcus aureus*.

SA was first observed as grape-like clusters by Sir Alexander Ogston, in the 1880s, in a slide preparation of pus from post-operative wounds and abscess patients^{134,135}. The observed SA

was further isolated and grown on a solid medium by Rosenbach in 1884. It was named *Staphylococcus aureus* (golden in Latin) due to its yellowish pigmented colonies. The pathogen is a facultative anaerobe, non-motile, and non-spore forming, which belongs to the phylum *firmicutes*, class *Bacilli*, and order *Bacillales*, family *Staphylococcaceae*, genus *Staphylococcus*. SA reproduces by binary fission and consists circular chromosome of 2.8 M base pairs with a shallow GC content of about 32.8 %. The genome comprises 2700 coding sequences, showing approximately 38 % with unknown functions.

The repertoire of various virulence genes determines the pathogenicity of SA towards the host immune system. SA infects the innate immune system with the production of surface proteins, extracellular toxins and enzymes^{136,137}. Surface proteins of SA such as clumping factors, fibronectin protein A aids in bacterial adhesion, and tissue invasion. Toxins such as hemolysin, leukotoxin, exfoliative toxin, enterotoxin, and toxic shock syndrome toxin-1, destruct host cells and tissues. Coagulase, proteases, and staphylokinase act as enzymes aiding bacterial evasion and penetration of the host. All these virulence factors are the products of the pathogen, causing damage to the host immune system. Various genome-wide approaches show that the expression of virulence factors in SA is regulated at multiple levels; including transcription, translation, and mRNA degradation. The regulatory systems and trans-acting factors such as sigma factors, two-component systems, metabolite responsive regulatory proteins, RNA binding proteins, and regulators RNAs are responsible for modulating the virulence genes¹³⁸.

1.5.2 Staphyloxanthin

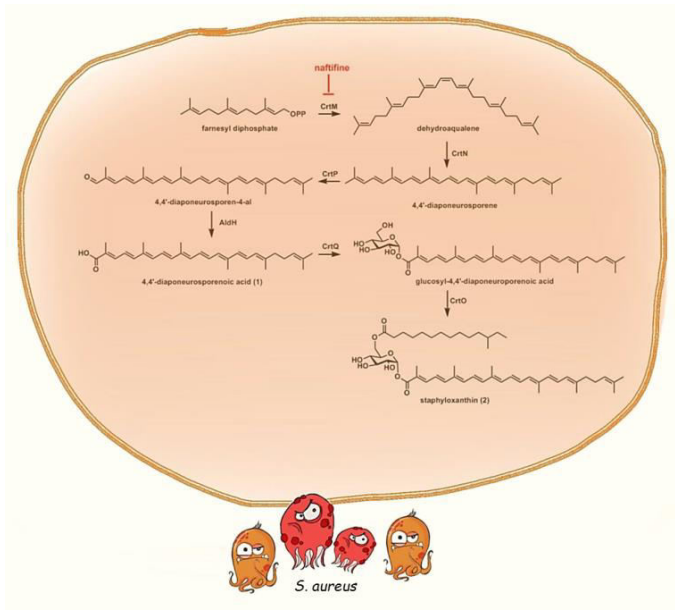


Figure 7: Staphyloxanthin biosynthetic pathway in *S. aureus*: Head to head condensation of two molecules of farnesyl diphosphate forms dehydroqualene, catalyzed by the dehydroqualene synthase CrtM. Dehydroqualene is dehydrogenated by the dehydroqualene desaturase CrtN to form the yellow intermediate 4,4'-diaponeurosporene. Following oxidation of the terminal methyl group of 4,4'-diaponeurosporene catalyzed by a mixed function oxidase, CrtP, to form 4,4'-diaponeurosporenic acid. Then, glucosyl 4,4'-diaponeurosporenoate is formed by esterification of glucose at the C-1 position of 4,4'-diaponeurosporenic acid via CrtQ, a glycosyltransferase. Finally, glucose at the C-6 position is esterified with the carboxyl group of 12 methyltetradecanoic acid by the acyltransferase CrtO to yield staphyloxanthin (2). (Figure adopted from reference 151).

As depicted in the figure, the first step in the synthesis of staphyloxanthin is catalyzed by enzyme dehydro-squalene synthase (CrtM). It executes head to head condensation of two molecules of farnesyl diphosphate to produce dehydrosequalene with an intermediate of presequalene diphosphate. Successive dehydrogenations with enzymes CrtN, CrtP yield 4,4'-diaponeurosporene, which is then further glycosylated and esterified with CrtQ to give carotenoid staphyloxanthin (**Fig 7**). Genes involved in staphyloxanthin synthesis on crtOPQMN operon are regulated by sigma B¹⁴⁴ while the activity of sigma B is encoded by Rsb proteins through rsbUVWsigB system. Hence, it shows that rsbUVWsigB system and crtOPQMN operon is essential for the pigmentation in *S. aureus*¹⁴⁵.

Over 90% of SA causing human infections are golden-organ pigmented and are named as staphyloxanthin by Marshall and Rodwell, in 1972¹³⁹. The carotenoid pigment is one of the key virulence factors, which protects *S. aureus* from innate immune defense system^{140,141}. Staphyloxanthin is a product of the C30 triterpenoid carotenoid biosynthetic pathway with a peculiar structure of long carbon chain with two terminal rings¹⁴². A purified staphyloxanthin was identified as β -D-glucopyranosyl-1-O-(4,4'-diaponeurosporene-4-oate)-6-O-(12-methyltetradecanoate) through NMR demonstrating esterified glucose with a triterpenoid carotenoid carboxylic acid at C1 position and C15 fatty acid at C6 position¹⁴³. Genes responsible for the biosynthesis of staphyloxanthin are located in crtOPQMN operon and

requires the newly discovered enzyme aldH. As depicted in the figure, the first step in the synthesis of staphyloxanthin is catalyzed by enzyme dehydro-squalene synthase (CrtM). It executes head to head condensation of two molecules of farnesyl diphosphate to produce dehydrosequalene with an intermediate of presequalene diphosphate. Successive dehydrogenations with enzymes CrtN, CrtP yield 4,4'-diaponeurosporene, which is then further glycosylated and esterified with CrtQ to give carotenoid staphyloxanthin (**Fig 7**). Genes involved in staphyloxanthin synthesis on crtOPQMN operon are regulated by sigma B¹⁴⁴ while the activity of sigma B is encoded by Rsb proteins through rsbUVWsigB system. Hence, it shows that rsbUVWsigB system and crtOPQMN operon is essential for the pigmentation in *S. aureus*¹⁴⁵.

Host phagocytes mainly eliminate pathogens with the release of reactive oxygen species (ROS), O_2^- , H_2O_2 , and HOCl produced by nicotinamide adenine dinucleotide phosphate (NADPH)¹⁴⁶. Staphyloxanthin shows antioxidant property due to the presence of many conjugated double bonds absorbing excess energy from ROS¹⁴⁷. Carotenoid pigments increases virulence and neutrophil resistance in SA as a result of the antioxidant activity, significantly promoting the development of a subcutaneous abscess in the mouse model¹⁴⁸.

Anti-virulence drugs developed targeting the various enzymes in the staphyloxanthin biosynthetic pathway can be therapeutic to SA infections¹⁴⁹. The cholesterol biosynthetic pathway in humans involves squalene, which is similar in structure to dehydrosqualene in the staphyloxanthin biosynthetic pathway. The SACrtM and human squalene might possess structural similarities (30 % identity, 36 % similarity) found by clustal amino acid alignment. The crtM enzyme is inhibited by cholesterol biosynthetic inhibitor BPH-652 and representing virulence therapy against *S. aureus*¹⁵⁰. Moreover three phosphonosulfonates also block staphyloxanthin biosynthesis in-vitro inhibiting crtM activity¹⁵⁰. FDA approved antifungal agent, naftifine hydrochloride, and its 47 derivatives have shown to block staphyloxanthin biosynthesis by targeting CrtN¹⁵¹.

S. aureus regulates the full range of virulence factors establishing acute and chronic human infections. The complex global regulatory system is known as accessory gene regulator (Agr), which primarily orchestrate the expression of exoprotein genes responding to environmental signals such as bacterial cell density (quorum sensing), nutritional status and energy availability^{152,153}. Several regulatory systems functioning coordinately or independently are; Staphylococcal accessory regulator A (Sar A)¹⁵⁴, *S. aureus* exoprotein expression (Sae) operon¹⁵⁵ and the staphylococcal alternative sigma factor B (Sig B).

1.5.3 Accessory Gene Regulator system

A pivotal regulator of virulence factor; *agr* locus is 3.5 kb in size,¹⁵² which represents the prototype of quorum sensing in Gram-positive bacteria¹⁵⁶. An *agr* operon organizes two divergent promoters P2 and P3, generating transcripts, RNAII and RNAIII, respectively¹⁵⁷. RNAII encodes genes AgrB, AgrD, AgrC and AgrA. The *agr* system activates with a threshold concentration of extracellular auto inducing peptide (AIP), which varies in length from 7-9 amino acids and contains five-membered rings. SA produces sufficient amounts of thiolactone containing AIP to enable quorum sensing. AgrD is the propeptide encoding precursor of auto inducing peptide (AIP) pheromone. The structure of AgrD typically consists of an N-terminal amphipathic leader, the middle region of 7-9 residues that are processed into

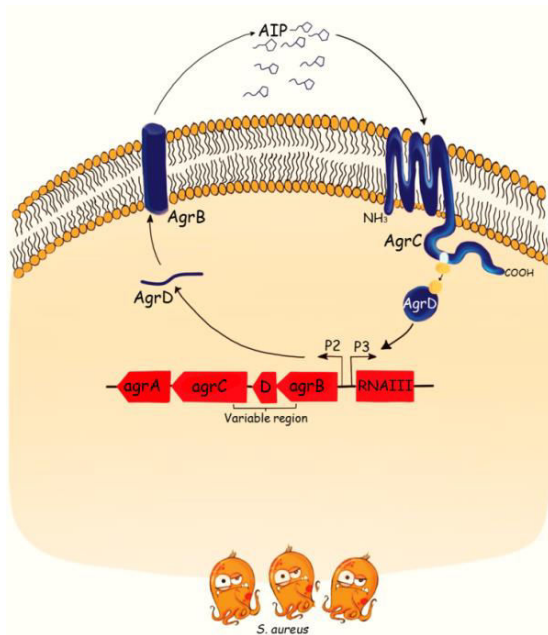


Figure 8: AGR (accessory gene regulator) quorum sensing system in *S. aureus*: RNAII and RNAIII are the divergent transcripts of agr locus. RNAII contains four genes, agrBDCA, which are required to synthesize AIP that activate the regulatory cascade. Briefly, AgrD is the precursor peptide of AIP, AgrB is a membrane protease involved in generating AIP, AgrC is a histidine kinase that is activated by binding AIP, and AgrA is a response regulator that induces transcription of RNAII and RNAIII through the P2 and P3 promoters respectively. (Figure adopted from reference 156).

the two-component signal transduction system¹⁶¹. AgrC is a 46 kDa membrane protein belonging to the histidine protein kinase (HPK) family, which is a critical receptor protein for the signal transduction system. It mainly consists of N terminal membrane integrated sensor molecule that detects and binds AIP. Apart from this, it has several transmembrane domains and a C terminal histidine kinase molecule. Conformational changes occur in the AgrC cytoplasmic helix after the binding of AIP to the N-terminal sensor molecule. Ligand receptor (AIP-AgrC) and AgrC-AgrA interaction have been extensively studied, which shows that the leucine residue at position 171, when substituted, shows altered activity¹⁶².

AgrA, which is primarily the response regulator for the agr quorum-sensing system, is 27 kDa in size. It belongs to the family of conserved response regulators with CheY-like receiver domains¹⁶³. AgrA is highly conserved among different SA species as compared to the AgrB, AgrC, and AgrD. Upon binding of quorum-sensing signal AIP, AgrC phosphorylates AgrA, which in turn activates the P2 and P3 promoter along with other transcriptional targets¹⁵⁷. Hence, two divergent transcripts RNAII and RNAIII are transcribed through P2 and P3,

the mature AIP thiolactone structure, and a negatively charged C-terminal recognition sequence. AgrB is a 22 kDa endopeptidase responsible for the proteolysis of AgrD through specific recognition sequence. It has six transmembrane segments consists of four hydrophobic transmembrane α helices and two hydrophobic loops with several positively charged amino acid residues¹⁵⁸. The N terminal, specifically the first 34 residues, is highly conserved in Agr B¹⁵⁹.

Further, the linear peptide is processed by the addition of the thiolactone group at the C terminus. The C terminus tail of AgrD play a critical role in the cleavage of AgrB and AIP production¹⁶⁰. Mutations in the histidine residue at position 77 (H77), and cysteine residue at position 84 (c84) is essential for the

processing of AgrD. The AgrC and AgrA form

respectively, creating a positive feedback loop. Koenig et al. demonstrated that purified AgrA binds to the RNAIII-agr intergenic region of P3 promoter with high affinity than the P2 promoter¹⁶⁴. The function of AgrA in activating the quorum sensing system is impaired when an extra adenine is inserted to the seven continuous adenines in the C-terminal. AgrA is shown to activate the other three chromosomal operons, such as *psm* α , *psm* β , and MW00370/0372. The expression of PSM is through the direct binding of AgrA to PSM promoter regions independent of RNAIII¹⁵⁹.

1.5.4 Regulatory RNA

The ability of an organism to use the small, non-coding RNA (sRNA) for gene regulation is well established. After the discovery of novel small RNA in *E. coli*, genome-wide approaches have revealed complex and dynamic RNA-mediated regulation in *S. aureus*. The first significant and regulatory RNA in SA, RNAIII was discovered in 1993 (which will be discussed in detail later). Almost a decade later, Pichon and Felden demonstrated sRNA encoded on pathogenicity islands of *S. aureus*. They used computational methods to identify seven sRNA (*spr A-spr D*) produced by horizontally acquired genomic islands. Further, bioinformatic predictions were used to identify RsaO genes and eleven Rsa genes that function by masking the ribosomal binding site^{165,166}. High throughput sequencing and cDNA libraries were used to identify *sau* genes and *Teg* genes, respectively^{167,168,169}. To date, approximately 250 regulatory sRNA in *S. aureus* have been studied.

Most of the sRNAs of SA are located randomly in the core of genome and mobile accessory elements. Some of the sRNAs are also present in multiple copies. Regulatory RNA, including the housekeeping RNA; 4.5S, RNase P, and tmRNA target mRNA either in trans (targeting other RNAs and protein) or in cis (affecting adjacent or associated sequences). They function at the levels of transcription or translation or both of the target mRNA by controlling the gene expression of the bacteria to adapt to the environment¹⁷⁰. Cis-regulatory elements that encode the cis-regulatory RNA may be located in the 5' or 3' untranslated regions in bacteria. These RNAs in a particular condition can sense environmental signals such as metabolites (Riboswitches), uncharged tRNAs (T-boxes), metal ions, pH, and temperature (thermoswitches) which regulate the expression of downstream genes by a conformational change. Protein targeting RNAs modulate the activity of proteins by interacting with them and acting as a regulatory RNA. This regulatory RNA is expressed in several stress conditions, including starvation, antibiotic treatment, and host infections. In the current thesis we will focus on RNAIII of SA in host pathogen interaction.

1.5.5 RNAIII

RNAIII is the known effector of the *S. aureus agr* quorum-sensing system, which mediates the regulation of virulence genes^{171,161}. During the growth phase of *S. aureus*, RNAIII accumulates with maximal expression in the late exponential and stationary phase. RNAIII meets all the requirements of the multifunctional RNA; as it is 514 bp long RNA possessing intricate fold of 14 stem-loops (H1-H14) and three long-distance helices¹⁷². RNAIII acts as a switch between the early expression of surface proteins and the late production of exotoxins. Sixteen genes encoding toxins and enzymes are up-regulated by RNAIII, which represses at least seven genes encoding surface proteins. The strategy of RNAIII to mediate the gene regulation is to control the target gene expression at multiple levels, such as transcription, translation, and mRNA stability. The expression of numerous genes involved in virulence and cell wall metabolism has been regulated by RNAIII by antisense pairing and at a post-transcriptional level. So far, accumulation of RNAIII in high cell density is shown to repress the enzymes involved in peptidoglycan turnovers such as hydrolases and amidases. Hence, RNAIII represents a paradigm in the field of bacterial RNAs to show an influence on pathogenesis.

Moreover, RNAIII plays a role in regulating the hemolytic, and microbial activities due to the presence of δ -hemolysin peptide (Hld) in its 3' end^{173,174}. RNAIII acts both as an activator and a repressor of a particular mRNA target, coordinating the complex regulatory network for various trans-acting sRNAs. For example, RNAIII initiates the translation of *hla* mRNA, which encodes for hemolysin¹⁷⁵. Hence, in the absence of RNAIII, the 5' end of *hla* mRNA undergoes conformational change blocking the access to ribosome on the Shine-Dalgarno (SD) sequence. Hairpins H3 and H7 of RNAIII interact with the 5' UTR of *hla* mRNA and provides access to the SD sequence triggering the α -hemolysin translation. RNAIII is shown to regulate the surface adhesion proteins as extracellular adherence protein (EAP) (also known as MAP) involved in *S. aureus* immune evasions. The MAP production is upregulated by RNAIII interaction with the *map* mRNA via antisense pairing¹⁷⁶.

On the other hand, RNAIII regulates various target genes by inhibiting the translation through binding at the TIS of mRNA and triggering degradation. For example, RNAIII represses the translation of SA100 mRNA, one of the mRNA involved in *S. aureus* adhesion to host cells, *spa* mRNA encoding immune escape protein A as well as *rot* mRNA encoding toxin production^{171,177,178}. Recently, it was demonstrated that the opportunistic bacteria *S. aureus* contains 5'-NAD capped RNAIII which inturn led to the decrease expression of alpha and

delta toxins resulting in reduced cytotoxicity¹⁷⁹. Thus, RNAIII regulates several proteins, which are major virulence factors produced by SA during infection.

1.6 Extracellular vesicles

All the cellular life forms have an inherent feature to release extracellular vesicles (EVs). These small-sized lipid bilayers enclosed particles ranges from 20 to 500 nm in diameter, secreted by all domains of life such as eukarya, bacteria, and archaea. Extracellular vesicles are mainly known to cargo stimuli, including nucleic acids, toxins, lipoproteins, and enzymes that are critical in microbial physiology and pathogenesis. The presence of extracellular vesicles were first found in *E. coli* by electron microscopy that are referred as outer membrane vesicles (OMVs). The biogenesis of the OMV occurs by the accumulation of the phospholipids, followed by pinching off the outer membrane¹⁸⁰. OMVs are packed with multiple virulence factors that play a crucial role in bacterial pathogenesis¹⁸¹. Recently, OMVs are shown to act as immune modulators inducing innate and adaptive immune responses^{182,183}. *In-vivo* and *in-vitro* studies demonstrate the delivery of lipopolysaccharide through outer membrane vesicle triggering caspase-11 dependent responses¹⁸².

In Gram-positive bacteria, the biogenesis of extracellular vesicles is complex and poorly understood due to the presence of the thick peptidoglycan structure. In recent years, it is demonstrated that Gram-positive bacteria, including SA and *Bacillus subtilis*, naturally release membrane vesicles during growth cycles¹⁸⁴. Extracellular vesicles secreted by various Gram-positive bacteria; *Bacillus anthracis*, *Streptococcus pyrogens*, *S. aureus*, *Streptococcus pneumonia*, and *Streptococcus agalactia* carry a wide range of hemolysins and pore-forming toxins^{185,186,187,188}. Proteomic analysis of the SA shed membrane vesicles (MVs) showed the presence of beta-lactamase, which is essential for antibiotic resistance allowing the poly microbial community to evolve against antibiotics¹⁸⁴. *S. aureus* membrane vesicles cause skin barrier disruption in mice leading to skin inflammation due to the presence of toxins^{189,190}.

Group A streptococcus (GAS) releases MVs regulated by the two-component system and cargos; protein, lipids, and nucleic acids, mainly RNA¹⁸⁷. Recently, Group B streptococcus was shown to produce membrane vesicles, which, when exposed, lead to fetal compromise and preterm termination during pregnancy¹⁸⁸. Disease development causing infection and colonization at distant site was observed through the transfer of MVs containing an array of molecules for immune invasion. Due to the association of various factors and enzymes such as coagulase, *S. aureus* membrane vesicles, when added to serum, can induce cloth

formation^{184,191}. Membrane vesicles thus aid the formation of fibrin networks around pathogens leading to a protective environment avoiding access to the innate immune system. Extracellular vesicles from community-associated methicillin resistance *S. aureus* shows the presence of alpha-type phenol soluble modulins, which promote the biogenesis of EVs by disrupting the cytosolic membrane. EVs purified from the mutant *S. aureus* are immunogenic in mice, as they induce cytolytic neutralizing antibodies protecting in lethal sepsis model, which highlights the importance of EVs as a vaccine platform.

1.7 Lipoproteins

A significant class of surface proteins anchored into the plasma membrane of SA represents the bacterial lipoproteins¹⁹². These proteins are differentiated by the N-terminus lipid moiety and are synthesized as precursors followed by processing into the mature form at the cytoplasmic membrane. Initially, the N terminus of prototypical Braun's *E. coli* lipoprotein contains the unusual S-glycerol-cysteine residues (N-acyl-S-diacylglycerol cysteine) with modified three fatty acids¹⁹². Lipoproteins are synthesized as precursors with a unique 18-36 amino acid long signal peptide at its N-terminus. This consensus sequence is differentiated by the presence of C-terminus lipobox at three amino acid sequence in front of the cysteine residue (-Leu-3-Ser/Ala-2-Ala/Gly-1-Cys+1)^{192,193}.

Lipoproteins are modified and processed by three enzymatic reactions after the insertion into the cytoplasmic membrane via the Sec pathway. The first step in the biosynthesis of lipoproteins is the transfer of the diacylglycerol group from the phosphatidylglycerol to the sulphhydryl group of an invariant cysteine residue in the lipobox. The reaction is catalyzed by phosphatidylglycerol-pro-LPP diacylglyceroltransferase encoded by Lgt. After the translocation of lipoproteins through the cytoplasmic membrane, the specific signal peptidase II (Lsp) detects the diacyl-glycerol-modified lipo-signal peptide and cleaves between the -1 position of the amino acid and +1 position of the lipid-modified cysteine residue¹⁹⁴. In the last step of biosynthesis, the N terminus of the diacylglycerol-modified cysteine residue is fatty acylated by an N-acyltransferase (Lnt) to form N-acyl diacylglycerol-cysteine¹⁹⁵. All the three enzymes (Lgt, Lnt, Lsp) essential for the lipidation and biosynthesis of lipoproteins are located in the cytoplasmic membrane.

Lipoproteins in Gram-positive bacteria play a diverse role in protein secretion and folding of exoproteins, attachment, and invasion of host cells¹⁹⁶. Lipoproteins are essential in the host-pathogen interaction influencing the pathogenicity, immune responses and cytokines, and

chemokines secretions. Bacterial lipoproteins and synthetic lipopeptides bind and activate TLR2 leading to the NF- κ B activation¹⁹⁷. TLR2 heterodimers with TLR6 and TLR1 on detection of bacterial diacylated and triacylated lipoproteins respectively^{198,199}. Mutations in the Lgt and Lsp lead to impaired pathogenicity of the innate immune system.

2. STATE OF THE ART

Range of microbial ligands and bacterial toxins activate the inflammasome sensors either through direct or indirect mechanisms. The current state of art suggest that the bacterial toxins activate the NLRP3 inflammasome complex indirectly through various processes such as K⁺ efflux, lysosomal and mitochondrial damage, cathepsin B release and reactive oxygen species production^{200,201,202}. Initially, various ionophores such as nigericine, valinomycin and ATP were shown to deplete potassium in the cells and induce IL-1 β and IL-18 secretion and were dependent on inflammasome adaptor ASC and NLRP3 sensor^{203,204}. Munoz- Planillo also demonstrated that the drop in potassium content acts as a common signal triggered by bacterial pore forming toxins and other particulate matters to induce the NLRP3 inflammasome activation. In *S. aureus*, multiple pore forming toxins and hemolysins have shown to evolve NLRP3 inflammasome activation. Especially α -hemolysin is shown to release IL-1 β in caspase-1 dependent manner in both human and mouse monocytic cells²⁰⁵. Similarly, GBS pigment/ lipid toxin was also shown to induce membrane permeabilization which causes the efflux of intracellular potassium activating the NLRP3 inflammasome via caspase-1²⁰⁶. Hemolytic strains of GBS have been reported to induce NLRP3 inflammasome for the release of IL-1 β in murine dendritic cells and macrophages^{207,208}.

Apart from the pore forming toxins, other microbial ligands such as RNA play a crucial role in activation of inflammasome. Along with pore forming toxins endogenous GBS RNA when given cytosolically activated the canonical inflammasome pathway for the release of IL-1 β in murine macrophages²⁰⁸. Sha et al demonstrated that multiple types of RNA such as mRNA, tRNA rRNA and small ssRNA are sensed by human macrophages for the activation of inflammasome²⁰⁹. On the contrary murine macrophages can sense only mRNA components²¹⁰. Nonetheless, the upstream pathway of NLRP3 responsible for the release of IL-1 β is undefined. Recently, it was demonstrated that the cGAS-STING pathway is responsible for the IFN- β response upon detection of cytosolic DNA from GBS⁴⁸. The cGAS-STING pathway signals upstream of NLRP3 and is also independent to the IFN- β responses²¹¹. Nonetheless, *Brucella* infections showed STING dependent cGAS independent responses for the release of IL-1 β ²¹². Although, the involvement of STING and the mechanism involved in the delivery of Gram-positive bacterial RNA ligands for the activation of canonical inflammasome pathway for the release of IL-1 β is undefined.

Cytosolic delivery of PAMPs is the foremost step for the activation of NLRP3 inflammasome for the release of IL-1 β . Gram-positive bacteria mainly, *Mycobacterium ulceras*, *Bacillus*

anthracis, GBS and *S. aureus* release membrane vesicles^{184,213,185,189}. Gurung et al have reported that the membrane vesicles release by *S. aureus* are packed with effector molecules which interacted the the host causing cell death²¹³. Recently, membrane vesicles shed by GBS orchestrated events at the fetomaternal interface leading to membrane damage and fetal death in murine¹⁸⁸. Yet, the exact molecular structure of the varied vesicles secreted by Gram-positive bacteria and the mechanism to activate the NLRP3 inflammasome is undiscovered.

Activation of canonical and non-canonical inflammasome leads to release of alarmins, chemokines, cytokines and endogenous molecules which can show a host protective or deleterious effect during bacterial infections^{214,215}. The current literature posits that, canonical inflammasome pathway is been activated by Gram-positive bacteria while Gram-negative bacteria activates the non-canonical inflammasome pathway in THP1 macrophages and primary macrophages^{101,103}. Gram-negative bacteria specifically activate caspase-4/5 in human and are orthologue of caspase-11 in mouse¹⁰⁰. Caspase-4 and caspase-5 are similar genes but show apparent differences in their regulation and inflammasome activation^{216,217}. The current state of art lacks the link between non-canonical inflammasome activation and Gram-positive bacterial infection. Various endogenous molecules such as HMGB1, S100A9 and progranulin are released in the extracellular milieu orchestrating the deregulated inflammation, organ damage and poor outcomes in sepsis. Subsequent studies have highlighted the role of PGRN as it showed elevated levels in sepsis patients as compared to healthy individuals¹²⁴. Recently, progranulin was shown as a novel diagnostic marker for early onset sepsis^{218,219}. However, the involvement of caspase-5 and the signaling pathway activating inflammasome pathway through Gram-positive bacteria remains undiscovered.

The current thesis focuses on elucidating the signaling pathway involved in the activation of inflammasome pathway through GBS and *S. aureus* for the release of IL-1 β and PGRN.

AIM

Our aim is to clarify the mechanism by which Gram-positive bacteria deliver PAMPs for the activation of inflammasome in the release of IL-1 β and progranulin. To this end, extracellular vesicles shed by GBS and SA was characterized for the activation of inflammasome pathways and the following objectives were addressed.

1. To exhibit the release of extracellular vesicles through Gram-positive bacteria.
 - 1.1 Characterizing the varied types of vesicles released by Gram-positive bacteria.
 - 1.2 Activation of inflammasome pathway for the release of IL-1 β and progranulin by Gram-positive bacterial shed vesicles.
2. To elucidate the upstream pathway involved in the activation of canonical inflammasome pathway.
 - 2.1 Involvement of STING for the release of IL-1 β through Gram-positive bacterial infection.
3. Scrutinizing the Gram-positive microbial ligand involved in the activation of canonical inflammasome pathway via STING.
 - 3.1 Activation of canonical inflammasome pathway through Gram-positive bacterial RNA.
4. To explicate the type of RNA enclosed in the vesicles and its involvement in release of IL-1 β .
5. To verify the role of microbial polyunsaturated lipids in inflammasome activation.
6. Investigating the role of non-canonical inflammasome pathway involved in the secretion of alarmins such as progranulin.
 - 6.1 Demonstrating the role of lipoproteins in caspase-5 activation for the release of progranulin.
 - 6.2 To corroborate the role of TLR2 for the release of progranulin via caspase-5.
7. To study the relevance of discovered mechanisms with Gram-positive sepsis patients.
 - 7.1 To verify the hallmarks of inflammasome activation such as presence of RNAIII or caspase-5 and GSDMD cleavage in *S. aureus* sepsis patients.

3. MATERIALS AND METHODS

3.1 Materials

Table 1: Consumables for isolation of MLBs and MVs

Materials	Catalogue no /manufacturer
Sterile 0,22 µM syringe filter	107091
3.5 mL, Open-Top Thick wall Polypropylene Tube, 13 x 51mm	349623/Beckman coulter
13.5 mL, Open-Top Tube, 16 x 76 mm	326814/Beckman coulter
Ultracentrifuge rotor	TLA-100.3
Opti prep	1114542/Progen
HEPES	L1613 /Biochrom
NaCl	HN00.2/Roth
Phosphate Buffer Saline (PBS)	14190169/ThermoFisher

Table 2: Consumables for the characterization of MLBs

Materials	Catalogue no /manufacturer
Agar plating	
Sterial polystyrene loop	Ansa GmbH, Germany
BD Columbia Agar, 5 % sheep blood	254007/BD
Raman Spectroscopy	
Calcium fluoride slide	Crystal GmbH, Germany
Upright micro Raman setup, CRM300	WITec GmbH, Germany
Electron microscopy	
Carbon coated EM grids	400 meshes, quantifoil, Großlobichau, Germany
BAF400T freeze fracture unit	BAL-TEC, Lichtenstein
Zeiss EM902A electron microscope	Carl Zeiss AG, Oberkochen, Germany
Fixing solution (2.5 % glutaraldehyde in cacodylic acid buffer)	Sigma Alrich
Coating Unit CCU-010	Savematic GmbH, Bad Ragaz, Switzerland
Zeiss LEO 1530 SEM	Carl Zeiss AG, Oberkochen, Germany
Dynamic Light Scattering (DLS)	
Semi-micro cuvettes	108861
DLS	Zeta sizer nano series
Protein analysis	
Pierce™ Silver Stain Kit	24612/Thermo Fisher

Table 3: Constituents for LC-MS and isolation of staphyloxanthin

Materials	Catalogue no /manufacturer
UHPLC-MS	Shimadzu, Germany
High resolution mass spectroscopy	Thermo (Bremen, Germany)
Chromatography column	PHENOMENEX®, Germany
NMR	Bruker
Silica gel	Macherey-Nagel, Germany
Methanol	VWR, Germany
Water for HPLC	Millipore, Germany
Formic acid	Carl Roth, Germany

Acetonitrile	LC-MS grade, VWR
Media ingredients	Carl Roth, Germany

Table 4: RNA extraction constituents

Materials	Catalogue no /manufacturer
innuSPEED Lysis Tube Z	845-CS-1170050/Analytic Jena
QIAzol Lysis Reagent	79306/QIAGEN
SpeedMill Plus homogenizer	Analytic Jena, Germany
Total RNA mini spin columns	EM09C-050/7BioScience
miRNA mini spin columns	EM12C-050/7BioScience
Chloroform	VMR Chemicals
Total RNA extraction kit	QIAGEN
QIAexcel	QIAGEN

Table 5: RNA sequencing kit

Kit	Constituents	Catalogue no /manufacturer
SMARTer smRNA-Seq kit for Illumina	SeqAmp DNA polymerase SMARTer smRNA-Seq Package 1 and 2 NucleoSpin Gel and PCR Clean-up	TAKARA
Qubit RNA HS assay	Qubit [®] RNA HS Reagent (component A) Qubit [®] RNA HS Buffer (component B) Qubit [®] RNA HS standard 1 (component C) Qubit [®] RNA HS standard 2 (component D)	Q32852/Thermo Fisher Scientific
Qubit DNA HS assay	Qubit [™] 1X dsDNA HS Working Solution (Component A) Qubit [™] 1X dsDNA HS Standard 1 (Component B) Qubit [™] 1X dsDNA HS Standard 2 (Component C)	Q33230/Thermo Fisher Scientific
Quick Dephosphorylation Kit	CutSmart [®] Buffer (10X) Quick CIP	M0508S/ New England Biolabs

Table 6: Primers used in the study

The T7 polymerase promoter sequence is italicized and the restriction enzyme sites are underlined.

Gene Name	Annealing Temp (°C)	Primers
RNAIII (cloning in pET28a)	58°C	F: <u>GCGGAATTC</u> <i>CAGATCACAGAGATGTGAT</i>
		R: <u>GCGAAGCTT</u> <i>AAGGCCGCGAGCTTGGGA</i>

RNAIII (T7) (IVT)	66°C	F:TAATACGACTCACTATAGGGAGATCACAGAG ATGTGAT
		R: AAGGCCGCGAGCTTGGGA
1-213 RNAIII (IVT)	58°C	F:TAATACGACTCACTATAGGGAGATCACAGAG ATGTGAT
		R: ACTATACGAAGATAACAAAT
213-514 RNAIII (IVT)	58°C	F:TAATACGACTCACTATAGGGACTAAAAGTATG AGTTATTAA
		R: AAGGCCGCGAGCTTGGGA
202-514 RNAIII (IVT)	55°C	F:TAATACGACTCACTATAGGGCTTCGTATAGTA CTAAAAGT
		R: AAGGCCGCGAGCTTGGGA
202-317 RNAIII (IVT)	55°C	F:TAATACGACTCACTATAGGGCTTCGTATAGTA CTAAAAGT
		R: ATAGCACTGAGTCCAAGGA
Rsa C (IVT)	58°C	F:TAATACGACTCACTATAGGGGTTTACTTTGAT AGGCCAGA
		R: TCCCATATCGTGCGTTAAATA
WAN01CC66-rc (IVT)	58°C	F:TAATACGACTCACTATAGGGAAAAGCTCTCCA TCATCTA
		R: AGTGATATTTTGGGTAATCG
HP (IVT)	58°C	F:TAATACGACTCACTATAGGGTGGTAACCGCAC TCGTA
		R: AAACAAAATCATCTTAGCGT
Spinach	55°C	F:TAATACGACTCACTATAGGGACGCGACTGAAT GAAATGGTGAAGGACGGGTCCACTTCGTATA GTACTAAAAGTATGAGTTATTAAGCCATCCCA ACTTAATAACCATGTAAAATTAGCA
		R:GACGCGACTAGTTACGGAGCTCACACTCTA CTCAACAAATAGCACTGAGTCCAAGGAACT AACTCTACTAGCAAATGTTACTCACTTGCTAA TTTTACATGGTTATTAAGTT
Lgt oligos	60°C	F:GAAAATTTCCAATGGCCATATTACG
		R:AAACCGTAATATGGCCATTGGAAA

Table 7: Constituents for RNAIII Cloning

Materials	Catalogue no /manufacturer
EcoRI restriction enzyme	R0101S/ New England Biolabs
HindIII restriction enzyme	R0104S/ New England Biolabs
Q5® High-Fidelity DNA Polymerase	M0491S / New England Biolabs
Pet28a vector	Neosep lab
T4 DNA Ligase	M0202T/ New England Biolabs
<i>E.coli</i> competent cells	Neosep lab
NucleoSpin® Plasmid isolation kit	740588250/ Macherey-Nagel

Table 8: Constituents for *In-vitro* transcription

Materials	Catalogue no /manufacturer
Ribonucleotide Solution Mix	N0466S/New England Biolabs
Hi-T7 RNA Polymerase	M0658S/New England Biolabs
10X Hi-T7 RNA Polymerase Buffer	M0658S/New England Biolabs
miRNA mini spin columns	EM12C-050/7BioScience
RNA extraction kit	QIAGEN

Table 9: Constituents for CDN binding assay and spinach fluorescence assay

Materials	Catalogue no /manufacturer
8-Biotin-11-c-diAMP	B 156-001/BioLog Life science institute
Streptavidin	R&D systems
miRNA mini spin columns	EM12C-050/7BioScience
RNA extraction kit	QIAGEN
TMB substrate Reagent A and B	BioLegend
c-diAMP	C 088-01/ BioLog Life science institute
DFHBI	TE26/VWR

Table 10: Media and consumables for cell culture

Materials	Catalogue no /manufacturer
RPMI-1640 with GlutaMax	61870044 /Thermo Fisher
Fetal Bovine Serum	S0115/ Biochrom C0742C
Penicillin Streptomycin (1000U/ml)	15140122/Thermo
DMEM, Glutamax, High Glucose	61965059/ThermoFisher
Opti-MEM™ I Reduced Serum Medium	51985026, Thermo Fisher
Gentamycin 10mg/ml	A2712/Biochrom
Recombinant Human M-CSF	574804/Biolegend
DMSO	D8418/Sigma Aldrich
PBSwithout Ca ²⁺ , Mg ²⁺	14190169/Thermo Fisher
5, 10, 25ml Pipette	Greiner bio-one
25 cm ² , 75 cm ² cell culture flask	Greiner bio-one
Cryovials	LCR2BYSMY/National Lab
PMA	tlrl-pma/Invivogen

Table 11: Cell lines used in the study

Cell lines	Source/ media used
THP1 (ATCC)	Current study /RPMI+10% FCS+Pen/strep
<i>CASP5</i> ^{-/-}	Current study /RPMI+10% FCS+Pen/strep
<i>CNPY3</i> ^{-/-}	Current study /RPMI+10% FCS+Pen/strep
<i>CASPI</i> ^{-/-} (clone A5)	RPMI+10% FCS+Pen/strep ¹⁰¹
<i>CASP4</i> ^{-/-} (clone C11)	RPMI+10% FCS+Pen/strep ¹⁰¹
<i>ASC</i> ^{-/-} (clone C12)	RPMI+10% FCS+Pen/strep ¹⁰¹
<i>STING</i> ^{-/-} (Invivogen)	RPMI+10% FCS+Pen/strep
<i>cGAS</i> ^{-/-} (Invivogen)	RPMI+10% FCS+Pen/strep
<i>R-STING</i> ^{-/-} (Invivogen)	RPMI+10% FCS+Pen/strep

Table 12: Ligand and inhibitors

Materials	Catalogue no /manufacturer
LPS-EB	tlrl-3 pelps/ InvivoGen,
Pam3CSK4	tlrl-pms/ InvivoGen,
FSL	tlrl-fsl/ InvivoGen,
Lipofectamine 2000 Reagent	11668-027/ThermoFisher
Naftifin hydrochloride	Exoderil
Rnase A	7156.1/Roth
DNase1,	EN0525/Thermo
KCL	8121.1/Roth
Dynasore	ALX-270-502-MO25,Enzo
Human STING inhibitor H-151	PC-35312/ ProbeChem
NLRP3 Inhibitor, MCC950	CAS 256373-96-3/ Calbiochem
Nigericin	tlrl-nig/ InvivoGen

Table 13: Kits (ELISA and LDH)

Kits	Catalogue no /manufacturer/ Lot no
Human IL-1 β ELISA MAX TM Deluxe	437004/ BioLegend (B297865, B273362)
Human TNF alpha Duo Set ELISA	DY210-05/R&D systems (P209961, 1495856)
Human Progranulin DuoSet ELISA	DY2420 /R&D systems (P221723, P180201)
Human Galectin-1 Duo Set ELISA	DY1152-05/R&D systems (P199094)
LDH Cytotoxicity Detection Kit	MK401/Takara Clontech (AH2P024)
TMB substrate Reagent A and B	421101/BioLegend (B298138)

Table 14: Buffers for western blot

Buffer	Ingredients
20 X Nupage Running Buffer (500 ml)	50 mM MES-97.6 g, 50 mM TrisBase-60.6 g, 0.1% SDS-10 g, 1mM EDTA- 3 g, pH-7.3
20 X Nupage transfer Buffer (500ml)	40.8 g Bicin, 52.4 g BisTris, 3 g EDTA pH-7.2
10 X TBS-T (500ml)	12.114 g Tris HCl, 87 g NaCl, pH-7.4
Blocking Buffer	5 % skim milk in TBS, 5 % BSA

Table 15: Consumables for western blot

Materials	Catalogue no /manufacturer
10x Cell Lysis Buffer	9803S/ New England BioLabs
Sample Buffer, Laemmli	S3401-10VL/ Sigma
NuPAGE TM Novex TM 4-12% Bis-Tris Protein Gels, 1.0 mm, 15-well	NP0323BOX/ life technologies
PVDF Membrane	IPVH00010/ Merck
Blotting paper	TE26/ VWR
Western Bright ECL	541004/ Biozym
Page Ruler TM Prestained Protein Ladder, 10 to 180 kDa	26616/ Thermo fisher
Restore Western Blot Stripping Buffer	21059/ Thermo Fisher
SuperSignal TM West Pico PLUS Chemiluminescent Substrate	34580/ Thermo Scientific

Table 16: Primary and secondary antibodies for western blot

Protein	Catalogue no /manufacturer	Dilution	Concentration
Caspase-1	GTX133447/ GeneTex	1:1000	1 µg/ml
Biotin anti-human IL-1β Antibody	508301/ Biologend	1:1000	25 µg/ml
Human STING/TMEM173 Antibody	MAB7169-SP/ Bio-Techne GmbH	1:1000	25 ng/ml
GAPDH	GA1R/ Thermo	1:5000	1 µg/ml
Human Progranulin/PGRN Antibody	MAB2420-SP/ R&D	1:1000	83 µg/ml
Anti-Caspase-5 antibody	ab69641/ Abcam	1:1000	1 µg/ml
GSDMD Polyclonal AB	20770-1-AP/ Proteintech	1:1000	33 ng/ml
a-Rabbit-hrp labeled	074-1506/ KPL	1:1000	1 µg/ml
a-Mouse-hrp labeled	074-1806/ KPL	1:1000	1 µg/ml

Table 17: Constituents for Immunofluorescence

Materials	Catalogue no /manufacturer
Coverslips	ECN 631-1577/ VWR
Dapi	6335.1/ Roth
LAMP1	25630/ Abcam ab
Alexa Fluor 647 conjugated Streptavidin	016-600-084/ dianova
Alexa Fluor 488 conjugated Streptavidin	016-540-084/ dianova
Permeabilization Buffer	LS00833356/ Invitrogen
Zeiss LSM 780 Confocal microscope	Zeiss, Germany

Table 18: Constituents for infection model

Materials	Catalogue no /manufacturer
Wax worm <i>Galleria mellonella</i>	Biosystems Trularv, UK
Insulin syringe	BD microfine, 0.5 ml
Recombinant Human Progranulin Protein, CF	2420-PG-050/ R&D systems

Table 19: Constituents for generation of Lgt knockout

Materials	Catalogue no /manufacturer
pnCasSA-BEC vector	Quanjianji Ji's lab
T4 DNA Ligase	M0202T / New England Biolabs
T4 Polynucleotide Kinase	M0201S / New England Biolabs
NaCl	P029.2 /Roth
NEB Golden Gate Assembly Kit (BsaI-HFv2)	E1601S / New England Biolabs
Dam/Dcm ^{-/-} Competent <i>E. coli</i>	C2925I / New England Biolabs
Electroporation Cuvettes	165-2083/BioRad

Table 20: List of software's used for the study

Name	Developer
Graph Pad prism; ZEN Black 2.3 SP1 (Carl Zeiss GmbH)	Origin 9.0; Project 4 &5 (WITec GmbH, Germany)
Tecan i-Control	Malvern zetaser software 7.12
GNU R windows platform with R packages	Department of Biophotonics, Jena, Germany

Peaks, HyperSpec	
SeqMan Pro Array star and Gen Vision Pro	DNASTAR
Lab Solutions	Shimadzu, Germany
Thermo Xcalibur 4.0	Thermo
TopSpin 3.2	Bruker
ChemBioDraw Ultra 13.0	ChemBioDraw
Zeitasizer nano series	Malvern Panalytical
FastScan-CCD-camera, acquisition softwareEMMANU4v4.00.9.17	TVIPS, Munich, Germany

3.2 METHODS

3.2.1 Isolation and characterization of MLBs and MVs

3.2.1.1 Isolation

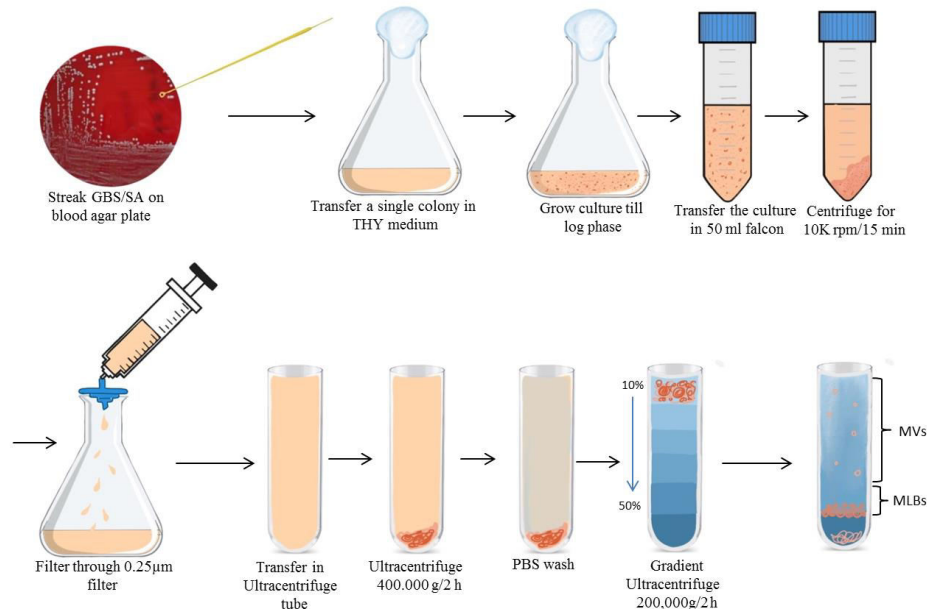


Figure 9: Diagrammatic representation of isolation of MLBs and MVs

MLBs and MVs were isolated from wild type *S. aureus* strain LS1, wild type GBS strain NEM316, mutant $\Delta cylE$ and naftine treated GBS.

Previously established method for the isolation of outer membrane vesicles from Gram-negative bacteria was used with some modifications. The MLBs and MVs were isolated in sterile conditions under the lamellar air flow as shown in fig. 9. Briefly, SA and GBS were grown till late log phase in THY medium at 37 °C. The grown culture was transferred to 50 ml falcon and centrifuged at 10,000 rpm for 15 min at 4 °C. The supernatant devoid of the bacteria was further filtered through 0.22 µm filter to get rid of any cell debris. The filtered supernatant was used to isolate the MLBs following ultracentrifugation at 400,000 g for 2 h. The ultracentrifugation was carried at 4°C using Beckman coulter rotor TLA-100.3 rotor and clear open top tubes. The tubes were balanced and weighed before the ultracentrifugation. Following the ultracentrifugation, a reddish orange pellet was obtained at the end of each tube. The supernatant was discarded and the pellet was washed with PBS for 1 h at 400,000 g using the similar rotor. This pellet contains MLBs as well as MVs, they were further purified using gradient ultracentrifugation. Opti prep with 10 mm HEPES, 0.85% NaCl was used to prepare gradient from 50-10 %. The pellet obtained was over layered on top and ultracentrifuged at 200,000 g for 2 h at 4 °C. After the completion of the ultracentrifuge, the tubes

were slowly removed and four fractions of 2.5 ml were collected. These fractions were further mixed with 7.5 ml of PBS and washed for 1 h at 200,000 g at 4 °C. The upper three fractions pelleted MVs while the MLBs were pelleted in the fourth fraction. The collected fractions were washed with PBS and further characterized.

3.2.1.2 Characterization

The collected pellets were further characterized as described below.

1. Agar plating

This is a primary characterization to verify contamination in the isolated MVs and MLBs. Each batch of preparation of the vesicles was streaked on the blood agar plate. The streaked plates were incubated at 37 °C overnight. The MLBs and MVs which do not show any growth were characterized further.

2. Raman measurement

Raman measurement was performed in collaboration with Core Units Biophotonics, CSCC Jena, Germany. The detailed procedure for the Raman measurement is mentioned in the appendix section.

3. Electron microscopy

Electron microscopy for the Gram-positive bacterial vesicles was performed in collaboration with Center of Electron microscopy, Jena, Germany. The detailed procedure for the electron microscopy is mentioned in the appendix section.

4. Dynamic Light Scattering

The size distribution of the isolated MLBs and MVs were measured using Zetasizer nano series. The purified vesicles were diluted 1:1000 with PBS in the spectrophotometric cuvette. The cuvette was placed in the zetasizer holder at measured at 25 °C. For thermotropic analysis of the MLBs, the diluted MLBs were continuously measured from 15 °C to 60 °C with an interval of 5 °C. The results presented were in the log form.

5. Silver staining of MLBs and MVs

To detect the proteins in the isolated MVs and MLBs from *S. aureus*, silver staining was performed. Equal concentration of the MLBs and MVs were re-suspended in the SDS-PAGE sample buffer (Thermo) and boiled for 10 mins. A sample corresponding to 10 µg of protein was separated SDS-PAGE was performed as described below. The separated gel was further subjected to silver staining using manufactures instruction (Pierce silver staining kit).

6. LC-MS of lipids and c di-AMP in MLBs

Detection of lipids through LC-MS was performed in collaboration with Leibniz Institute for Natural Product Research and Infection Biology e.V., Jena, Germany. Similarly LC-MS for the detection of c di-AMP was performed at Mass Spectrometry Platform, Friedrich Schiller University Jena, Faculty of Chemistry and Earth Sciences Jena, Germany.

The detailed procedure for the detection of staphyloxanthin type of lipids and c di-AMP through LC-MS is mentioned in the appendix section.

3.2.2 Isolation of staphyloxanthin and its precursor from *S. aureus*

Standardization and isolation of staphyloxanthin and its precursor from *S. aureus* was performed in collaboration with Leibniz Institute for Natural Product Research and Infection Biology e.V., Jena, Germany. The detailed procedure is mentioned in the appendix section.

3.2.3 Molecular biology

3.2.3.1 RNA extraction

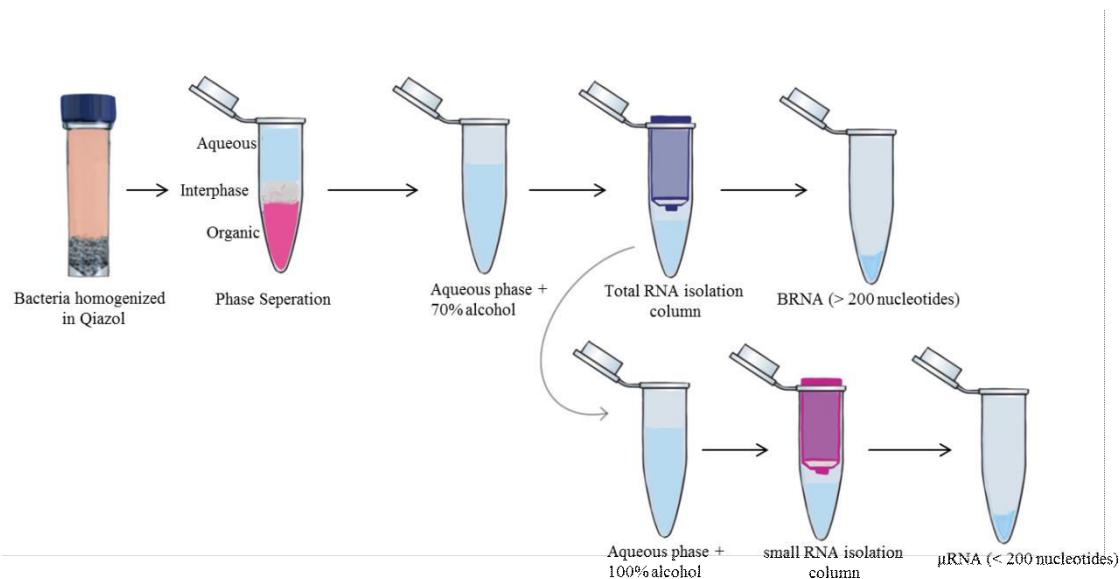


Figure 10: Diagrammatic representation of isolation of μRNA and BRNA from Gram-positive bacteria

For the extraction of Big RNA (>200 nucleotides) and μRNA (<200 nucleotides) from SA, GBS and MLBs manufactures protocol from Qiagen RNA extraction kit was followed. The protocol was modified as follows; bacteria grown till late log phase were collected and homogenized in 500 μl Qiazol in innuSPEED Lysis Tube Z (Analytic Jena, Germany) for 1 min by using the SpeedMill Plus (Analytic Jena, Germany) homogenizer. The tubes were centrifuged at high speed and the lysed supernatant was added with 200 μl of chloroform, vortexed and incubated for 3-5 min at RT. Samples were centrifuged for 15 mins at 12,000g to obtain phase separation: the lower red (Phenol-chloroform phase), the interphase and the

colorless upper phase. The upper phase contains the total RNA which was further isolated using two column method as shown in the Fig. 10. For the isolation of Big RNA, total RNA extraction kit was used (QIAGEN). The lysed bacteria were mixed with 1 V 70% ethanol and passed through the column. This was further followed with buffer washes as mentioned in the protocol. The flow through from the big RNA column were collected and mixed with 1.5 V 100 % ethanol following washes to remove the contaminants. Finally the column was washed with buffer warmed at 65 °C to remove the salts and metabolites. The high quality RNA from individual fractions was eluted with RNase free water. After completing the RNA isolation the concentration was measured using spectrophotometer, each fraction ranged around 500 ng to 3 µg. It was further analyzed on bioanalyser (QIAGEN advanced systems) for the size distribution of the particular fractions.

3.2.3.2 RNA sequencing

RNA sequencing was performed on µRNA isolated from wild type *S. aureus* (SA), Δagr mutant (SA- Δagr) and *S. aureus* MLBs (SA-MLBs). The RNA integrity of µRNA was checked using Qubit RNA HS assay (Thermo fisher scientific) with a Qubit fluorometer. The respective µRNA quantified more than 1.8 by A260/280 ratio were processed further.

Dephosphorylation of isolated µRNA: The quantified µRNA was dephosphorylated using Quick dephosphorylation kit (New England BioLabs) with manufactures protocol. The input of 5 µg of respective µRNA was dephosphorylated using Quick smart buffer and CIP followed by incubation for 10 min at 37 °C. The dephosphorylated µRNA were further purified using µRNA isolation columns. The purified dephosphorylated µRNA were again quantified using Qubit RNA HS assay.

Library preparation of RNA for sequencing: The libraries were prepared from dephosphorylated µRNA from SA, SA- Δagr and SA-MLBs using smRNA-seq kit (TAKARA) following manufactures instruction. Briefly, with the respective input of 1 µg µRNA including the positive and negative controls, library preparation followed polyadenylation, cDNA synthesis, PCR and clean up. Prepared libraries were finally quantified using Qubit DNA HS assay with Qubit fluorometer Each library gave yield of 18-20 ng/µl of cDNA. Each library prepared was also separated through 2 % agarose gel electrophoresis to verify the size and quality.

The prepared library was further pulled and sequenced using Illumina dual sided 250 base pair sequencing. The Pulled libraries were sequenced by MWG Biotech. The sequencing of

SA, SA- Δ agr and SA-MLBs gave approximately 3 million reads covering the entire region. The obtained sequences were analysed by NeoSep group member (Sachin D Deshmukh) following the scripts obtained from the collaborator in Uniklinik Keil, Germany and DNASTAR technical support. The sequenced reads were analyzed using DNASTAR software with the reference sequence of *Staphylococcus aureus* subsp. aureus 315 (accession number: NC_002745.2). SeqMan Pro and GenVision Pro programs were used to identify at least 2 fold differentially abundant reads in the respective samples.

3.2.3.3 RNAIII cloning

RNAIII was cloned from wild type *S. aureus* strain LS1 DNA using PCR. Primer design for PCR cloning of RNAIII gene was constructed according to previous study by Liu et al 2012, using genomic DNA as a template for PCR. The end of each primer contained a specific restriction enzyme (EcoRI and HindIII, respectively) as follows.

RNAIII_EcoRI (F): GCGGAATTCAGATCACAGAGATGTGAT

RNAIII_HINDIII (R): GCGAAGCTTAAGGCCGCGAGCTTGGGA

RNAIII was amplified using Q5 High-Fidelity DNA polymerase as follows

Components	Volume (25 μ l Reaction)
5X Q5 reaction buffer	5 μ l
10 mM dNTPs	0.5 μ l
10 μ M Forward primer	1.25 μ l
10 μ M Reverse primer	1.25 μ l
Q5 High-Fidelity DNA polymerase	0.25 μ l
5X Q5 high GC Enhancer	5 μ l
Template	X μ l (500 ng)
Nuclease free water	To 25 μ l

The reaction was assembled and amplified at annealing temperature 58 °C.

The amplified product is separated on 1-2 % agarose gel with ethidium bromide in TAE buffer. The respective band at 562 bp was sliced out on the UV table and subjected to PCR cleanup (Macherey-Nagel Nucleospin gel and PCR cleanup kit). The cleaned product was restricted digested using 1 μ l each of HINDIII and EcoRI restriction enzymes (NEB) in 1 X buffer overnight at 37 °C. Reaction product was separated on agarose gel and the respected

bands were sliced cleaned with PCR cleanup kit (Macherey-Nagel Nucleospin gel and PCR cleanup kit).

Purified vector Pet28a and insert were combined in a molar ratio of 1:3 (25 ng vector, 75 ng insert) with 5X ligation buffer and 1 μ l of ligase. The reaction was carried out in a volume of 20 μ l for 16 °C overnight. Next day, the ligated product was transformed to the bacteria. 100 μ l of competent cells (*E. coli* DH5 α) were thawed on ice, 20 μ l of the ligated product was added to the cells following incubation for 1 h on ice. The cells were given heat shock at 42 °C for 2 min and immediately placed on ice for 5 mins. Further the cells were allowed to grow for 1 h at 37 °C in 1000 μ L LB medium at 750 rpm. Pre-culture was streaked out on an LB agarplate with kanamycin as selection antibiotic and incubated at 37 °C overnight. For plasmid preparation, Miniprep cultures were grown in 10 mL LB medium, with 100 μ g/ mL kanamycin overnight shaking at 37 °C. Plasmid preparations were performed with the (Macherey-Nagel Plasmid isolation kit) kit according to the manufacturer's recommendations. Each newly created plasmid was controlled by test digestion to verify successfulligation. Positive clones were Sanger-sequenced (GATC Biotech, Jena) over theinsertion/ mutation sites.

3.2.3.4 *In-vitro*-transcription

In-vitro-transcription of the DNA templates was performed and standerized in the laboratory using following protocol. The DNA templates for the *in-vitro*-transcription were PCR amplified from the RNAIII clone using primers mentioned in the materials. The *in-vitro*-transcription was carried out using the Hi-Scribe RNA transcription kit (New England BioLabs). Briefly, the reaction was assembled at room temperature in the following order

Sample	Volume
Nuclease free H ₂ O	X μ l
NTPs (10 mM)	1 μ l
Template DNA (800 ng)	X μ l
1 \times reaction buffer	2 μ l
HiScribe™ T7 polymerase	2 μ l
Total	20 μ l

Mix and incubated at 37 °C for 2 h. Further, 2U of DNase treatment was given for 20 min at 37 °C. The transcribed RNA was further precipitated in 100 % ethanol with sodium acetate

for 16 h at -20 °C. Next day, the precipitated RNA was centrifuged to remove any precipitate and further purified using RNA purification columns following the manufacturer's instructions (QIAGEN). The RNA columns were washed twice with warm buffer heated at 65 °C. Quality control of IVT RNA was performed using QIAxcel capillary electrophoresis fragment analysis protocol to ensure lack of poor transcription template contamination and degraded RNA. Assurance of RNA purity and lack of contaminating DNA was further verified in the cellular assays using WT and cGAS deficient THP1 macrophages which can differentiate DNA dependent responses.

3.2.3.5 Binding assay for μ RNA and CDN

Binding assay was established and standardized in the laboratory. Following protocol was used to perform the assay.

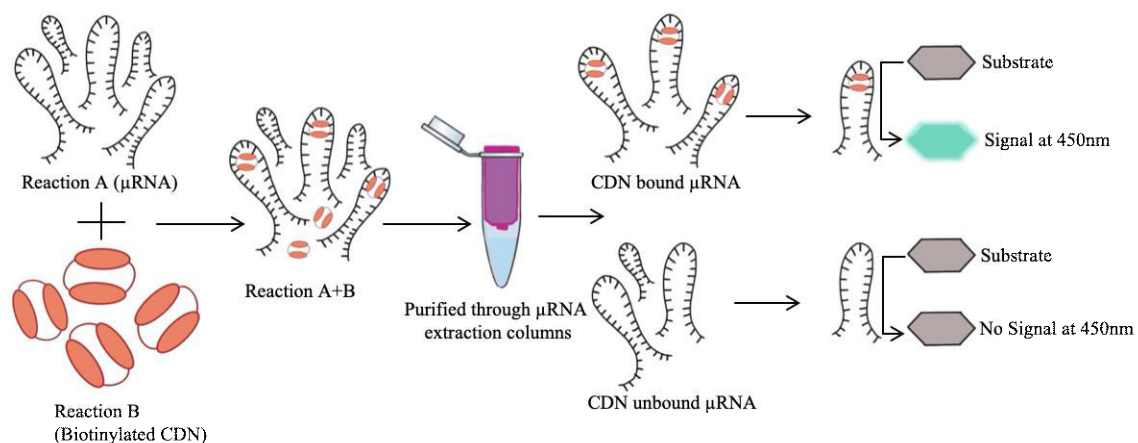


Figure 11: Procedure for the binding assay of RNA and CDN

Reaction A

Sample	Volume
μ RNA/BRNA (4 μ g)	X μ l
Buffer (20 mM tris-HCL pH 8.4, 50 mM KCl 0.1 mM MgCl ₂)	4 μ l
H ₂ O	X μ l
Total	40 μ l

The above reaction was mixed and heated at 80 °C for 10 min.

Reaction B

Sample	Volume
--------	--------

Biotin-c-di-AMP (16 μ M)	X μ l
Streptavidin-HRP	1 μ l
Buffer (20 mM tris-HCL pH 8.4, 50 mM KCl 0.1 mM MgCl ₂)	1 μ l
Total	10 μ l

The above reaction was mixed and heated at 37 °C for 30 min (reaction B).

Further, the reaction B was then added to reaction A and stepwise incubated for 37 °C for 10 min followed by 30 °C for 10 min, 25 °C for 10 min and, finally, 4 °C for 5 min.

The above reaction was mixed with 300 μ l cold water and 1.5 V 100% ethanol to elute water μ RNA. The extraction was performed using μ RNA extraction columns according to the manufacturer's instructions. Following this, RNA was eluted in 50 μ l and diluted with TMB substrate (1:1) in a 96 well plate. The reaction was stopped with 2N H₂SO₄ and absorbance measured at 450 nm.

3.2.4 LC-MS for binding of μ RNA and CDN

To check the binding of μ RNA and CDN, the above mentioned binding procedure was carried out. Following this the eluted RNA was diluted 1:100, 1:50 and 1:10 with RNase free water. The diluted RNA was subjected to ultra-high performance liquid chromatography coupled with high resolution mass spectrometry using THERMO (Bremen, Germany). The detailed procedure of LC-MS is described in the section entitled "LC-MS of c-di-AMP and derivatives in MLBs".

3.2.5 Spinach fluorescence assay

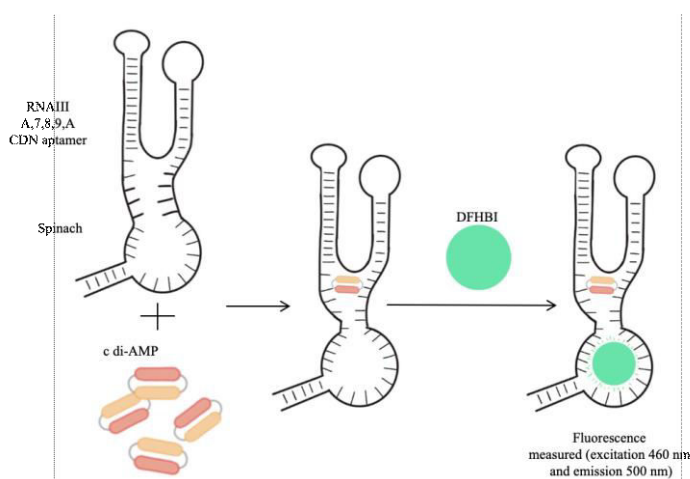


Figure 12: Schematic representation of Spinach Fluorescence assay

Spinach fluorescence assay was performed to validate the binding of the central domain of RNAIII and CDN. Previously characterized small molecule binding aptamer was used²²¹. The spinach DNA primers mentioned in the materials were amplified by PCR up to 25 cycles with DNA polymerase using annealing temperature of 55 °C as described above.

The PCR product was further separated on

2 % agarose gel and the respective bands were cut and sequence analysed.

The confirmed DNA was further *in-vitro*- transcribed using T7 RNA polymerase following precipitation and μ RNA column separation. The column was carefully washed with warm wash buffer to remove any impurities in the transcribed RNA. The spinach RNA was eluted in spinach reaction buffer (40 mM HEPES, 125 mM KCL, 3 mM $MgCl_2$). Proceeding with the fluorescence assay the *in-vitro transcribed* RNA was heated at 70 °C for 3 min, and then cooled down at room temperature over 5 min. For each measurement 100 nM of spinach RNA was used with 0.1 pM-10 nM CDN (c-di-AMP) and 10 μ M of DFHBI (3,5-Difluoro-4-hydroxybenzylidene) was added.

Samples were incubated at 37 °C in a black 96 well microtiter plate until equilibrium was reached. The fluorescence was then measured with a Tecan infinite plate reader at excitation 460 nm and emission 500 nm. Background fluorescence was subtracted and data were normalized.

3.2.6 Cell Culture

3.2.6.1 Maintenance of THP1 wild type and knockout cell line

Human monocytic suspension cell lines of THP1 wild type, *CASP1*^{-/-}, *CASP4*^{-/-}, *CASP5*^{-/-}, *ASC*^{-/-}, *STING*^{-/-}, *cGAS*^{-/-} deficient and *STING*^{R232} expressing *STING*^{-/-} cells were cultured. For the culturing of these cells the incubator was maintained at 37 °C with 5 % CO₂ in RPMI medium 1640 supplemented with L-Glutamine, sodium pyruvate, 10 % (v/v) FCS and 100 U/ml Penicillin-Streptomycin. *CASP4*^{-/-}, *CASP1*^{-/-}, *ASC*^{-/-} knockout THP1 cells were a kind gift from Prof. Veit Hornung and were phenotypically and genotypically confirmed. *STING*^{-/-}, *cGAS*^{-/-} and *STING*^{R232} expressing *STING* were purchased from Invitrogen and confirmed by western blot. THP1 *CASP5*^{-/-} cells with the deletion of *caspase-5* gene was prepared in the lab with sgRNA of caspase-5 purchased from Santacruz. The knockouts were confirmed with western blot and sequencing. A particular clone showing biallelic homozygous mutation on the border of exon 5 of gene caspase-5 isoform A was confirmed with sequencing and used in the study. Clones were further analysed by western blot and functional assays (data not shown). Similarly, THP1 *CNPY3*^{-/-} cells with the deletion of *CNPY3* gene were prepared in the lab by Mohamed Ghait using sgRNA and confirmed through western blot (Data not shown). Cells were spilt every 3 days in fresh medium to avoid overgrowth.

3.2.6.2 Cell Storage

THP1 and knock out suspended cells were frozen in 70 % RPMI-1640 media supplemented with 20 % FBS and 10 % DMSO in cryovials. The density of the cells in the cryo vials were around 2×10^6 cells/ml. The vials were frozen in -80 °C for 24 h in order to achieve the slow

cooling process. Next day the vials were transferred to the liquid nitrogen (-150 °C) for long term storage. Cells were thawed in a water bath at 37 °C following the re-suspension in warm medium. To avoid the effects of DMSO on cell viability the media was changed the same day.

3.2.6.3 Isolation of human blood derived primary macrophages

Peripheral blood mononuclear cells were obtained from healthy, informed and consenting volunteers. The PBMCs were isolated using Bicol separation solution followed by density gradient centrifugation. Briefly, collected blood was first diluted in the ratio 1:1 with Phosphate buffered saline (PBS). The diluted blood was layered slowly on top of Bicol in the ratio 8:3. The tubes were centrifuged at 800 g for 20 mins. Further, the interphase containing the mononuclear cells were transferred and washed three times with PBS. Finally the cells were suspended in DMEM media with 10 % FBS and ciprofloxacin. Macrophages were differentiated for 3 days from the mononuclear cells using recombinant human M-CSF (10 ng/ml). On day 4 the media was changed and the cells were ready for further experiments.

3.2.6.4 Cell Stimulations

Cultured wild type THP1 and knockout cell lines were counted using haemocytometer. Eighty thousand and five hundred thousand cells per well were seeded in 6 and 24 well plate respectively. Cells were differentiated into macrophages overnight using 100 ng/ml phorbol 12-myristate 13-acetate (PMA). Next day the cells were washed with pre-warmed PBS. For all the experiments, unless indicated the cells were primed for 3 h with Pam3CSK (400ng/ml) when LPS was the second stimulus or with LPS (100 ng/ml) when RNA was the second stimulus.

For evaluation of cells: Wild type THP1 and *CASP1*^{-/-}, *CASP4*^{-/-}, *ASC*^{-/-}, *CASP5*^{-/-} differentiated macrophages were stimulated intracellular with LPS (1 µg/100 µl) complexed with lipofectamine (LF). Extracellular LPS without lipofectamine and only lipofectamine were used a control. For positive control, nigericine (6.5 µM) was used.

MV and MLB stimulations: For the IL-1β and PGRN responses wild type THP1 and *CASP1*^{-/-}, *CASP4*^{-/-}, *ASC*^{-/-}, *CASP5*^{-/-}, *STING*^{-/-}, *cGAS*^{-/-} differentiated macrophages were washed with pre-warmed PBS and stimulated with 10 µg per well of MVs and MLBs.

RNA stimulations: For cytosolic activation of inflammasome using RNA, wild type THP1 and *CASP1*^{-/-}, *CASP4*^{-/-}, *ASC*^{-/-}, *STING*^{-/-}, *cGAS*^{-/-} differentiated macrophages were stimulated with bacterial RNA (5, 2.5, 1 µg/ml) and *in-vitro*- transcribed RNA with lipofectamine. Only RNA and lipofectamine are used as a control.

To determine the role of staphyloxanthin type of lipids, wild type THP1 and human blood derived macrophages were used. Bacterial RNA (5, 2.5, 1 $\mu\text{g/ml}$) was micelled with 0.125 μM of isolated lipids and stimulated to the cells. Stimulations of only RNA and lipid were used as a control. The respective solvent control of lipid (DMSO) was used to normalize the data.

Inhibitors: Wild type THP1 differentiated macrophages were treated with small molecule inhibitors for 1 h before the stimulations using following concentrations: H-151 (100 μM , 50 μM , 10 μM), Dynasore (150, 100 μM), KCL (75 mM, 60 mM, 45 mM), and MCC950 (5 μM , 10 μM). The cells treated with inhibitors were washed with pre-warmed PBS prior to the stimulations.

RNase A, DNase I treatment experiments: Wild type THP1 macrophages were pretreated using lipofectamine with RNase A and DNase I (100 ng/ml, 50 ng/ml and 10 ng/ml) for 2 h. The cells were washed with pre-warmed media prior to the bacterial infections and MLB stimulations. Heat inactivated RNase A was used as a control.

Bacterial infections: *S. aureus* strain LS1, Δagr *S. aureus* mutant, *S. aureus* strain RN4220, Δlgt mutant and GBS strain N316 and mutant ΔcylE were grown overnight at 37 °C in THY medium. Bacteria were harvested, washed with PBS and then calculated according to specific MOIs. Freshly cultured and differentiated wild type THP1 and *CASPI*^{-/-}, *CASP4*^{-/-}, *ASC*^{-/-}, *CASP5*^{-/-}, *STING*^{-/-}, *cGAS*^{-/-} macrophages were washed with pre-warmed optiMEM media prior to infection. Differentiated macrophages were infected for 1 h with strains and mutants of *S. aureus* and GBS with MOIs 10 and MOI 20 respectively with optiMEM media without antibiotics. Subsequently, after the infection the cells were washed with fresh optiMEM was containing 100 $\mu\text{g/ml}$ gentamycin and 250 UI/ml penicillin / 250 mg/ml streptomycin to kill the extracellular bacteria. The cells were further incubated overnight with opti MEM containing antibiotics.

Naftifine treated bacterial infections: *S. aureus* and GBS strains were grown overnight in THY medium with empirically optimized 50 μM naftifine. Wild type THP1 macrophages were infected with naftifine treated *S. aureus* and GBS. Experiments were carried out with intracellular stimulation with μRNA isolated from naftifine treated bacteria as mentioned above. At last, the supernatants were collected and cell lysate were used depending on the following method of investigation as mentioned later.

Cytosolic activation with lipoproteins: Pam3Cys and FSL were used for the cytosolic activation of macrophages and release of PGRN. Wild type THP1 and *CASP4*^{-/-}, *ASC*^{-/-}, *CASP5*^{-/-}, *CNPY3*^{-/-} macrophages were stimulated intracellular with 500 ng of Pam3Cys and FSL complexed with lipofectamine 2000. Supernatants and cell lysate collected were processed further.

3.2.7 LDH Assay

Lactate dehydrogenase is the cytoplasmic enzyme present in the cells which is released upon cell rupture and cell damage. Quantification of LDH release upon stimulation is the method to investigate the cell death. LDH assay is a calorimetric method for the quantification of LDH release due cell death. LDH assay was performed on the cell free supernatants with Pierce LDH Cytotoxicity assay kit. The assay is a two-step reaction in which the first step is the conversion of lactate to pyruvate where NAD^+ is reduced to NADH catalyzed by LDH. In the second step, diaphorase acts as a catalyst which transfers H/H^+ from NADH to tetrazolium salt which is reduced to formazan dye. The assay was performed according to the manufacturer's instructions with respective controls. Relative LDH release was calculated as LDH release (% cell death) = $100 \times ((\text{O.D of stimulated cells} - \text{O.D of unstimulated cells}) / (\text{O.D of lysis control} - \text{O.D of unstimulated cells}))$.

3.2.8 Cytokine and alarmin analysis by enzyme-linked immunosorbent assay (ELISA)

The concentrations of the cytokines and alarmins in the cell culture supernatants after stimulations were measured using IL-1 β , TNF- α , PGRN and Galectin-1 ELISA kits. The ELISA was performed as per manufacturer's instructions in the R&D system kits. Briefly, a sandwich ELISA which captures the analyte between two antibodies was used to detect the cytokines and alarmins. A 96-well polystyrene ELISA plate coated with special type of antibody or antigen was used. On day 1 the wells were coated with capture antibody for the binding of proteins of interest followed by overnight incubation at 4 °C. On day 2 the proteins from the cell culture supernatants bind to the coated antibody along with respective standards. When the proteins have been bound to the wells enzyme conjugated secondary antibodies are added. The secondary antibodies are specific for the antigens. A washing step is done to remove unbound species. Finally a substrate is added that is converted by the conjugated enzyme to a detectable product. The supernatants of the stimulated cells were collected after 16 h and diluted 1:5 for IL-1 β and TNF- α , 1:10 for PGRN and 1:10 for Gal-1. To measure the secreted PGRN and Gal-1 from patients, the plasma from the healthy controls, ICU and sepsis

patients was used with 1:10 dilution each. Each kit of PGRN ELISA was calibrated according to the signal to noise ratio.

3.2.9 Protein biochemistry

3.2.9.1 Protein isolation from supernatants

After the simulations, proteins from the supernatants were precipitated using chloroform-methanol method. Briefly, the collected supernatants were added with 1 V methanol and 1/4th V of chloroform. The solution was vortexed followed by centrifugation at 12000 rpm/ 5min at RT. The supernatant was discarded without disturbing the pelleted interphase. The pellets were washed with 1V methanol and dried at 50 °C. The dried pellets were then used further.

3.2.9.2 Protein extraction from cultured cells

Cells were washed with ice cold 1x PBS and incubated with lysis buffer on ice for 15 minutes. The lysate was then collected vortexed and centrifuged at 1105 X g for 15 minutes at 4 °C. Supernatant was collected and stored at -80 °C or used for sample preparation.

3.2.9.3 SDS-PAGE and Western Blotting

Pierce® BCA protein assay kit (Thermo scientific) was used to determine the concentration of unknown protein samples. To the required amount of protein (50 µg), 1X loading buffer was added and incubated at 95 °C for 5 min. After incubation, 20 µl of protein samples were loaded directly into the wells of SDS-polyacrylamide gel. The separation of proteins according to the size was determined together with a molecular size marker (Page Ruler Plus, Thermo Scientific).

Samples and the marker were separated using 4-12 % SDS-PAGE gels and were run with Nupage running buffer at 70 V constantly. The separated protein gel was further transferred to a PVDF membrane using a wet blot system. The western blot sandwich was prepared overlaying Whatman filter paper on each side of the PVDF membrane and the SDS-gel. The transfer was performed using a transfer buffer at 20 V for 1h. Later the membrane was blocked with a blocking solution mainly with 5 % skim milk or bovine serum albumin for 1 h. The blocked membrane was incubated overnight at 4 °C with the primary antibody. Next day the membrane was washed three times with 1X TBS-T with gentle agitation followed by diluted secondary antibody for 1 h. The washed membrane was immuno detected with freshly prepared ECL solution by G-BOX Chemi XX6 imaging device (Syngene). For reprobng the membrane was stripped with stripping buffer followed by TBS-T washes and primary antibody.

3.2.10 Immunocytochemistry

3.2.10.1 STING and LAMP1 co-staining

Three hundred thousand wild type THP1 cells were differentiated with 10 ng/ml of PMA on cover slips in 24-well plates. Following the stimulations and infections, cells were fixed with ice-cold methanol at -20 °C for 15 min. Fixed cells were rinsed with PBS for 5 mins followed by permeabilization. The permeabilization of the cells was carried out using permeabilization buffer containing saponin (Invitrogen). The cover slips with differentiated cells were stained with diluted (1:1000) primary antibody against STING and LAMP-1 for overnight at 4 °C. Next day, the cells were washed three times with PBS followed by secondary antibody. Anti-mouse labelled with Alexa Flour 488 and anti-rabbit labelled with Alexa Flour 647 were used as secondary antibody and incubated for 1 h. Finally after washing the cells were stained with DAPI and mounted on microscopic slides. Further, the images were acquired using a Zeiss LSM 780 confocal microscope with 63X objective. The quantification of the co-localized specks were calculated by using the formula number of co-localized yellow speckles/ number of red speckles *100.

3.2.11 Infection model

3.2.11.1 Infection of *Galleria mellonella*

Galleria mellonella was used as an infection model to study the pathogenesis of GBS and the vesicles secreted. The wax worm *Galleria mellonella* was purchased from Biosystems, Trularv, UK and maintained at room temperature in dark. After the purchase the larvae were used within 2 weeks. Larvae weighed between 150 mg to 300 mg at the time of the experiments. The selection of larvae was based on the size (around 15-25 mm in length) and color (creamiest with minimal grey markings). For each experiment 5-7 larvae each were injected with 50 µl of inoculum into the left proleg using a 0.3 -0.5 ml insulin syringe. For the priming experiments the sub lethal dose of MVs and recombinant progranulin (100 µg/ml) was used. Following the infection, each group of larvae were incubated at 37 °C in 9 cm petri dish upto the period of the experiment.

3.2.11.2 Monitoring of *Galleria mellonella* larvae.

Following the infection, *Galleria mellonella* larvae was observed at particular time points for the following attributes: survival, melanization, activity, and extend of cocoon formation. A score was provided to each larvae post infection contributing to the overall health index of the individual wax worm. The overall score ranges between 4-0. A healthy, uninfected larvae

generally scores 4 and the infected, dead larvae scores 0. For control purposes, wax worms were injected with 0.5 ml of PBS in each set of experiments.

3.2.12 Generation of the Lgt knockout strain

Lgt knockout strain of *S. aureus* was prepared in the lab with some assistance from medical student Laura Reng. Targeted single base mutant of Lgt was prepared by CRISPR RNA guided cytidine deaminase as described previously²²². The empty vector used for the lgt mutant, pnCasSA-BEC was a kind gift from Prof. Quanjianji Ji. The base editing plasmid pnCasSA-BEC-*lgt* was constructed using following steps

1. Oligo Design

20 bp- spacer sequences were selected before the PAM site (NGG) in the target site. Following two oligos were used for lgt sequences

Oligo F: GAAATTTCCAATGGCCATATTACG

Oligo R: AAACCGTAATATGGCCATTGGAAA

2. Phosphorylation of the oligos

For the phosphorylation of the oligos the reaction was assembled as follows

Sample	Volume
T4 DNA ligasebuffer (10x, NEB)	5 μ l
Oligo F (100 μ M)	1 μ l
Oligo R (100 μ M)	1 μ l
T4 polynucleotidekinase (NEB)	1 μ l
ddH ₂ O	42 μ l
Total	50 μ l

The mixture was further incubated at 37 °C for 1 h.

3. Annealing of the phosphorylated product

The phosphorylated product was mixed with 0.5 μ l of NaCl and annealed by incubating them at 95°C for 3min and steadily cooling down the mixture to the room temperature using a thermo cycler. The annealed mixture was diluted 10 times using ddH₂O.

4. Golden Gate assembly

The annealed spacer was followed by Golden gate assembly as follows

Sample	Volume
T4 DNA ligasebuffer (10x, NEB)	1µl
The pnCasSA-BEC plasmid (20 fmol/µL)	1µl
Annealed spacer (20 fmol/µL)	1µl
T4 DNA ligase (NEB)	0.5µl
BsaI-HF (NEB)	0.5µl
ddH2O	6µl
Total	10µl

This is followed by the reaction protocol in a thermo cycler

T(°C)	Time
37 °C	3 min } 25 cycles
16 °C	4 min } 25 cycles
50 °C	5 min
80 °C	15 min
10 °C	Forever

5. Transformation

The product from the Golden gate assembly was transformed to 100 µl of DAM/DCM⁻ *E. coli* (NEB) competent cell. The plate was incubated at 37 °C overnight and the successful construction of pnCasSA-lgt plasmid was verified with PCR and sequencing.

6. Base editing in the RN4220 strain

The PnCasSA-Lgt plasmid was transformed to RN4220 strain of *S. aureus* by electroporation. 1 µg of PnCasSA-Lgt plasmid was mixed with 50 µl of the RN4220 competent cells. The mixture was transferred to 1-mm electroporation cuvette (Bio-Rad) at room temperature. Electroporation was pulsed at 2.1kV/mm, 100 Ω, and 25 µF, the cells were immediately supplied with 950 µL Todd's soya broth (TSB) and recovered at 30 °C for 1–2 h. Further, 1 ml of cells were centrifuged and plated onto a TSB plate containing 10 µg/ml chloramphenicol. The plate was incubated at 30 °C for 24 h. The successful mutation in the target site was confirmed with sequencing. The colonies with desired mutation were further processed for plasmid curing.

6. Plasmid curing

The bacterial cells with desired mutation were further cultured in TSB media containing 10 µg/mL chloramphenicol at 30 °C overnight. Next day, the cells were 1:1000 diluted and incubated at 42 °C for 12 h without adding chloramphenicol. The bacteria were plated onto a TSB plate in the absence of chloramphenicol. The plate was incubated at 37 °C overnight. Next day, several colonies were randomly picked and resuspended individually into 10 µL ddH₂O. The cells were streaked onto two different TSB plates in the presence or absence of 5 µg/mL chloramphenicol. The successful curing of the plasmid was confirmed when the cells could only grow on the plate without chloramphenicol.

3.2.13 Patient Samples

Samples infected with Gram-positive bacterial infection were collected through a clinical cohort study performed on the multidisciplinary intensive care unit (ICU) of Jena University Hospital. All patients admitted to the ICU were screened within 2 h of admission for evidence of a systemic inflammatory response syndrome (SIRS) resulting from possible or proven infection. When sepsis was diagnosed, all adult patients with organ dysfunction according to the old criteria for sepsis (Sepsis-2) were eligible for study inclusion. All samples are thus in accordance with the new Sepsis-3 definition. Blood samples were collected within 24 h after clinical diagnosis. *S. aureus* patient isolates were obtained from the department of Microbiology, Jena, Germany. After approval by the local ethics committee (IDs: 2160-11/07, 2712-12/09 and 3824-11/12), all patients or legal surrogates gave informed consent for genetic analyses, blood collection and data evaluation. Fifty bacterial isolates from sepsis patients showing blood culture positive for *S. aureus* were obtained from medical microbiology department of Uniklinikum Jena. Characteristics of patients are mentioned in the appendix section.

3.2.14 Statistics

Data were analysed using Graph Pad Prism software version 6. Data are presented as mean +/- SEM. Data were analysed for statistically significant differences using paired t test for two conditions or groups. The quantification of the microscopic STING+LAMP1 structures undertaken using a Mann Whitney test. Data shown are mean ±SD (n=3), representative of at least three independent experiments. Asterisks indicate statistically significant differences (*p < 0.05, **p < 0.01 and ***p < 0.001). For the *Galleria mellonella* infection experiments, Kalpan Meier survival test was used. P values of * < 0.05, **p < 0.01, ***p < 0.001, and <0.0001 were considered significant.

4. RESULTS

4.1 Gram-positive bacteria exhibit active production of multilamellar lipid bodies (MLBs) and uni-lamellar membrane vesicles (MVs)

Gram-positive bacteria such as Group B streptococcus, *S. aureus*, *Mycobacterium ulcerans*, and *Bacillus. spp* are known to shed membrane vesicles, yet their exact mode of action and delivery is undiscovered^{184,185,188,223}. To investigate the extracellular vesicles shed by Gram-positive bacteria, we first morphologically examined *S. aureus* strain LS1 and GBS strain NEM 316 using electron microscopic approaches. Both strains upon subjecting to scanning electron microscopy (SEM) displayed numerous spherical protrusions from the bacterial cell membrane (**Fig. 13a**). The diameter of these vesicular protrusions ranged from 50-100 nm in size (**Fig. 13a**). Detailed analysis of *S. aureus* under freeze-fracture electron microscopy exhibited the accumulation of vesicle-like structures both inside and outside of the cell membrane (**Fig. 13b**). We further analyzed if the observed vesicular structures are released freely from the membrane of Gram-positive bacteria.

To isolate the freely released extracellular vesicles we used ultracentrifugation approaches. The purified membrane fractions from ultracentrifugation of *S. aureus* culture supernatants were examined by negative staining transmission electron microscopy (TEM). The obtained EM micrographs have exhibited a heterogeneous sized population of vesicles. Following density gradient ultracentrifugation we identified two types of vesicles. I). low density 50 nm-sized uni-lamellar membrane vesicles (MVs) and II). High density several 100 nm-sized lipid-rich multilamellar structures (**Fig. 13c,d**). TEM examination of the later showed higher-order assemblies with concentric lipid layers and hence we named them multilamellar lipid bodies (MLBs).

As a complementary approach to determine the varying sizes of the vesicles, GBS, and *S. aureus* vesicles mixture (MLBs+MVs), purified MVs and MLBs were subjected to dynamic light scattering (DLS) (**Fig. 13e**). The Dynamic light scattering with a Zetasizer permitted the size distribution of MLBs and MVs. The vesicles mixture of SA and GBS revealed two distinct populations of 50-100 nm and 400 nm of MVs and MLBs respectively (**Fig. 13e**). MLBs isolated from GBS and SA exhibited a single broadly dispersed population of 400 nm supporting the TEM analysis (**Fig. 13e**). Taken together, the above data strongly support the notion that Gram-positive bacteria produce MLBs and MVs during cell growth.

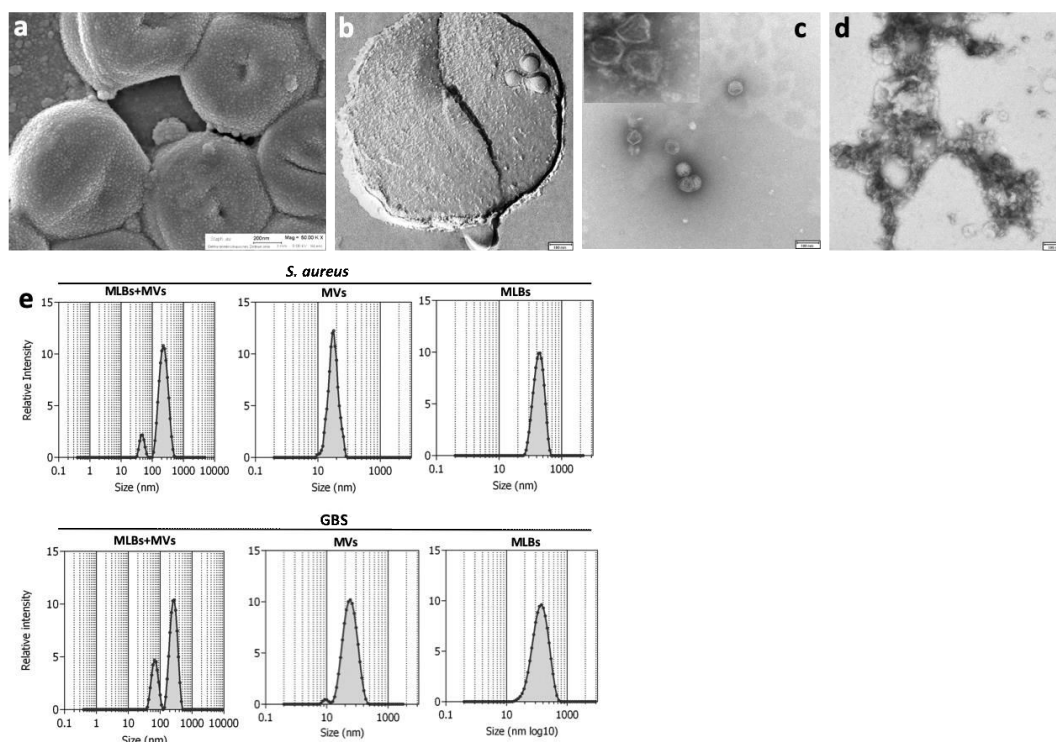


Figure 13: *S. aureus* and GBS secrete multi-lamellar lipid bodies and membrane vesicles

(a) Scanning electron microscopic images of SA, depicting multilamellar protrusions from the membrane. (b) Freeze fracture image of SA depicting cytoplasmic accumulation of lipid bodies. (c) Negative staining TEM image of membrane vesicles isolated from SA. (d) Negative staining TEM image of multilamellar lipid bodies (MLBs) isolated from *S. aureus*. (e) Size distribution of GBS and *S. aureus* vesicle mixture (MLBs+MVs), purified MVs and purified MLBs respectively. The x-axis is set to logarithmic scale.

To determine the composition of MLBs secreted by *S. aureus*, Raman spectroscopic analysis was carried out. The obtained Raman peaks demonstrated the presence of carbohydrates, proteins, nucleic acid and lipids (**Appendix Fig. 32a**). Detailed spectral analysis exhibited unsaturated fatty acids and long chain lipids at Raman peaks 2974, 2967, 1732, 1669, 1528 and 1163 cm^{-1} . This approach also identified the polyunsaturated lipids of *S. aureus* at Raman vibrations at 1009, 1163 and 1528 cm^{-1} (**Appendix Fig. 32a**). Comparison of the Raman peak profile of MLBs and *S. aureus* bacteria revealed that both *S. aureus* and its MLBs had similar lipid profile (**Appendix Fig. 32a**). The membranes of *S. aureus* contain staphyloxanthin, an unphosphorylated saccharolipid of isoprenoid nature that gives it an orange yellow color¹⁴³. Using liquid chromatography coupled with mass spectroscopy approach we attempted to determine if the vesicle secreted by *S. aureus* contains staphyloxanthin type of lipids. The precursor of staphyloxanthin biosynthetic pathway, 4', 4'-diaponeurosporonic acid was identified at m/z 432-433 in the vesicle mixture (MLBs+MVs), MLBs and the bacteria *S. aureus*. Surprisingly, MVs of *S. aureus* failed to detect the presence of 4', 4'

diaponeurosporonic acid at m/z 433 (**Appendix Fig. 33a**). In addition to the differences in lipids contents, total protein isolated from MVs and MLBs were subjected to silver staining. Similar to the lipids, silver staining gel demonstrated the differences in the protein in MLBs and MVs. The variability in the protein content of the vesicles indicates involvement of contrasting sorting mechanism (**Fig. 13f**). Moreover, the LC-MS profile revealed the presence of cyclic di-nucleotides (CDN) and its derivate pApA in the *S. aureus* MLBs at the retention time of 2.73 and 2.75 min respectively (**Fig. 13g**). Altogether, the above data characterizes the newly discovered MLBs which consists of nucleic acids, lipids and proteins.

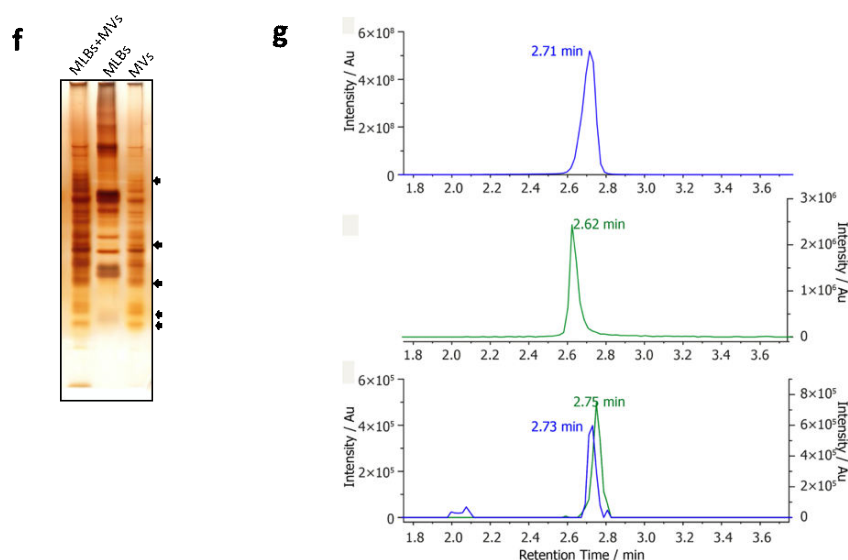


Figure 13. *S. aureus* secrete multi-lamellar lipid bodies and membrane vesicles

(f) Silver staining gel of vesicle mixture (MLBs+MVs), purified MLBs and purified MVs from *S. aureus*. (g) Mass spectra of I) c-di-AMP (Blue) II) derivative pApA (Green) III) c-di-AMP and its derivative in *S. aureus* MLBs.

4.2 CRISPR macrophages demonstrated canonical and non-canonical inflammasome pathway

To examine the immunological relevance of *S. aureus* released vesicles, the study focuses on the usability of CRISPR macrophages. To commence with the inflammasome activation in the human system we examined macrophages differentiated from monocytic cell line; THP1. According to the previous literature, the THP1 cell line has the scope to activate both canonical and non-canonical inflammasome pathways¹⁰¹. To elucidate the inflammasome pathways, THP1 cells deficient for *ASC*, *CASP1*, *CASP4*, *CASP5*, were generated using CRISPR/Cas9 (Clustered regularly interspaced short palindromic repeats/CRISPR associated protein 9). Upon LPS transfection, THP1 wild type and knockout cells elicited pronounced cell death and IL-1 β responses measured by lactate dehydrogenase (LDH) and IL-1 β Elisa

respectively (**Fig. 14a,b**). The non-canonical inflammasome pathway was activated upon LPS transfection showing caspase-4/5 dependent but ASC and caspase-1 independent cell death response (**Fig. 14a**). On the other hand, the canonical inflammasome activation for the release of IL-1 β was ASC and caspase-1 dependent (**Fig. 14b**). Of note, the extracellular LPS and the transfection vehicle lipofectamine lacked LDH and IL-1 β release (**Fig. 14a,b**). Based on these inflammasome activation profiles of cytosolic receptors the cells were used further.

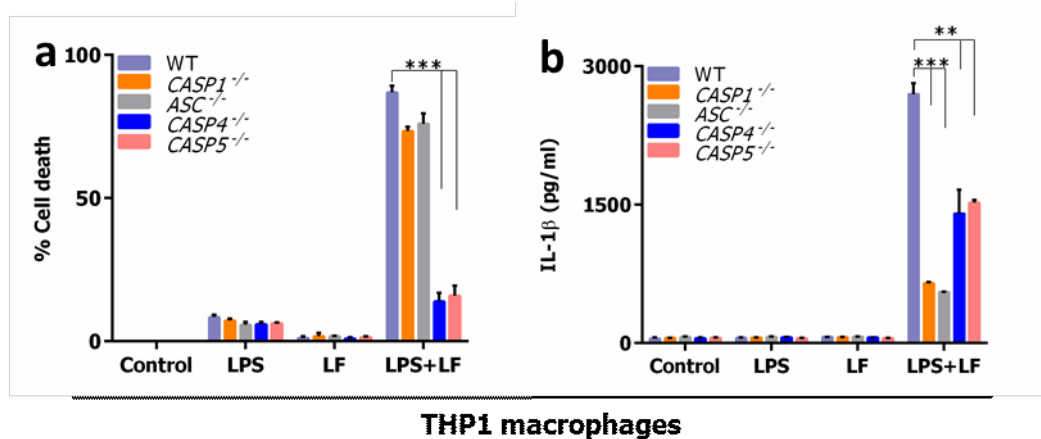


Figure 14: CRISPR macrophages demonstrated canonical and non-canonical inflammasome pathway

(a,b) Cell death and IL-1 β responses measured in THP1 (Purple), CASP1 deficient (Orange), ASC deficient (Grey), CASP4 deficient (Blue) and CASP5 deficient (Pink) THP1 macrophages when stimulated with intracellular LPS (LPS+LF), extracellular LPS and lipofectamine (LF).

4.3 Gram-positive bacterial RNA is a potent agonist for inflammasome activation

Following the evaluation of the THP1 macrophages for the inflammasome activation, we investigated the microbial ligand responsible for the release of IL-1 β . Bacterial RNA is a potent trigger for the innate immune responses such as Type-1 interferon, pro-inflammatory and inflammatory cytokines^{209,224,225}. Previously, GBS RNA was shown to induce NLRP3 inflammasome for the release of IL-1 β in mouse macrophages²⁰⁸. To determine the role of Gram-positive bacterial RNA in human macrophages, RNA isolated from *S. aureus* was transfected in THP1 macrophages. Robust activation of NLRP3 inflammasome was observed through the release of IL-1 β (**Fig. 15a**). On the other hand, extracellular RNA and lipofectamine by themselves did not confer cytokine release (**Fig. 15a**). To further validate the role of bacterial RNA in inflammasome activation we transfected RNase A, DNase I, and heat-inactivated RNase A (RNase HI) into human THP1 macrophages following SA infections and measured IL-1 β responses. Only RNase A, DNase I and RNase HI with lipofectamine were used as a control. Transfection of RNase A but not DNase I and heat-

inactivated RNase A (RNase HI) diminished IL-1 β upon infection with *S. aureus* (**Fig. 15b,c,d**). These results laid the paradigm where Gram-positive bacterial RNA activates the NLRP3 inflammasome pathway for the release of IL-1 β . Bacterial RNA contains mRNA, tRNA and three different sizes of rRNA (23s, 16s, and 5s), of which the only mRNA is sensed by murine bone marrow-derived macrophages (BMDMs) while all other types are sensed by human macrophages^{209,210}. To verify which type of RNA is responsible for inflammasome activation, different sizes of RNA were purified. Big RNA (BRNA) which contains >200 nucleotides and small RNA (μ RNA) containing 15-200 nucleotides were isolated from Gram-positive bacteria. This purified RNA was run on qiaexcel capillary gel electrophoresis (QIAGEN) to certify the size and purity. As expected the capillary gel demonstrated that big RNA has more than 200 nucleotides while the μ RNA contained less than 200 nucleotides and confirmed the purity of each fraction (**Fig. 15e**).

Gram-positive bacteria are known to synthesize cyclic di-nucleotides as a second messenger which are involved in several processes such as biofilm formation, cell wall homeostasis, and virulence gene expression^{226,227}. According to the recent discovery, the 5' untranslated region of riboswitches named RNA aptamers senses the specific metabolites through direct interactions. We hypothesized that the bacterial RNA could sense the cyclic di-nucleotides released by the Gram-positive bacteria. To evaluate this further, we established CDN binding absorption assay. For this assay, we used horse radish peroxidase (HRP) labeled c-di-AMP and μ RNA and BRNA from GBS as depicted in Fig 11. Non-biotinylated c-di-AMP was used as a control. Upon incubating respective RNA with HRP labeled CDN, we purified the bound fraction following the addition of the substrate. Surprisingly, the assay revealed that Gram-positive μ RNA has a strong capacity to bind CDN whereas big RNA failed to bind CDN (**Fig. 15f**). Hence, the above results confirm the CDN binding capacity of Gram-positive bacterial μ RNA.

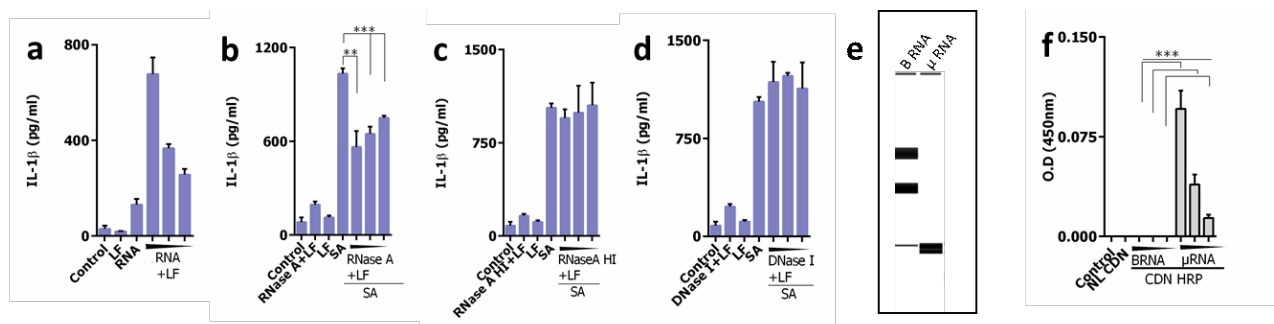


Figure 15: Gram-positive bacterial RNA is a potent agonist for inflammasome activation

(a) IL-1 β production measured in THP1 macrophages when transfected with increasing concentration of RNA, extracellular RNA and lipofectamine LF. (b,c,d) THP1 macrophages were pre-treated with increasing concentrations of cytosolic RNase A (RNase A+LF), DNase I (DNase I+LF) and heat-inactivated RNase A (RNase A HI+LF) respectively followed by infection with SA. IL-1 β production was measured. (e) Capillary gel electrophoresis of two types of purified GBS RNA (Big-BRNA, micro- μ RNA) run on Qiaxcel advanced system. Please note lower most band in B RNA sample is a capillary electrophoresis marker. (f) Optical density at 450 nm measured in binding assay of GBS μ RNA, BRNA (BRNA) with HRP-labelled CDN (c-di-AMP). Non-labelled CDN (NL c-di-AMP) was used as a control.

4.4 *S. aureus* MLBs accumulates different species of small RNA

Establishing the importance of the bacterial RNA in inflammasome activation and exhibiting the strong CDN binding capacity of μ RNA, the question of its presence in the MLBs remains unanswered. Cyclic dinucleotides in bacteria act as signal transducers and play a crucial role in quorum sensing^{226,227}. In *S. aureus* the quorum sensing system is regulated by accessory gene regulator locus which is responsible for virulence genes and pathogenesis. Recently, it was shown that GAS bacterial extracellular vesicles contain small RNA which can activate the immune system¹⁸⁷. To characterize and analyse the packaging of μ RNA in *S. aureus* MLBs, deep RNA sequencing of μ RNA purified from *S. aureus* MLBs (SA-MLBs), wild type *S. aureus* (SA) and Δagr mutant (SA- Δagr) was performed. Sequencing through Illumina dual sided-250 base-pair leads approximately 3 million reads per sample of SA-MLBs, SA, and Δagr covering the 15-200 nucleotides region. The obtained sequencing reads were mapped on *S. aureus* subsp. *aureus* N315 (accession number: NC_002745.2). Altogether 2-fold differentially abundant reads were obtained when analysed on the μ RNA analysis algorithms of SeqMan Pro ArrayStar and GenVision Pro.

Our analysis revealed the presence of 2828 different genomic locations enriched in the RNA sequencing reads. Focusing on the non-coding intergenic regions, we eliminated the reads obtained from rRNA, antisense, and coding regions. A total of 186 genomic regions were found to be differentially abundant when mapped on the *S. aureus* N315 genome (**Fig. 16a**). Of these, abundantly present 22 genomic regions were in common to SA, SA- Δagr and SA-MLBs and 41, 8, and 5 genomic regions overlapped in SA, SA- Δagr and SA-MLBs (**Fig. 16b**). Detailed analysis revealed the presence of various small regulatory RNAs (sRNA) from *S. aureus* which are responsible for various virulence activities. In together it demonstrated the presence of 106 small RNA (sRNA) from eight different sRNA families of N315 genome (**Appendix Fig. 34a**).

Analysing the NGS reads further, we manually curated and mapped on all sRNA identified in SA, SA- Δagr , and SA-MLBs. (Data obtained through collaboration from Uniklinikum Keil, Germany and technical assistant DNASTAR). Calculation of percentage reads estimated that the pseudogenes originating 6s RNA, 4.5s RNA and tmRNA were abundant in all the three μ RNA (Appendix Fig. 34a). In our analysis, genes encoding spr such as spr A-G were absent. Rsa A, C, E, F, H, I were differentially expressed in SA, SA-MLB, and SA- Δagr . Rsa A which is σB dependent is only expressed in SA- Δagr , Rsa F which is strain-specific to *S. aureus* showed expression which was relatively less in SA-MLB and SA- Δagr as compared to SA. Consistent with the literature, Rsa E which is regulated by quorum sensing system showed decreased levels in SA- Δagr . Rsa O genes were also differentially expressed. Rsa OG and Rsa OT levels were low in SA-MLB as compared to SA and SA- Δagr . None of the Sau genes were expressed in SA-MLBs. Out of the five σB -regulated genes sbr only sbr B, C, and D were found in our analysis. There was no expression of sbr B and D in SA-MLBs but sbr C was only expressed in SA and SA-MLBs and was completely dependent on SA- Δagr . The levels of WAN01CC66-rc were high in SA-MLBs as compared to SA and absent in SA- Δagr . Teg genes were also identified in our analysis of SA, SA-MLB, and SA- Δagr μ RNA. Teg 57 was only present in the SA-MLBs while absent in SA- Δagr and SA. Riboswitches such as Teg 1 and Teg 76 were absent in all of the three μ RNA. RNAIII which is one of the best-characterized regulators was found to be SA- Δagr dependent and exclusively present in the SA-MLBs. Surprisingly, we found small RNAs such as Rsa C, sbr-C, RNAIII, and WAN01CC66 were exclusively present in SA-MLBs (Appendix Fig. 34b). Altogether the above results concluded the presence of small RNA in MLBs with differential enrichment from the originating bacteria.



Figure 16: *S. aureus* MLBs accumulates different species of small RNA

(a) Heat map of differentially abundant μ RNA sequence reads obtained through deep sequencing in SA, SA-MLB and SA- Δagr . The reads were mapped on *S. aureus* subsp. aureus N315 (accession number: NC_002745.2) corresponding to 186 differentially abundant

genomic regions. **(b)** Venn diagram summarizing the overlap between differentially abundant reads mapped on genomic regions of N315 obtained by deep sequencing of SA (Blue), SA-MLB (Grey) and SA- Δ agr (Pink) μ RNA.

4.5 RNA aptamers present in MLBs activate the canonical inflammasome pathway via STING

After establishing the presence of small RNA in MLBs, the signaling pathway remains undiscovered. We further investigated the role of entrapped small RNA for the inflammasome activation and release of IL-1 β . To elucidate the pathway, purified MLB RNA was transfected to human THP1 macrophages along with *CASP1* and *CASP4* deficient cells. Results depicted that intracellular MLB RNA activated canonical inflammasome pathway as it showed caspase-1 dependent but caspase-4 independent response for IL-1 β and cell death (**Fig. 17a,b**). Pharmacological inhibition of NLRP3 by MCC950²²⁸ inhibited IL-1 β secretion in response to transfected MLB RNA (**Fig. 17c**). These results concluded that entrapped MLB RNA activates the canonical inflammasome pathway for the release of IL-1 β . The robustness of MLB RNA was further tested through enzymatic treatment with RNase A, DNase I, and heat-inactivated RNase A (RNase A HI). Degradation of RNA ligands by RNase A abrogated the inflammasome activation while DNase I and heat-inactivated RNase A showed no difference in IL-1 β release (**Fig. 17d,e,f**). Thus, the above results show that RNA entrapped in the MLBs is a potent activator of the canonical inflammasome pathway for the release of IL-1 β .

In concordance with the crucial role of endogenous second messenger cyclic di-nucleotides (CDN) in activation of STING for type I interferons^{41,42,48} and affinity of bacterial μ RNA towards CDN (**Fig. 15f**). We further unraveled the activation signal of bacterial and MLB RNA upstream of NLRP3. To do so, first, we evaluated the canonical inflammasome activation for the release of IL-1 β in wild type THP1 along with *CASP1*, *ASC*, *CASP4*, *STING*, and *cGAS* deficient macrophages. Nigercine a potent inducer of canonical inflammasome pathway showed caspase-1, ASC dependent while *STING*, *cGAS*, and caspase-4 independent IL-1 β responses (**Fig. 17g**). Further, to elucidate the role of *cGAS* and *STING* in canonical inflammasome activation, μ RNA from SA, GBS, and MLBs were purified and cytosolically transfected to wild type THP1 macrophages along with *STING* and *cGAS* deficient macrophages. Surprisingly, Gram-positive bacterial RNA activated *STING* dependent but *cGAS* independent canonical inflammasome pathway (**Fig 17h,j**). MLB μ RNA also showed aligned response for the release of IL-1 β which was *STING* dependent (**Fig. 17i**). On the other hand, the surface stimulations of RNA and lipofectamine did not activate the inflammasome pathway for the release of IL-1 β . In

conclusion, RNA aptamers entrapped in the MLBs activate STING upstream of NLRP3 for the canonical inflammasome activation.

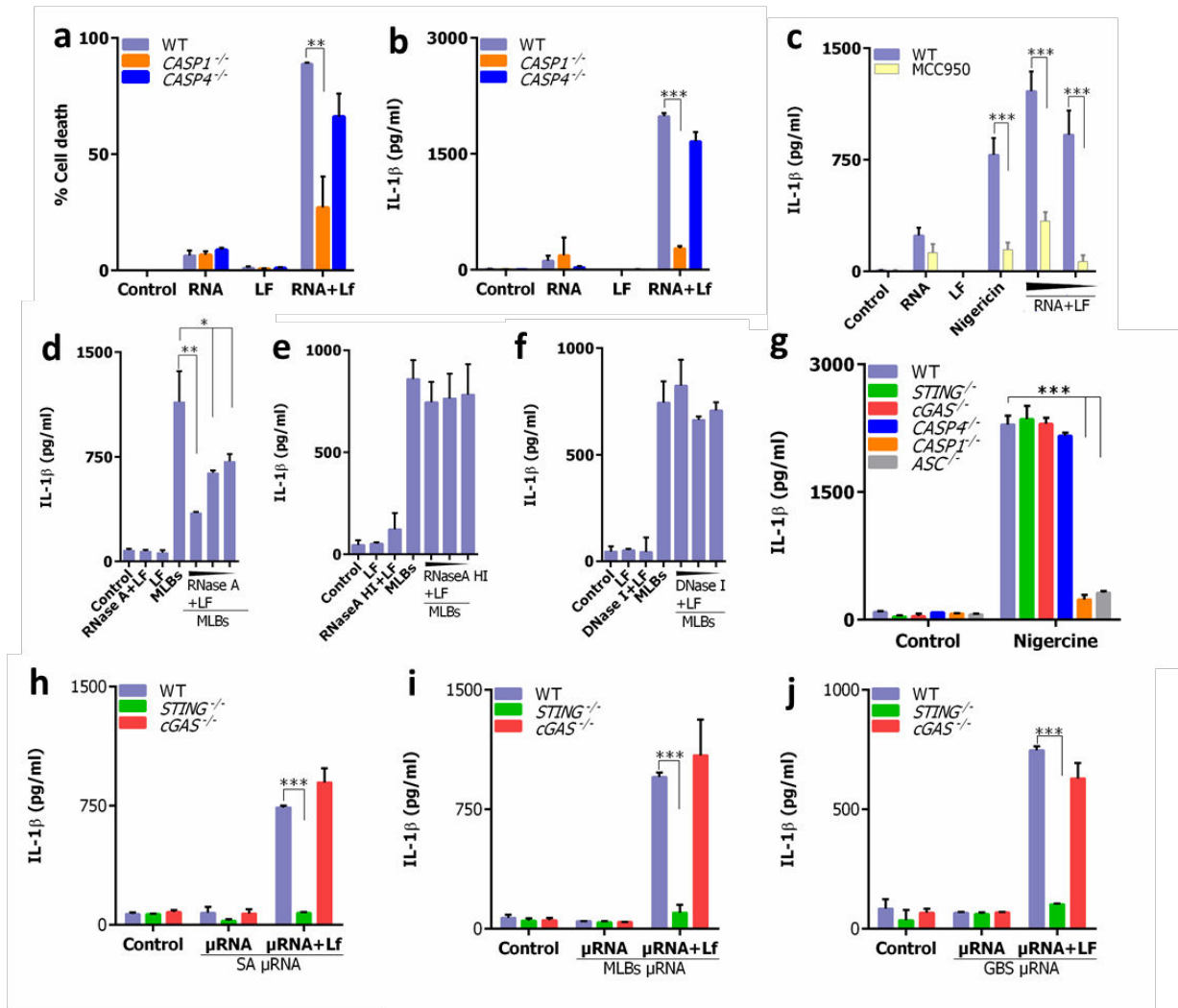


Figure 17: RNA aptamers present in MLBs activate the canonical inflammasome pathway

(a,b) THP1 (Purple), *CASP1* deficient (Orange), *CASP4* deficient (Blue) macrophages were stimulated with MLB RNA, cytosolic MLB RNA (RNA+LF). IL-1 β and cell death were measured. (c) THP1 (Purple) macrophages were pre-treated with increasing concentrations of MCC950 inhibitor (Yellow) and stimulated with *S. aureus* RNA, lipofectamine, nigericin, cytoplasmic RNA (RNA+LF) IL-1 β were determined. (d,e,f) THP1 (Purple) macrophages were pre-treated with increasing concentrations of cytosolic RNase A (RNase A+LF), DNase I (DNase I+LF) and heat-inactivated RNase A (RNaseA HI+LF) followed by stimulation with SA MLBs, IL-1 β was determined. (g) IL-1 β secretion was measured by ELISA in wild type, *STING* deficient (Green), *cGAS* deficient (Red), *CASP1* deficient (Orange), *ASC* deficient (Grey), THP1 macrophages when stimulated with nigericin (h,i,j) THP1 (Purple), *STING* deficient (Green) and *cGAS* deficient (Red) macrophages were stimulated with SA, MLB and GBS μ RNA (μ RNA), cytosolic μ RNA (μ RNA+LF) and IL-1 β production measured.

4.6 Gram-positive bacteria and its vesicles activate inflammasome for the release of IL-1 β and progranulin

In light of critical importance of entrapped RNA in activation of inflammasome, we turned our attention to the biological activity of the intact vesicles with respect to the inflammasome activation. Upon activation of the inflammasome pathway various cytokines and unconventional proteins are been released⁸². The current study focusses on the release of IL-1 β and progranulin upon stimulation of Gram-positive bacteria shed vesicles. In this setting, THP1 macrophages were stimulated with MLBs and MVs isolated from *S. aureus*. Upon measuring the IL-1 β responses, MLBs led to the activation of NLRP3 inflammasome pathway with abundant release of IL-1 β while MVs lacked the capacity to release IL-1 β (**Fig. 18a**). On the contrary, MVs led to the robust release of PRGN along with MLBs and *S. aureus* (**Fig. 18b**). In contrast to the IL-1 β and PGRN release, MLBs and MVs could activate the TLR mediated TNF α production (**Fig. 18c**). In summary, *S. aureus* secreted MLBs have the capacity to activate the inflammasome for the release of IL-1 β and PGRN while MVs could release only PGRN.

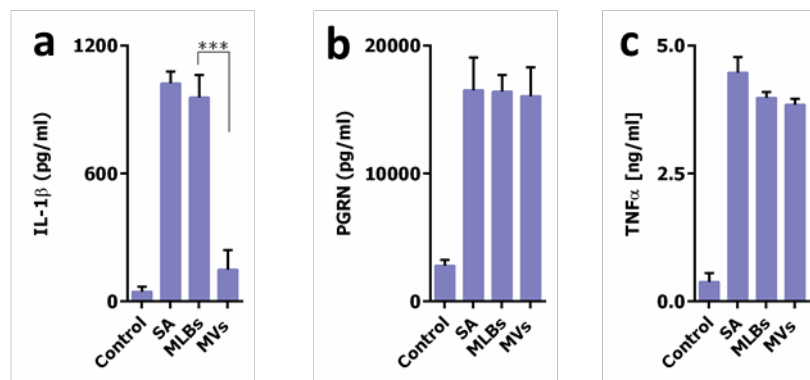


Figure 18: Gram positive bacteria and its vesicles activate the inflammasome for the release of IL-1 β and PGRN

(a,b,c) IL-1 β , PGRN and TNF α production measured in THP1 (Purple) macrophages following stimulations with MLBs, MVs and *S. aureus* infection.

4.7 Gram-positive bacteria mediates canonical inflammasome via STING

Taking advantage of the robust activation of inflammasome through bacterial μ RNA, GBS and SA shed vesicles, the next step was to elucidate the pathway activated by Gram-positive bacteria mainly SA and GBS. To do so, live bacterial infections were performed on wild type THP1 macrophages along with the *CASP1*, *CASP4*, *ASC*, *STING* and *cGAS* deficient macrophages. Surprisingly, similar to the μ RNA stimulations, IL-1 β response after infections with GBS and SA activated the canonical inflammasome pathway with STING dependent but

cGAS independent (**Fig. 19a,b**). These results were further confirmed through immunoblots which showed caspase-1 cleavage and cleaved IL-1 β in wild type THP1 and cGAS deficient cells in contrast to STING (**Fig. 19c**). We further validated STING deficiency using cells expressing variant of STING with arginine at 232 position (STING^{R232}). The main advantage of this approach was to confirm the utilization of STING in activation of canonical pathway and to rule out any interventions caused during the STING deficient cells preparations. Under these conditions, STING expressing STING^{R232} cells were able to retrieve the IL-1 β release upon SA and GBS infections (**Fig. 19d**). These results confirm the possible role of STING in Gram-positive bacteria activation of canonical inflammasome pathway. Moreover, infections with SA and GBS on STING and cGAS deficient cells showed no change in inflammasome independent cytokines such as TNF- α (**Fig. 19e**).

We went on to further characterize the involvement of STING in canonical inflammasome pathway by using STING specific antagonist. H-151 was recently shown to inhibit hSTING as it abrogated the type I IFN responses through reduction in the TBK phosphorylation and also suppressed the STING palmitoylation²²⁹. Subsequently to rule out the effect of immortalized cells, human primary blood derived macrophages were used to determine the inhibition of STING for IL-1 β responses. Cells were pre-treated with three different concentrations of H-151 (100 μ M, 50 μ M, 10 μ M) following infections with SA and GBS. Pretreatment of STING antagonist abrogated the release of IL-1 β by 80 % (**Fig. 19f,h**). H-151 treatment in primary blood derived macrophages had no effect on the TNF α production after the infections with SA and GBS (**Fig. 19g,i**). Taken together these results highlight the role of STING in canonical inflammasome pathway activated by Gram-positive bacteria.

Given the well documented role of potassium efflux in inhibiting the NLRP3 activation the crucial role of STING-signaling and lysosome was investigated. To unravel the activation signal from STING to NLRP3, human wild type THP1 macrophages were infected with *S. aureus* and GBS and stained with anti-STING and anti-LAMP1 antibody. To this end confocal microscopy revealed that upon activation STING, it concentrated in small vesicle like punctate structures presumably lysosomes (**Fig. 19j**). Co-localization of STING and LAMP-1 was pronounced upon SA and GBS infections in THP1 macrophages (**Fig. 19j**). In summary, Gram-positive bacteria activates STING signaling in human macrophages leading to IL-1 β release with possibly through K⁺ efflux upstream of NLRP3 activation.

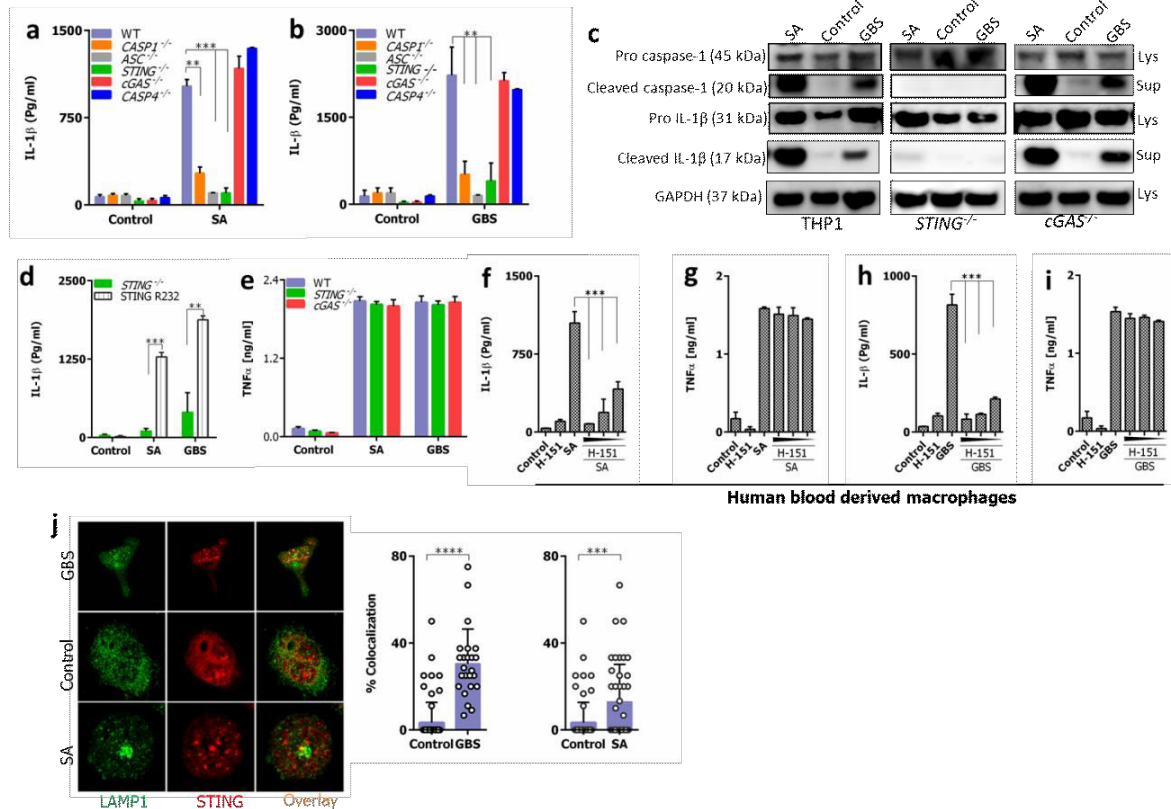


Figure 19: Gram-positive bacteria mediates canonical inflammasome via STING

(a,b) IL-1 β responses measured in wild type THP1 (Purple), *CASP1* deficient (Orange), *ASC* deficient (Grey), *CASP4* deficient (Blue), *STING* deficient (Green) and *cGAS* deficient (Red) macrophages when infected with SA and GBS. (c) Immunoblots showing IL-1 β and caspase-1 processing in wild type, *STING* deficient, *cGAS* deficient THP1 macrophages following infection with GBS and SA. (d) *STING* deficient (Green) and *STING*^{-/-} expressing *STING*^{R232} (pattern) were infected with SA and GBS, IL-1 β responses were measured. (e) TNF- α production measured in wild type, *STING* deficient (Green), *cGAS* deficient (Red) THP1 macrophages when infected with SA and GBS. (f,g) Human blood derived macrophages were pre-treated with increasing concentrations of STING inhibitor (H-151) for 1 h and then infected with SA. IL-1 β and TNF α production measured. (h,i) Human blood derived macrophages were pre-treated with increasing concentrations of STING inhibitor (H-151) for 1 h and then infected with GBS. IL-1 β and TNF α production is measured. (j) THP1 macrophages were infected with GBS and SA for 3 h. The cells were fixed and stained with anti-STING (Red) and anti-LAMP-1 (Green) specific antibodies. Percent co-localization was measured.

4.8 Gram-positive bacterial MLBs activate canonical inflammasome pathway via STING

In order to study the underlying signaling cascade activated by Gram-positive bacterial MLBs, wild type THP1 macrophages along with *CASP1*, *ASC*, and *CASP4* deficient cells were stimulated. As expected, IL-1 β responses triggered by GBS and SA MLBs followed the canonical inflammasome pathway showing independent response to caspase-4 but caspase-1, *ASC* dependent (Fig. 20a,c). These results were similar to live bacterial infections (Fig.

19a,b). Unravelling the pathway further the IL-1 β release measured in supernatants stimulated with SA and GBS MLBs showed that NLRP3 inflammasome activation required the presence of STING but was cGAS independent (**Fig. 20b,c**). The pretreatment of MCC950, a potent NLRP3 inhibitor²²⁸ on human THP1 macrophages abrogated the release of IL-1 β following stimulations with SA MLBs (**Fig. 20e**). These results followed the similar activation pattern as the live bacterial infections concluding the activation of STING for the release of IL-1 β .

It has been noted that activation of canonical NLRP3 inflammasome assembles on efflux of intracellular potassium, which is sufficient to activate the inflammasome⁸⁵. Determining the NLRP3 activation through efflux upon MLB stimulations; we cultured THP1 macrophages in presence of increasing concentration of potassium chloride following MLBs stimulations. As expected, canonical inflammasome mediated IL-1 β responses were completely blocked upon inhibition of potassium efflux following MLB and nigericin stimulations (**Fig. 20f,g**). Similar to Gram-negative bacteria secreted outer membrane vesicles; MLBs engrossed by the cell through dynasore-sensitive dynamin dependent endocytic pathways (**Fig. 20h**). Altogether these results conclude that MLBs secreted by Gram-positive bacteria follow canonical inflammasome pathway via STING for a robust IL-1 β response.

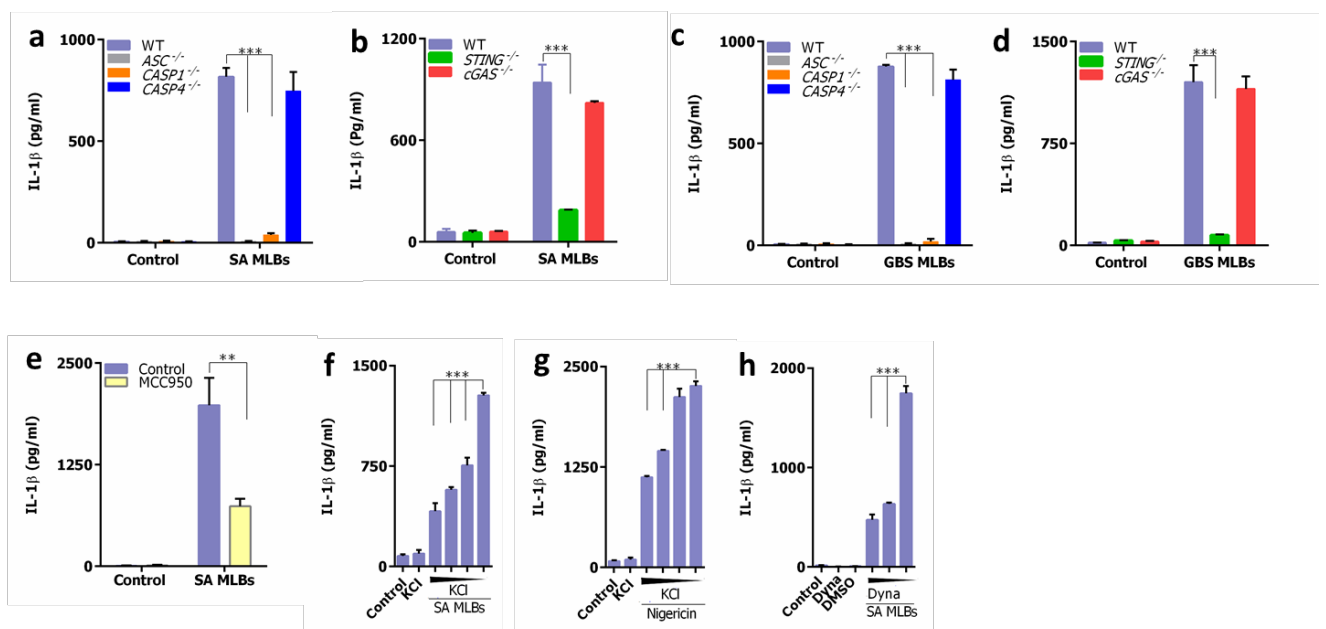


Figure 20: Gram-positive bacterial MLBs activate canonical inflammasome pathway via STING

(a,b,c,d) THP1 (Purple), ASC deficient (Grey), CASP1 deficient (Orange), CASP4 deficient (Blue), STING deficient (Green) cGAS deficient (Red) macrophages shows IL-1 β production following stimulations with *S. aureus* and GBS MLBs respectively. (e) THP1 macrophages

(Purple) were pre-treated with and without MCC950 inhibitor (yellow) for 1 h and stimulated with SA MLBs; IL-1 β was measured in the supernatant. (f,g) THP1 macrophages were pre-treated with increasing concentrations of KCl and stimulated with SA MLBs and nigericin. (i) THP1 macrophages cells were pre-treated with increasing concentrations of dynasore inhibitor for 1 h and stimulated with SA MLBs.

4.9 Accessory gene regulator system of *S. aureus* locus is engaged in RNA aptamer mediated inflammasome activation

In line of the notion that wild type *S. aureus* and Δagr mutant MLBs depict differential accumulation of small RNA, the effect of Δagr in inflammasome activation was further investigated. To this end, human blood derived macrophages and human THP1 wild type macrophages were infected with wild type *S. aureus* (SA) and mutant Δagr . To our surprise Δagr mutant bacteria failed to activate the inflammasome in THP1 and human blood derived macrophages in comparison with wild type *S. aureus* (Fig. 21a,b). Immunoblotting for cleaved caspase-1 and IL-1 β confirmed these results (Fig. 21c). To analyze this further, μ RNA from wild type *S. aureus* and mutant Δagr were purified and analyzed through capillary gel electrophoresis. We observed the equal production of μ RNA from *S. aureus* and mutant Δagr when analyzed on qiagen capillary gel electrophoresis (Fig. 21d). To examine the capacity of the isolated μ RNA in inflammasome activation, THP1 wild type macrophages were stimulated with *S. aureus* and mutant Δagr μ RNA intracellular and extracellular. Surface stimulations of Δagr μ RNA showed equal production of TLR dependent TNF α production in comparison to the wild type *S. aureus* μ RNA (Fig. 21e). Surprisingly, Δagr μ RNA failed to activate the NLRP3 inflammasome pathway in comparison with wild type *S. aureus* μ RNA with no release of IL-1 β (Fig. 21f). As the inflammasome response lacked in mutant Δagr , it can raise a possibility that the *S. aureus* mutant Δagr lacks CDN binding aptamers.

Analyzing it further the CDN binding capacity of the respective μ RNA was tested in an assay using horse raddish peroxidase-labelled c-di-AMP. μ RNA from wild type *S. aureus* showed more CDN binding capacity than Δagr μ RNA towards c-di-AMP (Fig. 21g). Further we used spectroscopic studies and subjected the μ RNA-CDN bound fractions to LC-MS. We observed that, CDN was detected in wild type *S. aureus* μ RNA fraction at retention time 3.31 min while Δagr μ RNA failed to show presence of bound CDN (Fig. 21h). Collectively the above results indicate the prominent role of AGR locus in expressing CDN binding RNA aptamers which are crucial for the activation of inflammasome. Furthermore, confocal microscopy revealed that STING trafficked through lysosome following stimulation with wild type *S. aureus* μ RNA through co-localization of STING and LAMP1. While Δagr μ RNA showed

significantly less lysosome like punctact structures (**Fig. 21i**). This additionally confirmed that STING activation through bacterial μ RNA pass triggers NLRP3 through lysosome.

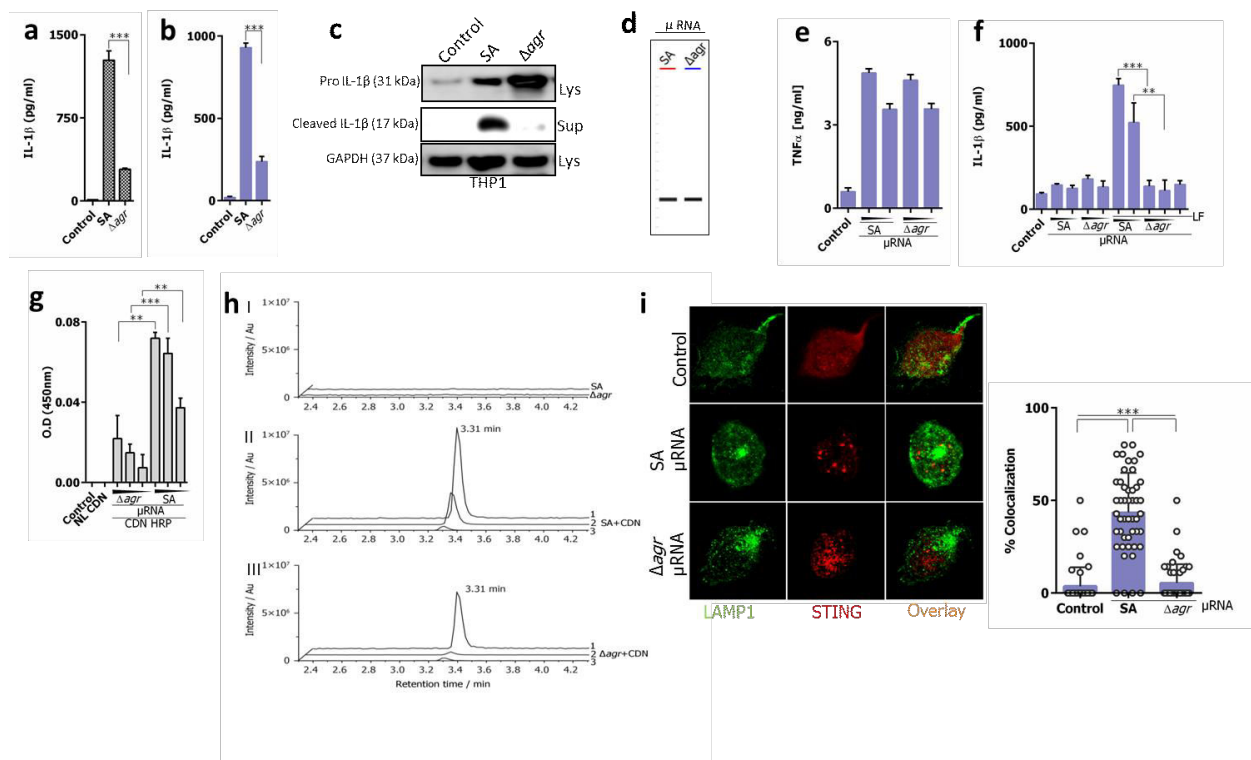


Figure 21: Accessory gene regulator system of *S. aureus* locus is engaged in RNA aptamer mediated inflammasome activation

(a,b) IL-1 β responses measured in THP1 (Purple) macrophages and human blood derived macrophages (pattern) when infected with SA and Δagr mutant bacteria. (c) Immunoblots showing processing of IL-1 β when infected with wild type SA and Δagr . (d) Capillary electrophoresis gel of μ RNA from *S. aureus* and Δagr mutant bacteria run on Qiaxcel advanced system. (e) TNF- α response measured in THP1 macrophages when stimulated with increasing concentration of *S. aureus* and Δagr mutant μ RNA (e) IL-1 β production measured in THP1 (Purple) macrophages when stimulated with μ RNA from *S. aureus* and Δagr mutant on the surface (SA and Δagr) and into the cytosol (SA+LF, Δagr +LF) and only LF. (g) Optical density at 450 nm measured in binding assay of bacterial μ RNA from *S. aureus* and Δagr mutant with HRP labelled CDN (c-di-AMP). Non-labelled CDN (NL c-di-AMP) was used as a control. (h) Mass spectra of c-di-AMP detected in I) μ RNA of *S. aureus* (SA), Δagr . II) Different concentration of SA μ RNA bound CDN fractions. III) Different concentration of Δagr μ RNA bound CDN fractions. (i) THP1 macrophages were transfected with μ RNA from SA, Δagr for 3 h. The cells were fixed and stained with anti-STING (Red) and anti-LAMP-1 (Green) specific antibodies. Percent co-localization was measured.

4.10 *S. aureus* RNAIII activates inflammasome pathway for the release of IL-1 β

Considering our sequencing analysis of μ RNA from wild type *S. aureus*, mutant Δagr and *S. aureus* MLBs we investigated small RNA which were only expressed in MLBs and are Δagr dependent. Interestingly, we found three small RNA named Rsa C, RNAIII and

WAN01CC66-rc which showed exclusive presence in MLBs (**Appendix Fig. 34b**). Visualizing the genomic reads of these small RNA showed utter dependencies on Δagr (**Fig. 22a**). (Data obtained through collaboration with Uniklinikum Keil, Germany and DNASTAR technical support). We hypothesized that the identified small RNA were the possible candidates to activate the inflammasome through μ RNA aptamers.

RNAIII is one of the regulatory RNA encoded by the AGR locus which controls several genes related to virulence and cell wall associated proteins^{230,231}. To further unravel the role of RNAIII in inflammasome activation we *in-vitro*-transcribed RNAIII and evaluated its role in inflammasome activation. Wild type THP1 macrophages were stimulated intracellular and extracellular with *in-vitro*-transcribed RNAIII. The IL-1 β responses demonstrate that cytoplasmic delivery of RNAIII activates the NLRP3 inflammsome (**Fig. 22b**). In contrast the surface stimulation and the lipofectamine lacked the capacity to release IL-1 β (**Fig. 22b**). As our previous results demonstrate a strong binding of bacterial μ RNA with CDN hence we assessed CDN binding capacity of RNAIII. Assay using horse raddish peroxidase and mass spectroscopic approaches demonstrated a strong binding of *in-vitro*-transcribed RNAIII and cyclic di-nucleotide (**Fig. 22c,d**). The above results laid a paradigm demonstrating the involvement of *S. aureus* regulatory RNAIII in inflammasome activation for the release of IL-1 β .

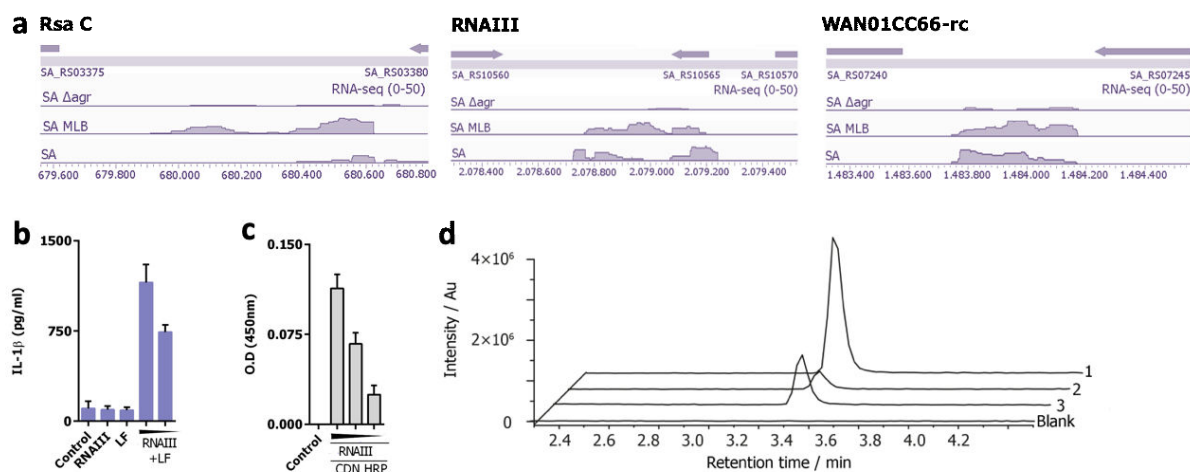


Figure 22: *S. aureus* RNAIII activates inflammasome pathway for the release of IL-1 β

(a) Visualization of read coverage of genomic locations of Rsa C, RNAIII, and WAN01CC66-rc identified by deep sequencing on wild type *S. aureus* (SA), *S. aureus* Δagr (SA- Δagr) and *S. aureus* MLBs (SA-MLB). The reads of each gene are shown in red color. (b) IL-1 β responses measured in THP1 (Purple) macrophages following stimulations with *in-vitro*-transcribed cytosolic RNAIII (RNAIII+LF), surface RNAIII and LF. (c) Optical density

at 450 nm measured in binding assay of *in-vitro*-transcribed RNAIII with CDN. **(d)** Mass spectra of c-di-AMP detected in different concentration of RNAIII bound CDN fractions.

4.11 A unique fragment of RNAIII with A, 7, 8, 9, A hairpins present in SA-MLBs activate the inflammasome pathway

We further investigated the structural importance of RNAIII for the activation of inflammasome. The obtained RNA seq reads of SA and SA-MLBs were mapped on *S. aureus* RNAIII genomic locus consisting of 514 bp (**Fig. 23a**). (Data obtained through collaboration with Uniklinikum Keil, Germany and DNASTAR technical support). We observed that the obtained sequenced reads overlapped with the RNAIII genomic locus. Scrutinizing it further, we found the exclusive presence of central domain A, 7, 8, 9, A corresponding to 202-317 nt in MLBs (**Fig. 23a**). Apart from the central domain, presence of 3' and 5' regions corresponding to 1-380 and 202-514 nt respectively of RNAIII were observed in SA-MLBs (**Fig. 23a**). To analyze the immunological relevance of the overlapping stretches 3' region (1-380 nt) and 5' region (202-514 nt) were *in-vitro*-transcribed. The 3' and 5' stretches of RNAIII when given cytosolically activated the inflammasome with release of IL-1 β (**Fig. 23b**). As the sequencing shows the exclusive presence of central domain A, 7, 8, 9, A (202-317 nt) in the MLBs we *in-vitro*-transcribed along with small RNA Hp as a control. Intracellular and extracellular stimulations on THP1 cells showed that the central domain activated the inflammasome with robust release of IL-1 β while Hp lacked the activation (**Fig. 23c**). To confirm the presence of central domain in MLBs, PCR amplification of 202-317 (A, 7, 8, 9, A) was carried out in SA, SA- Δ agr and SA-MLBs prepared cDNA. The following results validated the presence of central domain which was amplified only in SA-MLBs with slight presence in SA but absent in SA- Δ agr (**Fig. 23d**). Hp sRNA expressed in all three μ RNA was used as control, showed amplification in all cDNA (**Fig. 23d**).

We have shown that μ RNA from Gram-positive bacteria binds to CDN and is a crucial event in the activation of STING for the result of IL-1 β (**Fig. 15f, 17h,i,j**). Hence, we sought to analyze the binding capacity of the central domain to CDN. To confirm the CDN binding capacity of central domain A, 7, 8, 9, A we used spinach aptamer with conditionally fluorescent molecule difluoro-4-hydroxybenzylidene imidazolinone (DFHBI)²²¹. The fluorescence of spinach aptamer depends on the formation of a second stem loop. Hence, the second stem loop was replaced with the *in-vitro*-transcribed aptamer domain A,7,8,9,A of RNAIII. As anticipated, the A,7,8,9,A central domain linked to spinach aptamer exhibited strong fluorescence activation in a concentration-dependent manner from 0.1 to 10 nM c-di-AMP (**Fig. 23e**). Consistent with the previous results the intracellular transfection of *in-vitro*-

transcribed central domain confirmed the requirement of STING for the release of IL-1 β . These results confirm the involvement of RNAIII central domain in activating the inflammasome via STING through binding of CDN.

The central domain of RNAIII also contains the ribosomal binding site which is involved in the translation of the delta hemolysin¹⁷² and in the inflammasome activation (**Fig. 23b**). Hence, to characterize it further, we *in-vitro*-transcribed two stretches of RNAIII cutting the helix A. The 3' region from 1-213 nt and 5' region from 213-514 nt were *in-vitro*-transcribed and transfected to THP1 macrophages. Surprisingly, these regions failed to activate the inflammasome abrogating the release of IL-1 β when compared to the full length RNAIII (**Fig. 23g**). These results show that the helix A of RNAIII is crucial for the activation of inflammasome for the release of IL-1 β .

In order to evaluate the other identified small RNA for the inflammasome activation, we *in-vitro*-transcribed RsaC, WAN01CC66-rc, and RNAIII of non-aureus Staphylococcal species *S. carnosus* (TB300). All the sRNA lacked high sequence similarities but were predicted to have structural similarities. *In-vitro*-transcribed sRNA of Rsa C, WAN01CC66-rc, and TB300 when given cytosolically activated the inflammasome pathway with abundant release of IL-1 β (**Fig. 23h**). The above results conclude that the activation of inflammasome through sRNA is not sequence specific but structure specific.

Dimerization of STING is major event in response to the cytosolic DNA for IFN β induction³⁹. We monitored the dimerization of STING upon cytosolic stimulation of *in-vitro*-transcribed RNAIII, μ RNA from wild type *S. aureus* and Δagr in THP1 macrophages. The Immunoblots detected STING dimer in RNAIII and wild type μ RNA stimulations while the Δagr lacked the dimer formation (**Fig. 23i**). These results show the potential role of μ RNA for the activation of STING.

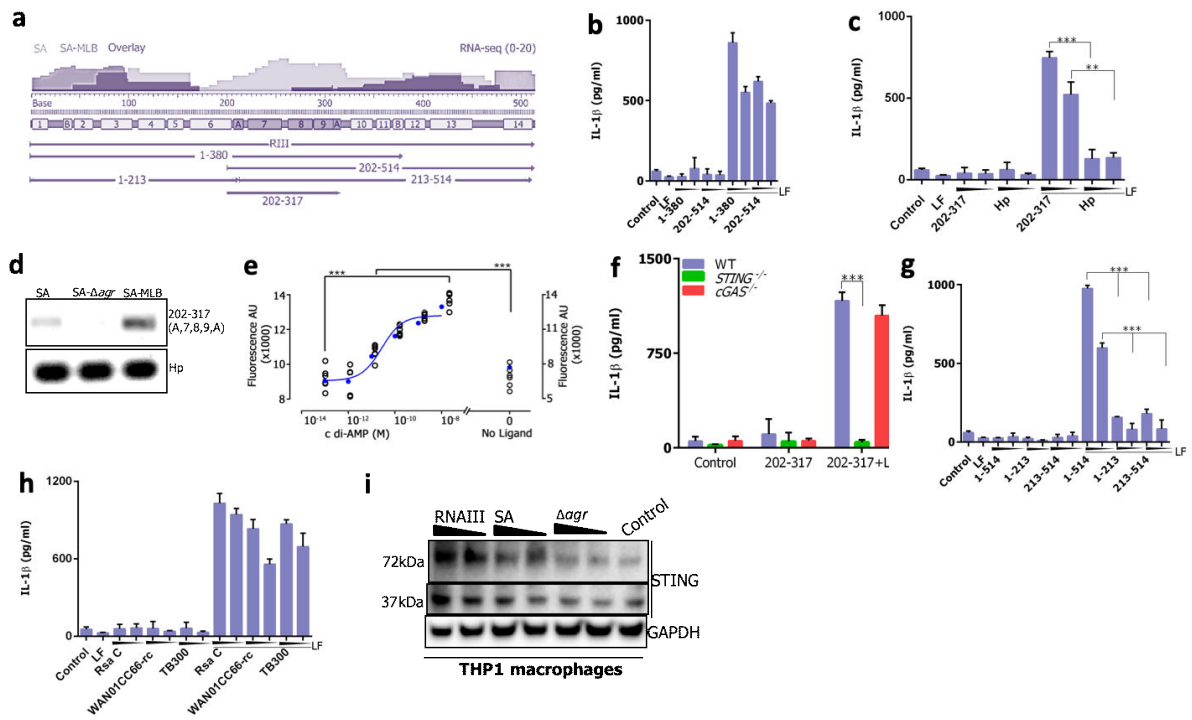


Figure 23: A unique fragment of RNAIII with A, 7, 8, 9, A hairpins present in SA-MLBs activate the inflammasome pathway

(a) Visualization of differentially abundant sequencing reads of SA (Light Purple) and SA-MLB (Medium Purple) and overlaid (Dark Purple) mapped on 514 base RNAIII cloned genomic locus of SA (LS1). (b) IL-1 β production measured in THP1 (Purple) macrophages following stimulations with *in-vitro*-transcribed RNAIII from 1-380 nt, 202-514 nt on surface and into the cytosol (1-380+LF, 202-514+LF) and LF. (c) IL-1 β production measured in THP1 (Purple) macrophages following stimulations with *in-vitro*-transcribed RNAIII from 202-317 nt on surface and into the cytosol (202-317+LF), HP RNA (HP+LF) and LF. (d) Semi quantitative PCR analysis of RNAIII central domain A,7,8,9,A (202-317 nt) in SA, SA- Δ agr and SA-MLB. HP RNA was used as a control. (e) Analysis of *in-vitro*-transcribed RNAIII central domain A,7,8,9,A spinach binding to c-di-AMP at 37 °C in presence of DFHBI (10 μ M) and different concentrations of c-di-AMP (0.1 pM-10 nM). Data from replicates (black) and mean (blue) are shown. Background fluorescence was subtracted from all data points. (f) THP1 (Purple), *STING* deficient (Green) and cGAS deficient (Red) macrophages were stimulated with *in-vitro*-transcribed RNAIII from 202-317 nt on surface and into the cytosol (202-317+LF), and IL-1 β production measured. (g) THP1 macrophages (black) were stimulated with *in-vitro*-transcribed RNAIII from 1-514 nt, 1-213 and 213-514 nt on surface and into cytosol (1-514+LF, 1-213+LF, 213-514+LF) and LF. IL-1 β production measured. (h) IL-1 β production measured in THP1 macrophages (Purple) following stimulations with *in-vitro*-transcribed Rsa C, WAN01CC66-rc, and *S. carnosus* (TB300) on surface and into cytosol (Rsa C +LF, WAN01CC66-rc +LF, TB300+LF) and LF. (i) Control THP1 macrophages incubated with μ RNA from (SA), Δ agr and *in-vitro*-transcribed RNAIII were used in STING dimerization assay followed by semi-native gel electrophoresis and resolution of STING monomer (37 kDa) and dimer (72 kDa) were observed. GAPDH was used as a loading control.

4.12 Staphyloxanthin type of lipids targets RNA PAMPs to mediate inflammasome activation

Establishing the crucial role cytoplasmic RNA as a potent activator of STING, the transfer of the RNA PAMP still remains undiscovered. In light of the fact that Raman spectroscopy, electron microscopy and mass spectroscopy identified the presence of staphyloxanthin type of lipids in MLBs, we investigated the role of lipid in inflammasome activation. To this end, we HPLC purified the staphyloxanthin (St2) and pathway precursor 4, 4'-diaponeurosporonic acid (St1) from *S. aureus* and subjected to Raman spectroscopy. Raman spectra identified carotenoid specific vibrations at 975, 1014, 1168, 1210, 1294, 1451, 1528 and 1581 cm^{-1} (**Appendix Fig. 32b,c**). These spectra were similar to SA, GBS and respective MLBs.

To further evaluate the role of St1 and St2 in inflammasome activation, empirical optimization of a sub-lethal dose of lipids was performed. THP1 macrophages and human blood derived macrophages were stimulated with intracellular and extracellular St1 and St2 with and without RNA respectively. IL-1 β responses revealed that the surface stimulation of lipids (St1, St2) and RNA did not activate the inflammasome while the combination of lipids with RNA (St1+RNA, St2+RNA) showed a robust activation of inflammasome (**Fig. 24a,b**). These results reveal the mechanism of MLBs to deliver RNA with the help of staphyloxanthin along with pathway precursor 4, 4'-diaponeurosporonic acid to the cytosol.

In order to further validate the role of staphyloxanthin biosynthetic pathway, recently discovered small molecular inhibitor, naftifine was used¹⁵¹. Here, GBS were grown in the presence of naftifine and plated on the Granada agar plate. It was observed that the naftifine inhibition had no effect of the growth of GBS but rendered GBS colonies colorless (**Fig. 24c**). To confirm the inhibition of the biosynthetic pathway, the SA and GBS inhibited bacteria were subjected to Raman analysis. Reduction in the Raman spectra at wavenumber 1528, 1168, 1013 cm^{-1} and 1528, 1129, 1012 cm^{-1} of SA and GBS respectively was observed (**Appendix Fig. 32d,e**).

Further the inflammasome activation was evaluated in human blood derived human macrophages. Here the naftifine inhibited SA and GBS bacteria were infected and IL-1 β and TNF α responses were measured. The inflammasome activation was reduced in naftifine treated bacteria with less amount of IL-1 β (**Fig. 24d,e**). In contrast the naftifine treated SA and GBS had no effect on TLR mediated TNF α response (**Fig. 24f,g**). To determine if the naftifine inhibition had any effect on the production of CDN binding aptamer, μ RNA was isolated from inhibited bacteria. THP1 wild type macrophages were simulated with SA and

GBS naftifine inhibited μ RNA. A pronounced IL-1 β secretion was observed in supernatants stimulated with inhibited μ RNA (Fig. 24h,i).

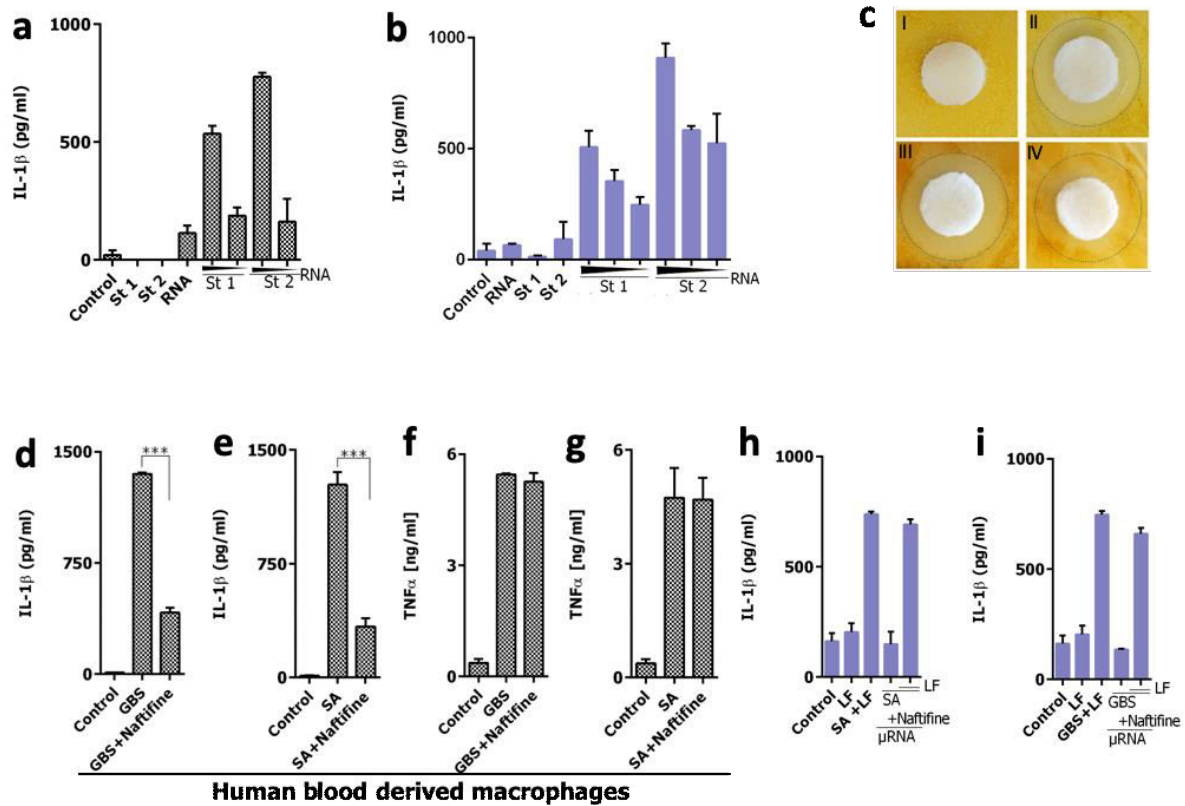


Figure 24: Staphyloxanthin type of lipids targets RNA PAMPs to mediate inflammasome activation

(a,b) IL-1 β production in human blood derived macrophages and THP1 (Purple) following stimulations with increasing concentrations of SA RNA, HPLC purified 4,4'-diaponeurosporenoic acid (St1), staphyloxanthin (St2), and 4,4'-diaponeurosporenoic acid (St1), staphyloxanthin (St2) micelles with RNA (St1+RNA, St2+RNA). (c) Inhibition of the staphyloxanthin biosynthetic pathway using the small molecular drug naftifine, I. Paper disc (white) with PBS as control showing no inhibition of biosynthetic pathway leading to golden yellow pigmentation over bacterial lawn (II,III,IV). Increasing concentrations of naftifine applied on paper disc (white) inhibiting the biosynthetic pathway leading to a zone of decolourization and opaque growth of GBS. (d,e) Human blood-derived macrophages were infected GBS and GBS treated with naftifine (GBS+Naftifine) and SA and SA treated with naftifine (SA+Naftifine). IL-1 β was measured in supernatant. (f,g) Human blood-derived macrophages showing TNF- α production when infected with GBS and GBS treated with naftifine (GBS+Naftifine) and SA and SA treated with naftifine (SA+Naftifine). (h,i) THP1 macrophages (Purple) were stimulated on surface and into cytosol with naftifine treated SA and GBS μ RNA (SA (Naftifine)+LF) (GBS (Naftifine)+LF) respectively. IL-1 β production was measured.

4.13 Gram-positive bacteria and its vesicles activates non-canonical pathway for the release of progranulin

After the establishment of the pathway required for Gram-positive bacteria to release IL-1 β , the signaling cascade required for the release of unconventional secretory protein progranulin and galectin-1 still remains undiscovered. Active IL-1 β and pyroptosis is triggered by sensing cytosolic LPS in THP1 macrophages (**Fig. 14a,b**). To verify if these endogenous molecules are secreted through intracellular sensing of LPS, we stimulated THP1 macrophages with surface as well as intracellular LPS. Similar to IL-1 β , galectin-1 and PGRN were robustly secreted in the extracellular space as a consequence of intracellular LPS detection (**Fig. 25a,b**). In contrast, surface stimulation of LPS and transfecting vehical lipofectamine lacked the release of galectin-1 and PGRN.

Further, to elucidate the pathway for the release of progranulin upon activation with Gram-positive bacteria, wild type THP1 along with *CASP1*, *ASC*, *CASP4*, *CASP5* deficient macrophages were used. Surprisingly, progranulin release in GBS infected supernatants showed independent response to canonical inflammasome pathway (**Fig. 25c**). In contrast to the canonical inflammasome, progranulin release was caspase-4 independent but caspase-5 dependent upon Gram-positive infections (**Fig. 25c**). Immunoblots also detected released progranulin when infected with GBS in wild type THP1 macrophages at 70 kDa. In contrast to the wild type THP1 macrophages, *CASP5* deficient cells completely blocked the release of progranulin (**Fig. 25d**). This laid the paradigm of the involvement of non-canonical inflammasome pathway for the release of progranulin in Gram-positive bacteria. To further validate these results we infected wild type THP1 macrophages along with *CASP1*, *ASC*, *CASP4* and *CASP5* deficient cells with wild type *S. aureus* and Δagr mutant. The PGRN release in the supernatants infected with wild type *S. aureus* showed canonical inflammasome independent response but were dependent on caspase-5 (**Fig. 25e**). In contrast to the IL-1 β response, Δagr mutant showed pronounced release of PGRN dependent on caspase-5 (**Fig. 25f**). Hence, these results conclude the involvement of non-canonical inflammasome pathway for the release of PGRN.

Cleavage of GSDMD is an important event for the activation of non-canonical inflammasome activated through LPS⁸². To evaluate the requirement of caspase-5 for the release of PGRN, autolytic self-cleavage of inflammatory caspase-5 and GSDMD was determined. Immunoblotting for caspase-5 and GSDMD from supernatants of infected GBS and SA were performed. Probing for cleaved caspase-5 in wild type THP1 macrophages revealed the

activation of caspase-5 upon GBS and SA (**Fig. 25g**). The unstimulated supernatants were used as control which did not detect the cleaved caspase-5 upon GBS and SA infections (**Fig. 25g**). Similarly, the downstream target for inflammasome activation, GSDMD showed detectable cleavage upon GBS and SA infections (**Fig. 25g**)

To validate the role of caspase-1 independent response for PGRN release upon GBS and SA infections, *CASP1* deficient macrophages were used. Immunoblots detected the presence of cleaved caspase-5 and GSDMD similar to wild type THP1 macrophages (**Fig. 25g**). Taken together the above results demonstrated the requirement of caspae-5 and GSDMD upon GBS and SA infections.

According to the previous results of *S. aureus* secreted MVs for the release of PGRN we further elucidated the pathway THP1 macrophages along with *CASP1*, *CASP4* and *CASP5* deficient cells were stimulated with *S. aureus* MLBs and MVs. Consistent to the previous results, PGRN responses triggered by MLBs and MVs were independent on caspase-1 and caspase-4 but dependent on caspase-5 (**Fig. 25h,i**). These results were similar to live bacterial infections for the release of PGRN through non-canonical inflammasome pathway.

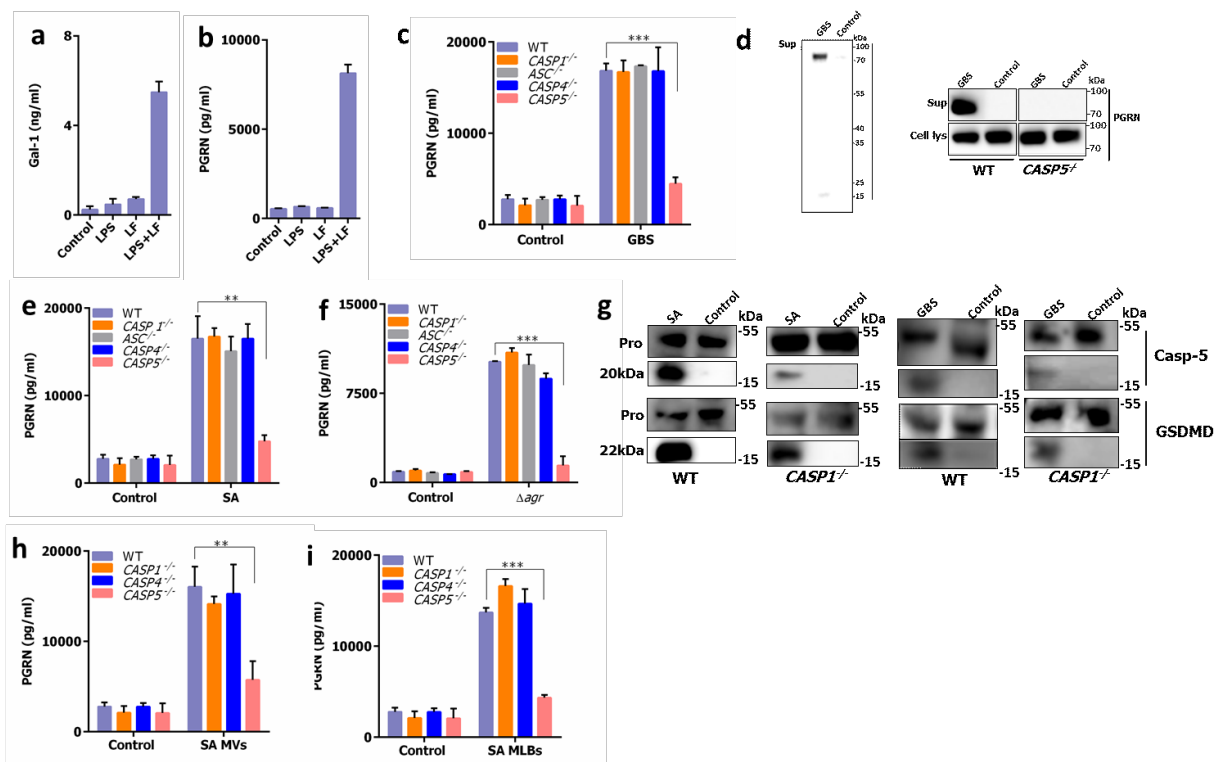


Figure 25: Gram-positive bacteria and its vesicles activates non-canonical pathway for the release of progranulin

(a,b) Galectin-1 and PGRN released measured in THP1 (Purple) macrophages upon stimulation of surface LPS, LF and intracellular LPS (LPS+LF). (c) Wild type THP1 (Purple),

CASP1 (Orange) deficient, *ASC* (Grey) deficient, *CASP4* (Blue) deficient, *CASP5* (Pink) deficient macrophages were infected with GBS, PGRN release was measured. (d) Immunoblot showing PGRN release in supernatant and cell lysate when infected with GBS in THP1 and *CASP5* deficient macrophages. (e,f) Wild type THP1 (Purple), *CASP1* (Orange) deficient, *ASC* (Grey) deficient *CASP4* (Blue) deficient, *CASP5* (Pink) deficient macrophages were infected with wild type *S. aureus* and Δagr respectively, PGRN release was measured. (g) Immunoblots showing Pro caspase-5 (48 kDa), cleaved caspase-5 (20 kDa), Pro GSDMD (55 kDa) and cleaved GSDMD (22 kDa) in THP1 and *CASP1* deficient macrophages when infected with GBS and SA respectively. (h,i) Wild type THP1 (Purple), *CASP1* (Orange) deficient, *CASP4* (Blue) deficient, *CASP5* (Pink) deficient macrophages when stimulated with *S. aureus* MVs and MLBs respectively, PGRN release was measured.

4.14 Gram-positive bacterial lipoproteins mediate progranulin release via caspase-5 yet bypassing TLR2

S. aureus lipoproteins have a defined role in activation of immune system through TLR2 signaling^{232,233}. To investigate the role of lipoproteins for the release of PGRN, diacylated lipoprotein FSL-1 and triacylated lipoprotein Pam3Cys (P3C) were used. To this end wild type THP1 macrophages were stimulated with intracellular and extracellular P3C and FSL. The immunoblots for PGRN release from supernatants revealed that surface stimulations of FSL and P3C did not release PGRN (Fig. 26a). In contrast the cytosolic delivery of FSL and P3C resulted in pronounced release of PGRN as compared to the unstimulated control (Fig. 26a). The PGRN in the cell lysates remained intact and was detectable.

To further evaluate the pathway activated by FSL and P3C for the release of PGRN, *CASP1*, *CASP4* and *CASP5* deficient macrophages were stimulated. Probing for PGRN revealed that the intracellular delivery of P3C was independent of caspase-4 and caspase-1 while dependent for caspase-5 for the release of PGRN (Fig. 26a). In contrast, supernatants from lipofectamine stimulation along with unstimulated control did not detect PGRN release. Resembling the Gram-positive bacterial infections, these results report that the lipoprotein activates caspase-5 for the release of PGRN. The above results show that the release of PGRN is independent of TLR2. In order to validate further, *CNPY3* deficient cells were used. *CNPY3* is a chaperon responsible for the surface translocation of plasma membrane TLRs. Consistent with the literature, FACS of *CNPY3* deficient cells reveals the absence of TLR2 while *CASP1* deficient and *CASP5* deficient cells used as control showed the presence of TLR2 (Fig. 26b). These macrophages were further stimulated with surface P3C and FSL. This approach was used to test the functionality of TLR2 in *CNPY3* deficient cells. To this end *CNPY3* macrophages failed to release TNF α while the caspase-1 and caspase-5 showed robust release of TNF α (Fig. 26c). Validating the results further, *CNPY3* deficient cells showed PGRN released in supernatants stimulated with intracellular P3C and FSL along with SA and GBS

infections (**Fig. 26d**). The cell lysate of CNPY3 deficient cells showed intact progranulin (**Fig. 26d**). The above results, confirmed that the release of progranulin independent of TLR2.

In *S. aureus* lipoprotein diacylglyceryltransferase (*lgt*) gene is responsible for the maturation of lipoproteins to activate TLR2²³⁴. In order to validate the independent role of TLR2 in progranulin secretion, we created Δlgt mutant. The CRISPR mediated point mutant of *lgt* was created using CRISPR RNA-guided cytidine deaminase (pnCasSA-BEC), enabling highly efficient gene inactivation and point mutations in *S. aureus*. The point mutation of *lgt* was created in RN4220 strain of *S. aureus* through electroporation following gated cloning. The screened Δlgt mutant created through CRISPR revealed mutation in the *lgt* gene of RN4220 at stop codon at Q75X amino acid of the N terminus. The sequenced clone of *lgt* mutant along with wild type RN4220 strain of *S. aureus* was used in further experiments. Consistent to the literature the Δlgt mutant of *S. aureus* failed to release IL-8 due to the lack of TLR2-binding lipoproteins (data not shown). To further validate the role of TLR2 in PGRN release, wild type RN4220 strain and Δlgt mutant were infected in wild type THP1 macrophages. We found that the PGRN release was completely abrogated in Δlgt mutant while the wild type RN4220 and SA showed a pronounced response (**Fig. 26e**). In contrast to PGRN release, Δlgt mutant has no effect on IL-1 β responses similar to wild type RN4220 and SA (**Fig. 26f**). Furthermore, immunoblots revealed that Δlgt mutant failed to release PGRN while had a robust activation of caspase-1 (**Fig. 26e,f**). The above results concluded human macrophages release progranulin through bacterial lipoproteins independent of TLR2.

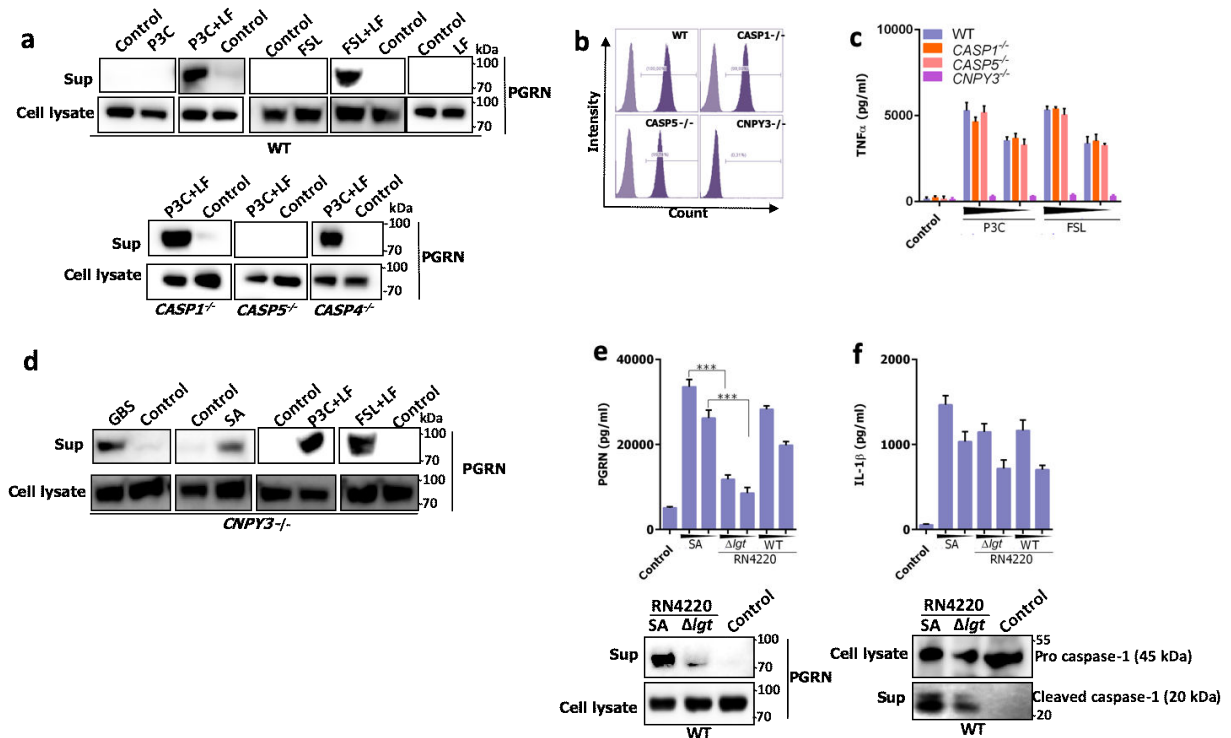


Figure 26: Gram-positive bacterial lipoproteins mediated progranulin via caspase-5 yet bypassing TLR2

(a) Immunoblots showing release of progranulin in supernatants and cell lysate following intracellular and extracellular stimulations of P3C and FSL with control lipofectamine (LF) in THP1, *CASP1* deficient, *CASP4* deficient, *CASP5* deficient macrophages. (b) FACS analysis for TLR2 in THP1, *CNPY3* deficient, *CASP1* deficient and *CASP5* deficient cells. (c) TNF α production measured in THP1, *CASP5* deficient, *CASP1* deficient and *CNPY3* deficient macrophages when stimulated with increasing concentrations of surface P3C and FSL. (d) Immunoblots showing release of progranulin in *CNPY3* deficient cells stimulated with intracellular P3C, FSL and infected with GBS and SA. (e) Progranulin release measured in THP1 macrophages following infection with wild type (RN4220) and Δlgt mutant *S. aureus*. (f) IL-1 β release measured in THP1 macrophages following infection with wild type (RN4220) and Δlgt mutant *S. aureus*.

4.15 Membrane vesicles enriched with lipoproteins show protective effect in *Galleria mellonella* via progranulin

We have observed that MVs shed from *S. aureus* has no effect of IL-1 β release but show robust secretion of progranulin (Fig. 18a,b). From these results we postulated that *S. aureus* MVs behaves as a commensal to the host immune system. To validate the following hypothesis, an infection model of GBS in *Galleria mellonella* larvae was established. Infection of GBS in *G. mellonella* demonstrated different degrees of melanization at various doses and time intervals eventually leading to death (Fig. 27a,b). Further, *G. mellonella* were infected with WT and $\Delta cyle$ mutant of GBS and observed its survival over 40 h. It was observed that WT GBS infected *G. mellonella* larvae die rapidly within 30 h while larvae

infected with $\Delta cylE$ mutant GBS survived without major signs of infection (**Fig. 27c**). To further verify the role of MVs, *G. mellonella* were primed with a sub-lethal dose of MVs isolated from $\Delta cylE$ for three days prior to GBS infection and observed for survival over 40 h. We observed pronounced protection from infection in primed *G. mellonella* larvae as compared to un-primed infected larvae (**Fig. 27d**).

To further consolidate these results, *G. mellonella* were infected with naftifine treated GBS. This rendered GBS into non-lethal bacteria in *G. mellonella* model (**Fig. 27e**). Consistent with this, vesicles isolated from WT GBS that contain granadaene were lethal in *G. mellonella* model whereas vesicles isolated from naftifine treated GBS were unable to cause melanization and death of larvae (**Fig. 27f**). We further postulated that MVs isolated after treatment with naftifine may protect larvae from infection. Hence, in a priming experiment, we primed *G. mellonella* with MVs isolated from naftifine treated GBS for three days followed by infection with GBS. Unprimed larvae rapidly succumbed to infection within 30-40 h, compared to primed larvae which showed significant survival till end of the experiment (**Fig. 27g**).

Encouraged with these results we primed *G. mellonella* larvae with P3C followed by infection with GBS. Similar to our results in MV priming experiments, unprimed larvae rapidly succumb to infection within 30-40 h, whereas P3C primed larvae show significant survival after GBS infection till end of the experiment (**Fig. 27h**). To validate the protective effect by progranulin, we primed *G. mellonella* larvae with recombinant human PGRN followed with GBS infection. Consistent with the previous results PGRN priming resulted in complete protection of the larvae (**Fig. 27i**). Hence, these results support the possibility that lipoprotein induced granulin release may bestow a protective effect during bacterial infection.

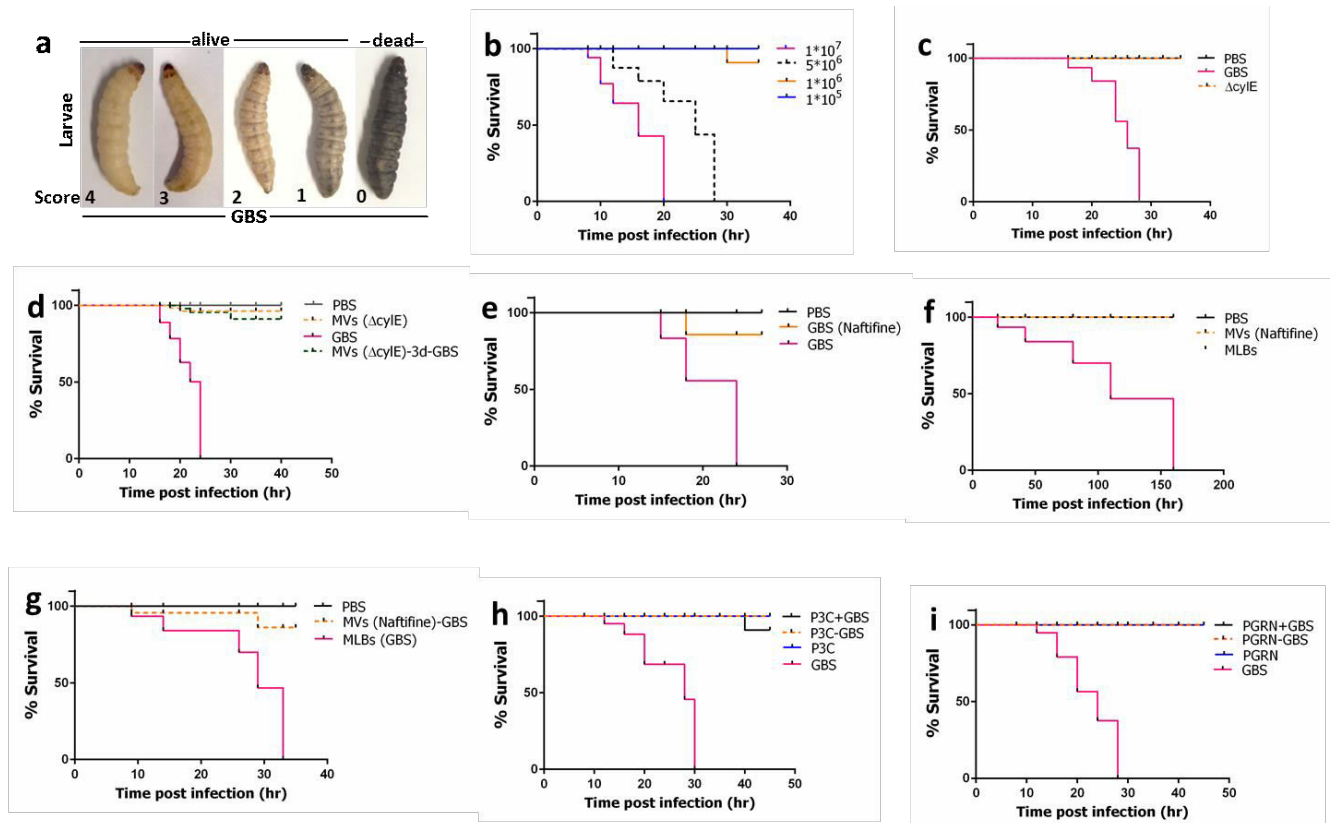


Figure 27: Membrane vesicles enriched with lipoproteins show protective effect in *Galleria mellonella* via progranulin

(a) *G. mellonella* infection model showing different stages of melanization correlating with disease scores. (b) Kaplan-Meier survival curves of *G. mellonella* infected with different dose of GBS. (c) Kaplan-Meier survival curves showing *G. mellonella* infected with GBS, $\Delta cyle$ mutant (5×10^6 CFU). (d) *G. mellonella* primed with MVs isolated from $\Delta cyle$ GBS and infected with GBS (5×10^6 CFU) after 3 days, GBS, MVs and PBS were used as control, showing Kaplan Meier survival curve (e) Kaplan-Meier survival curves of *G. mellonella* infected with GBS, and GBS grown in presence of naftifine (5×10^6 CFU). (f) Kaplan-Meier survival curves of *G. mellonella* infected with 300 mg/kg GBS MLBs and MVs isolated from naftifine treated GBS. (g) Kaplan-Meier survival curves of *G. mellonella* primed with MLBs isolated from GBS or MVs isolated from naftifine treated GBS followed by infection with GBS (5×10^6 CFU) after 3 days, only GBS, MVs and PBS were used as control (h) Kaplan-Meier survival curves of *G. mellonella* primed with 50 ng of Pam3Csk (P3C) and then infected with GBS (5×10^6 CFU) after 3 days. PBS, Pam3Cys and GBS were used as a control. (i) Kaplan-Meier survival curves of *G. mellonella* primed with 50 ng of recombinant PGRN and then infected with GBS (5×10^6 CFU) after 3 days. PBS, recombinant PGRN and GBS were used as a control.

4.16 Inflammasome activation associated with organ damage during sepsis

In light of the established pathways for inflammasome activation we turned our attention for its relevance in the sepsis patients. To investigate the conserved role of RNAIII in *S. aureus* mediated sepsis, we collected fifty *S. aureus* patient isolates with infection focus of urosepsis, intravascular catheter, wound infection, cellulitis (Fig. 28a). According to the sepsis-3

definition, 10 % of the total blood culture positive patients had sepsis. We observed that 84% of the patient isolates had detectable RNAIII (**Fig. 28a**).

To further consolidate the results, we isolated μ RNA from three RNAIII positive (P5, P11, P27) and negative (P14, P15, P36) *S. aureus* isolates. THP1 macrophages were transfected intracellular and extracellular with the isolated patient μ RNA. RNAIII positive μ RNA (P5, P11, P27) activated the inflammasome with abundant release of IL-1 β while the RNAIII negative (P14, P15, P36) μ RNA lacked the activation (**Fig. 28b**). These results correlated to the fact that inflammasome activation in Gram-positive sepsis is mediated through μ RNA.

Further, activation of inflammasome was screened in an independent cohort through the autolytic cleavage of GSDMD. The plasma from four *S. aureus* sepsis patients were subjected to western blot analysis along with control plasma collected from non-septic patients undergoing cardiac surgery pre-operatively (T1) and post operatively (T6). Probing for GSDMD revealed the cleaved GSDMD band at 22 kDa in sepsis patients which was undetectable in the controls (**Fig. 28c**). In order to further validate the role of μ RNA in sepsis, μ RNA from control and sepsis patients were isolated and stimulated to THP1 macrophages. μ RNA from the sepsis patients activated the inflammasome pathway with release of IL-1 β while the control μ RNA failed to activate the inflammasome (**Fig. 28d**).

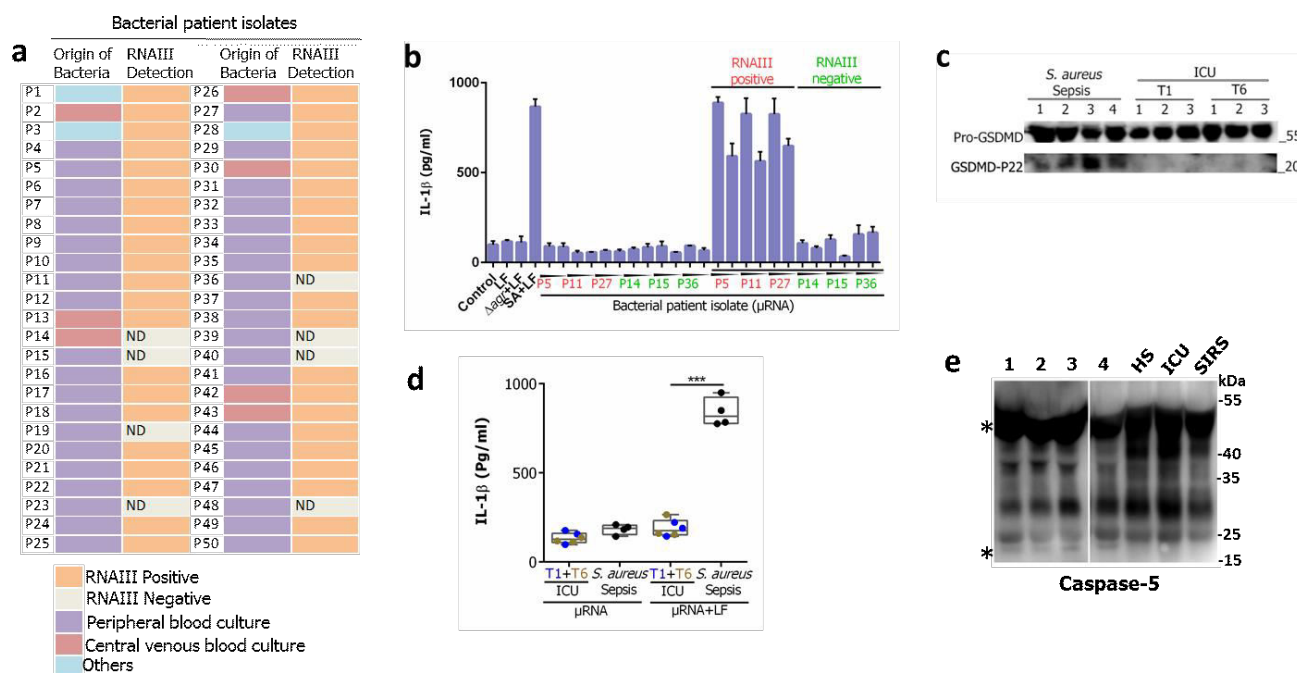


Figure 28: Inflammasome activation associated with organ damage during sepsis

(a) Diagrammatic representation of characteristics of *S. aureus* patient isolates (n=50) showing the presence of RNAIII (Orange), absence of RNAIII (Beige) and origin of bacteria. (b) THP1 macrophages (Purple) were stimulated with bacterial μ RNA of patient isolates P5,

P11, P27, P14, P15, P36 on the surface and cytosolically (P5+LF, P11+LF, P27+LF, P14+LF, P15+LF, P36+LF). IL-1 β production was measured. (c) Immunoblots showing active GSDMD (22 kDa) in plasma of *S. aureus* sepsis patients (1-4), ICU patients T1 (1-3), T6 (1-3). (d) THP1 macrophages were stimulated on the surface and cytosolically with μ RNA isolated from human plasma of *S. aureus* sepsis patients (n=4) and ICU controls pre operation and post operation (n=3). IL-1 β production was measured. (e) Immunoblots showing active caspase-5 (20 kDa) in plasma of Gram-positive sepsis patients (1-4), healthy donors (HS), ICU and SIRS patients.

Consistent with the PGRN release upon Gram-positive bacterial infection in THP1 macrophages, the plasma of Gram-positive sepsis patients showed hallmarks of cytosolic inflammation activation. When blotted against caspase-5, plasma of sepsis patients were detected with cleaved caspase-5 while the control lacked the activation of caspase-5 (**Fig. 28e**). Further, we verified the relevance of unconventional protein secretion such as galectin-1 and progranulin as a result of inflammasome activation in sepsis patients. High levels of galectin-1 was secreted in septic patients in comparison with the ICU patients (T1 and T6) and healthy volunteers (**Fig. 28f**). The septic patients accumulated galectin-1 around 50-80 ng/ml while the healthy volunteers showed around 20 ng/ml. Similarly, strong accumulation of PGRN in sepsis patients was seen with approximately 300 ng/ml while the healthy volunteers showed 2-50 ng/ml of PGRN secretion (**Fig. 28g**). High correlation with the levels of PGRN and sequential organ failure score of sepsis (SOFA) was observed (**Fig. 28h**). Further the level of PGRN also co-related to the liver and kidney failure markers such as creatinine, bilirubin, HST and CRP (**Fig. 28i,j,k,l**). We observed that PGRN levels showed strong correlation with HST and creatinine (**Fig. 28k,l**) while CRP and bilirubin showed no correlation (**Fig. 28i,j**). Collectively, these results underline the presence of cytosolic inflammasome markers in sepsis patients.

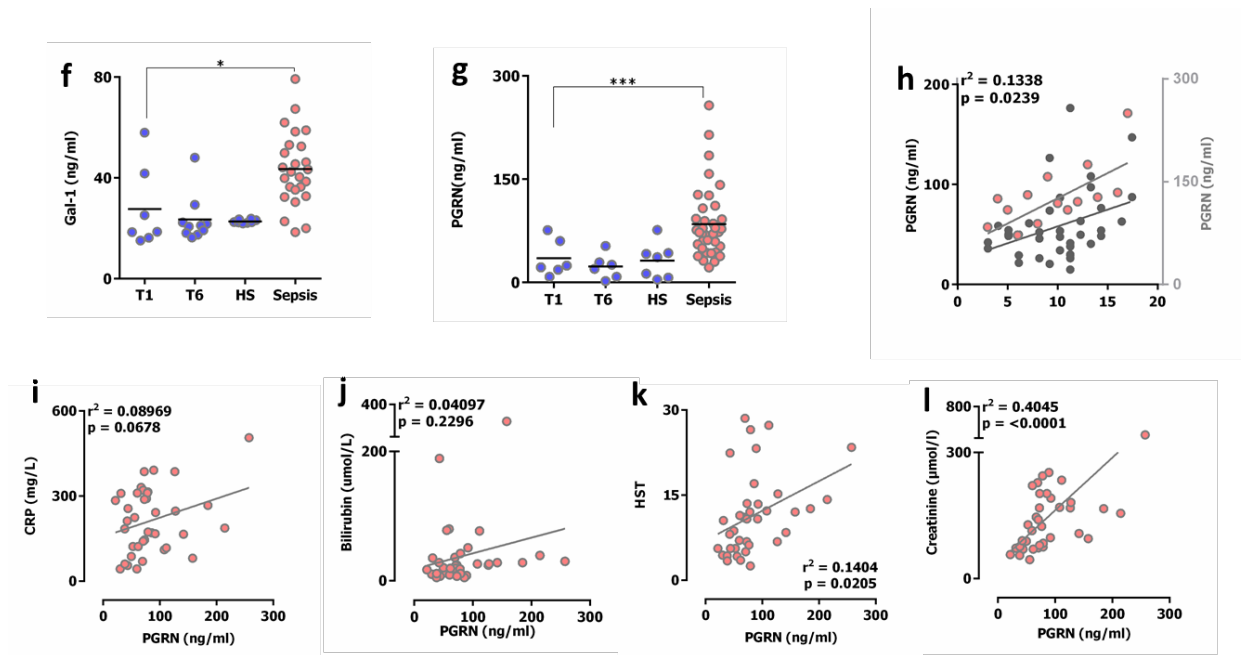


Figure 28: Inflammation activation associated with organ damage during sepsis

(f) Galectin-1 release measured in ICU patient's pre (T1) and post (T6) surgery, healthy volunteers and sepsis patients. (g) PGRN measured in sepsis patients and ICU patient's pre (T1) and post (T6) surgery and healthy donors (HS). (h) PGRN in sepsis patient correlated with the mean SOFA scores (black line) and PGRN in sepsis patients correlating with the respective SOFA scores (grey line). (i-l) PGRN in sepsis patient correlated with, HST, Creatinine, Bilirubin and CRP respectively. Significant results from Mann-Whitney non-parametric tests are indicated: * $P < 0.05$; ** $P < 0.01$; *** $P < 0.001$.

5. DISCUSSION

Over the years, significant progress is made in understanding the host-pathogen interaction of the Gram-positive bacteria. Infection with GBS and SA promotes the release of cytokines, chemokines, and alarmins that lead to deregulated host response with organ failure causing sepsis²³⁵.

Various studies have demonstrated the importance of inflammasome as an emerging strategy for the clearance of the bacteria. Activation of cytosolic caspases following gasdermin D cleavage is responsible for the release of cytokines and alarmins in the extracellular milieu. In this study, we addressed the cargo of microbial RNA and lipoproteins through extracellular vesicles secreted by Gram-positive bacteria following the inflammasome activation for the release of cytokines and alarmins.

The main aims of the current study were

- To isolate and characterize the extracellular vesicles shed by Gram-positive bacteria.
- To elucidate the inflammasome pathway activated by Gram-positive bacteria and its vesicles for the release of cytokines and alarmins.
- To investigate the relevance of inflammasome activation in Gram-positive sepsis.

5.1 Gram-positive bacteria secrete multilamellar lipid bodies and membrane vesicles

Microbial extracellular vesicles are described as the particles naturally released by the bacteria with lipid bilayer membranes²³⁶. The characteristics and diverse functions of the outer membrane vesicles shed by Gram-negative bacteria are well established. Several studies demonstrated that Gram-positive bacteria such as *Mycobacterium ulcerans*, *Bacillus anthracis*, GBS and *S. aureus* release membrane vesicles. This ruled out the possibility of Gram-positive bacteria to produce extracellular vesicles due to the presence of thick peptidoglycan layer in the cell wall structure^{184,15,188,189,213}. These studies highlight the production of membrane vesicles from Gram-positive bacteria as an evolutionarily conserved secretory mechanism. In the current study, we present a comprehensive analysis of the structure of Gram-positive bacteria released vesicles and their role in bacterial pathogenesis.

For the ultrastructural characterization of the vesicles shed by GBS and SA, we employed various microscopic techniques. Scanning electron microscopy revealed the blebbing of vesicular structures from the surface of GBS and SA (**Fig. 13a**). Meticulous isolation of these structures through density gradient ultracentrifugation revealed varying sizes of vesicles,

which showed known membrane vesicles (MVs) and newly discovered multilamellar lipid bodies (MLBs). As demonstrated earlier, the isolated membrane vesicles from SA and GBS shared common structural features with those of Gram-negative bacteria^{184,236}. MVs depicted spherical structure with a bi-layer of size around 50-100 nm and floating density of 1.16-1.20 g/ml. On the other hand, our analysis of electron microscopy and dynamic light scattering evaluations of MLBs revealed sizes of around 100-400 nm with a structure representing concentric lipid layers (**Fig. 13d,e**). Such heterogeneity was previously observed for SA under different growth conditions²³⁷. Moreover, Raman spectroscopy analysis in the current study revealed the presence of nucleic acids, proteins, lipids and carbohydrates in SA MLBs. Fingerprint Raman spectra at wave numbers 1009, 1163 and 1528 cm^{-1} indicated conserved polyunsaturated lipids in both SA and SA MLBs. These results suggest that the Gram-positive bacteria secrete varied types of vesicles into the extracellular milieu.

To further characterize the lipid cargo and examine potential enrichment of lipids in vesicles secreted by *S. aureus*, we undertook the mass spectroscopic approach. LC/MS analysis detected the presence of 4', 4'-diaponeurosporenoic acid, a precursor of the staphyloxanthin biosynthetic pathway in MLBs shed by *S. aureus*. Surprisingly, 4',4'-diaponeurosporenoic acid was absent in the MVs thus, suggesting differences in the advancement of lipids in the respective vesicles (**Appendix Fig. 33a**). These results were consistent with the findings where differences in the size and density of the isolated vesicles correlated with differences in the lipid: protein ratio and vesicle composition²³⁹. Enrichment of 4', 4'-diaponeurosporenoic acid particularly in the MLBs could be due to the selective sorting of lipids. Such type of sorting mechanism was previously observed in *P. gingivalis* that allowed specific packaging of virulence proteins and excluded outer membrane proteins from the cargo²³⁹. Similar to the lipid distribution, silver staining revealed differential protein content in MVs and MLBs (**Fig. 13f**). These results were analogous to the previous varied protein profiles in different isolates of *S. aureus*^{184,240}. It will be interesting to further investigate the differential sorting mechanism of proteins and lipids in MLBs and MVs of *S. aureus*. These results also suggest that bacterial effectors packed in the MVs and MLBs can be directly associated with the bacterial pathogenesis.

Apart from examining the structure and composition of the SA vesicles, the study also explored the biological function of the vesicles and their interaction with host cells. The focus was on the role of MLBs and MVs in the release of cytokines and alarmins. Interestingly, the present study found that MLBs have the capacity to activate the inflammasome for the release

of IL-1 β and progranulin (PGRN) (**Fig. 18a,b**). This was in contrast to the MVs that triggered the release of PGRN only (**Fig. 18a,b**). The inability of the MVs to activate the inflammasome for IL-1 β release supports the absence of staphyloxanthin type of lipids. This result confirms that one of the virulence factors, namely staphyloxanthin and its precursor that are packed in the MLBs are responsible for inflammasome activation and release of cytokines. Further studies on identifying similar virulence factors involved in host cell damage can provide insights into the MLBs-mediated pathogenesis.

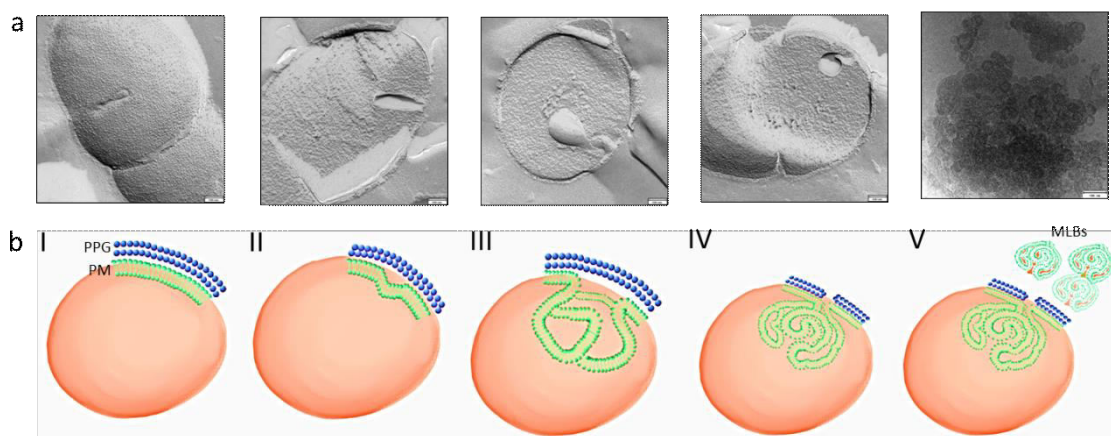


Figure 29: (a) Freeze fracture electron microscopy showing biogenesis of MLBs. (b) Graphical abstract depicting the hypothetical model of the formation of MLBs. (I) *S. aureus* showing plasma membrane (PM) and peptidoglycan (PPG) layer. (II) The origination of infolding of plasma membrane in the cytoplasmic space. (III) Formation of sac like structure due to the penetration of the plasma membrane. (IV) Concentric accumulation of folded plasma membrane. (V) Release of multi lamellar lipid bodies (MLBs) in the extracellular milieu.

The highlight of the current study is the discovery of unique vesicles shed by GBS and SA named multilamellar lipid bodies (MLBs). Hence, we sought to understand the biogenesis of these vesicles through freeze-fracture electron microscopy and establishing a hypothetical model. Apart from the presence of the thick peptidoglycan layer, the presence of staphyloxanthin type of lipids can initiate the destabilization of the underlying plasma membrane for the formation of these vesicles. The origination of MLBs initiates with the infolding of the plasma membrane in the extracytoplasmic space of SA (**Fig. 29b(II)**). We further observed the expansion and accumulation of the folded plasma membrane. Progressing the penetration of the folded plasma membrane forms a sac-like structure consisting of a concentric accumulation of lipids (**Fig. 29b(IV)**). This observation hinted the build-up of hydrophobic vesicles inside the formed a sac-like structure. It further tempts to hypothesize the entrapment of PAMPs in the MLBs which activate the inflammasome pathway. Following the sac formation the entrapped vesicles are released in the extracellular milieu (**Fig. 29b(V)**). According to the previous literature at this stage, various cell wall modifying enzymes like the peptidoglycan degrading enzymes can act on the release of these

vesicles. These enzymes may loosen the wall increasing the pore size and facilitate the release^{184,241}. Moreover, it was also shown that endolysin triggered the release of membrane vesicles in *S. aureus*. Further studies are needed to enhance the mechanistic explanation of the biogenesis of Gram-positive bacteria secreted vesicles to reveal the activation of the inflammasome pathway.

5.2 Bacterial small RNAs are enclosed in *S. aureus* shed MLBs

Since the characterization of MLBs indicated the presence of nucleic acids, the question of which nucleic acids packed in the MLBs are involved in regulating the host-pathogen interaction remained open. Indeed, bacterial small regulatory RNAs (sRNAs) between 50-200 nucleotides in length modulate gene expression by regulating transcription, translation, or by destabilizing mRNAs^{242,243}. These sRNAs are recognized as key players in bacterial metabolism and regulate virulence gene expression in host-pathogen interactions. Prior studies have noted the importance of sRNAs in the outer membrane vesicles of *P. aeruginosa* which can modulate the host immune responses^{244,245}. The subsequent discovery of small bacterial RNA prompted us to address the role of sRNAs enriched in MLBs during host-pathogen interaction.

To approach this, our approach of RNA sequence analysis revealed the presence of numerous small RNAs in SA-MLBs (**Fig. 16a**). Moreover, a high degree of intragenic sRNA species was observed in the MLBs, unlike the SA bacteria (**Fig. 16b**). In the current thesis, we observed approximately 160 previously studied small regulatory RNA genes through high throughput RNA sequencing. These genes enclosed in the MLBs were identified mainly from the WAN, Rsa, Teg, and sbr families of small RNA (**Appendix Fig. 34a**)²⁴⁶. The highlight of the thesis is the identification of RNAlII in SA-MLBs which is known to regulate various expressions of genes encoding virulence factors¹⁷¹. Detailed analysis of this small RNA revealed that Rsa C, WAN01CC66-rc and RNAlII genes showed AGR locus dependencies but were completely independent of SA and SA MLBs (**Appendix Fig. 34a,b**). Previous studies have identified that Rsa C carries a small ORF (open reading frame) similar to RNAlII suggesting their role in the pathogenicity of *S. aureus*.

Nonetheless, consistent with the previous literature, Rsa E which is regulated by a quorum sensing system showed a decreased level of expression in Δagr mutant μ RNA. In contrast to Rsa E, we found σ^B dependent gene Rsa A only expressed in SA- Δagr mutant. Analysis of the small RNA lacked the expression of Sau gene in SA-MLBs, while out of five σ^B regulated *sbr*

genes only *sbr* B, C and D were identified. SA and SA-MLBs showed precise expression of *sbr* C but SA-MLBs lacked *sbr* B expression. The lack of Teg 1 and Teg 76 expression in all the analysed μ RNA ruled out the involvement of riboswitches in the SA-MLBs. Altogether, the study highlights the dependency of Rsa C, WAN01CC66-rc and RNAIII on AGR locus suggesting the involvement of AGR in oxidative stress response. These results are consistent with the literature showing that *S. aureus* sRNA participates in the regulation of gene cascades²³⁰. Our sequencing analysis also suggests that the bacteria are prone to have feasible mechanisms for the sorting and packaging of the sRNAs in MLBs. The current study provides the first hint of sRNA presence in SA MLBs and the involvement in various gene regulations.

5.3 Bacterial μ RNA is a potent activator of the canonical inflammasome via STING

Following the identification of small RNA in SA-MLBs, we further highlight the role of these sRNA in inflammasome activation. The innate immune system activates the inflammasome upon cytosolic detection of microbial nucleic acids for the induction of type I interferon and pro-inflammatory cytokines. Previously, the role of bacterial RNA in inflammasome activation was studied mostly in murine bone marrow-derived dendritic cells (BMDCs) or bone marrow-derived macrophages (BMDMs)^{208,210}. Gram-positive bacterial RNA, especially streptococcal single-stranded RNA, was shown to be sensed by macrophages²²³. To date, research studies have failed to elucidate the mechanism of Gram-positive bacterial RNA in activating the inflammasome complex in human macrophages. In the current study, we show that human macrophages sense GBS and SA RNA cytosolically, thus, triggering the release of IL-1 β (**Fig. 17a**). Furthermore, the ability of RNase A treatment to abrogate the release of IL-1 β suggests that the Gram-positive bacterial RNA is indispensable for the inflammasome activation (**Fig. 15b,c,d**). These results are in line with that of another study in which the bacteria restored the capacity to activate the inflammasome in dead bacteria through prokaryotic messenger RNA referring them to viability associated PAMPs (vita PAMPs)²¹⁰.

While investigating the immunostimulatory role of bacterial RNA, we identified the involvement of μ RNA (less than 200 nucleotides) in the inflammasome activation. This μ RNAs from the MLBs activated the canonical inflammasome pathway through caspase-1 and NLRP3 (**Fig. 17b**). Moreover, enzymatic treatment with DNase I and heat-inactivated RNase I followed by MLB RNA stimulations showed no effect on the release of IL-1 β . This is supported by a previous study that showed the robust release of IL-1 β through caspase-1 in murine macrophages²⁰⁸. Altogether our results conclude that the μ RNA isolated from the

MLBs of Gram-positive bacteria activate the canonical inflammasome pathway. The activation of the inflammasome pathway through μ RNA coincides with the sequencing analysis and identified small RNA in MLBs (**Fig. 17c**).

Gram-positive bacteria produce cyclic-di-AMP (CDNs) as a second messenger required in several processes such as biofilm formation, cell wall homeostasis, bacterial growth and virulence gene expression^{226,227}. In the current study, we show that μ RNA from SA show high affinity towards CDN than the big RNA (more than 200 nucleotides) suggesting its possibility to function as a CDN binding RNA aptamer (**Fig. 15f**). STING is a well-defined receptor for CDN for the production of type I interferon⁴¹. In the current study, we identified STING as the main sensor for μ RNA in the upstream NLRP3 signalling pathway for the production of IL-1 β . These results suggest that sRNAs present in the MLBs function as RNA aptamers sequestering CDN ligands towards STING. Surprisingly, production of IL-1 β upon μ RNA stimulation was cGAS independent (**Fig. 17h,i,j**). Further experiments are needed to examine the origin and characteristics of the CDNs which activate STING.

Gram-positive bacteria, especially GBS, and viruses activate the cGAS/STING axis for the production of type I interferon^{41,48}. Previously, STING was identified as the primary upstream sensor for the release of IL-1 β in response to the Gram-negative *Brucella abortus* infection²¹². The report showed that the transfection of *Brucella* DNA activated the expression of type I interferon and guanylate-binding proteins (GBPs) in STING-dependent manner. Furthermore, the transfected DNA was shown to activate caspase-1 dependent on STING. The involvement of cGAS/STING in Gram-positive bacteria for the release of IL-1 β through inflammasome activation is undetermined. One of the key findings in the current study is the identification of STING involvement for the robust release of IL-1 β upon Gram-positive bacterial infection (**Fig. 19a,b**). These results were in line with the recent findings which revealed a distinct mechanism by which STING regulates the NLRP3 inflammasome for the IL-1 β secretion²¹¹.

Surprisingly, the release of IL-1 β was independent of cGAS following the SA and GBS infections. This observation was further strengthened by inhibition experiments with the small molecule inhibitor H-151 that abrogated the release of IL-1 β following GBS and SA infections (**Fig. 19f,g**)²²⁹. Interestingly, MLBs also activated the canonical inflammasome pathway via STING for the release of IL-1 β . These results confirm that MLBs are packed with microbial ligands necessary for the canonical inflammasome activation (**Fig. 20a,b**).

To dissect the pathway further, the mechanism by which STING activates NLRP3 for the release of IL-1 β was examined. Confocal microscopy results showed the co-localization of STING and LAMP1 suggesting the translocation of STING to the lysosome (**Fig. 19j**). Here, the STING triggered signaling pathway can cause lysosomal cell death, which in turn could lead to K⁺ efflux due to plasma membrane permeability. This efflux, in turn, triggers the activation of NLRP3 inflammasome for the release of IL-1 β . These results are in line with previous findings in which crystal and particulate matter induced the NLRP3 activation from K⁺ efflux during phagocytosis^{87,203,211}. Nonetheless, nigericin stimulated THP1 macrophages showed pronounced release of IL-1 β inducing NLRP3 (**Fig 17g**). Recently, wang et al 2020 also demonstrated two new approaches for the NLRP3 inflammasome activation: STING recruits NLRP3 and facilitates NLRP3 localization in the endoplasmic reticulum and secondly, STING interacts with NLRP3 and attenuates K-48 and K-63 linked ubiquitination of NLRP3. Apart from this mode of activation, the possible role of post-translation modifications in NLRP3 activation also cannot be ruled out and can be considered for further investigation.

5.4 RNAIII of *S. aureus* activates the canonical inflammasome pathway via STING

Following the μ RNA sequencing, the current thesis depicts the expression of well-known RNAIII in SA-MLBs. RNAIII, a 514 nt sized small RNA, in *S. aureus* is known to act as an effector of agr quorum-sensing system regulating various genes^{161,247}. Over the years, it has been shown that RNAIII regulates the gene expression by binding to the target mRNAs via an antisense mechanism^{157,172}. Moreover, RNAIII is capable of regulating protein A, a surface protein that plays a role in the inflammatory signaling pathway and evasion of the host innate immune system²⁴⁸. The present study found that RNAIII is capable of activating the canonical inflammasome pathway. When *in vitro* transcribed RNAIII was given cytosolically, it elicited a robust IL-1 β response (**Fig. 22b**). Moreover, RNAIII showed a strong binding affinity with CDNs in mass spectroscopy (**Fig. 22c**). This suggests the possibility of RNAIII as CDN binding aptamers activating the inflammasome pathway.

Detailed analysis of the μ RNA sequencing revealed that MLBs accumulated various stretches of RNAIII. Importantly, we identified that the central domain of RNAIII with hairpins H7, H8 and H9 is exclusively assembled in the MLBs with immunostimulatory capacity (**Fig. 23a,c**). The 3' and 5' ends of RNAIII showed similar response with respect to IL-1 β release and losing this function upon cleavage (**Fig. 23g**). Several modifications in RNAIII might play a

role in activation of inflammasome for the release of IL-1 β . Recently, it was demonstrated that the 5'-NAD capped RNAIII led to the decrease expression of alpha and delta toxins resulting in reduced cytotoxicity¹⁷⁹. Furthermore, similar to the μ RNA of SA, the central domain A,7,8,9,A of RNAIII showed strong binding towards CDN when measured via spinach binding assay. It showed higher fluorescence with increasing concentration of CDNs (**Fig. 23e**). These results are also suggestive of the central domain of RNAIII acting as a CDN binding aptamer. Hence, these *in vitro* experiments concluded that the central domain of RNAIII (A,7,8,9A) activates the inflammasome with robust release of IL-1 β . With respect to elucidating the immunogenic capacity of *S. aureus* RNAIII, the present study appears to be first of its kind.

Considering that the sequence of RNAIII is highly conserved in SA strains, similar sequence analysis were done for other *Staphylococcal* species such as *S. carnosus* which showed differences in the sequence. Nonetheless, RNAIII of *S. carnosus* activated the inflammasome with robust release of IL-1 β . Similarly, AGR dependent sRNAs such as RsaC, WAN01CC-66 and SbrC when given to macrophages activated the inflammasome pathway. Further studies are necessary to identify the active site for CDN binding and inflammasome activation in these sRNAs. Altogether these results suggest that the accumulation of small RNA in MLBs is a crucial event in host-pathogen interaction.

5.5 Staphyloxanthin type of lipids in *S. aureus* target RNA PAMPs for the activation of inflammasome

The current thesis further focusses on the identified staphyloxanthin type of lipids in SA MLBs. *S. aureus* is known for its peculiar golden orange color pigment staphyloxanthin, which is also one of its virulence factors¹⁴⁰. Staphyloxanthin has antioxidative properties due to its numerous conjugated double bonds that can scavenge reactive oxygen species (ROS) such as O₂⁻, H₂O₂, and HOCl^{148,249}. Studies have also shown that bacteria lacking staphyloxanthin exhibited normal growth but had no effect on the abscess formation due to their rapid killing by the host defense mechanisms¹⁴⁸. In the current study, we elucidated the effect of purified staphyloxanthin on inflammasome activation for the release of IL-1 β .

Following the mass spectroscopic detection of staphyloxanthin lipids in MLBs, we further scrutinized the role of these lipids in inflammasome activation. The Raman spectroscopic analysis of the HPLC purified staphyloxanthin and its precursor 4', 4'-Diponeurosporenic acid revealed its fingerprint spectra that matched with the *S. aureus* bacteria. The Raman peaks at 1528, 1168 and 1013 cm⁻¹ of staphyloxanthin and the bacteria added to the current

knowledge of microbial pigments (**Appendix Fig. 32b,c**). Similar study in GBS showed that the presence of carotenoids results in pigmentation of the bacteria^{250,251}. In conclusion, our results highlight the application of Raman spectroscopy in rapid assessment of bacteria from diagnostic point of view.

Following the above observations, the potential role of staphyloxanthin and its precursor 4', 4'-diaponeurosporenoic acid in host-pathogen interactions was examined. Interestingly, we found that these lipids are involved in transferring PAMPs to the cytosol for the activation of inflammasome. Staphyloxanthin and its precursor entrap Gram-positive bacterial RNA and deliver to the cytosol for the activation of caspase-1 and robust release of IL-1 β (**Fig. 24a,b**). These results provide a possible explanation to a previous finding study that showed the involvement of granadeane, a hemolytic pigment of GBS, in host cell lysis whose mechanism was unclear²⁰⁶. Our results emphasize the role of staphyloxanthin lipids in the pathogenesis of *S. aureus*.

The biosynthesis of staphyloxanthin involves five genes present on the crtOPQMN operon with a sigma B dependent promoter¹⁴³. Importantly, CrtM and CrtN are the key enzymes involved in the biosynthesis pathway in *S. aureus*. Inhibition of crtN enzyme with small molecule inhibitor, naftifine turned orange colored bacteria to colorless. These bacteria lacked the capacity to release IL-1 β evidenced by no fingerprint spectra (**Fig. 24d,e,f,g, Appendix Fig. 32d,e**). Overall, our data suggests the evolutionary interplay of the bacterial lipid toxins switching them from harmless to pathogenic. It further suggests the basis of rational drug design targets against the major sepsis causing pathogen.

5.6 Gram-positive bacteria activates the non-canonical inflammasome pathway for the release of progranulin

Establishing the activation of the canonical pathway for the release of IL-1 β through MLBs, the thesis focusses on the immunological relevance of MVs for the release of unconventional proteins. It is well known that Gram-positive and Gram-negative bacteria such as *E.coli*, *S. aureus*, and Group B streptococcus activate the inflammasome pathway for the release of cytokines^{7,90,252,253}. At the same time, the activated inflammasome pathway also releases unconventional proteins such as HMGB1, SH1000, and IL-1 α ^{254,90}. Earlier, it was shown that progranulin is one such unconventional glycoprotein playing a key role in physiological processes such as early embryogenesis, wound healing, and host-pathogen responses^{255,256}. Moreover, several studies have highlighted the role of PGRN in acute and chronic inflammation. However, the mechanism is still not clear. In the current study, we elucidate the

mechanism for the release of PGRN from macrophages upon infection with Gram-positive bacteria and its vesicles. In the course of this study, we found MVs is a potent inducer of PGRN from macrophages. Our results add to the current knowledge of the functions of membrane vesicles (MVs) from Gram-positive bacteria.

Human caspase-4/5 is activated mainly through a non-canonical pathway triggered by LPS from Gram-negative bacteria¹⁰⁰. As such, it has been generally accepted that Gram-negative bacteria activate the non-canonical pathway for pyroptosis while Gram-positive bacteria release IL-1 β through the NLRP3-ASC-CASP1 axis. Surprisingly, our data suggest that GBS and SA activate human caspase-5 for the release of progranulin (**Fig. 25c,d**). These results also suggest the simultaneous involvement of caspase-1 and caspase-5 for the release of IL-1 β and progranulin in GBS and SA respectively. To our knowledge this is the first report elucidating the role of non-canonical inflammasome pathway in Gram-positive bacterial pathogenesis. This is supported by findings that showed a balance of pro- and anti-inflammatory responses when the host reacts to infection that results in healing and recovery²⁵⁷.

Exploring the release of progranulin further, we show that Δagr mutant of SA respectively released progranulin that was caspase-5 dependent, but were unable to demonstrate the same for IL-1 β (**Fig. 25f**). These results support the possibility of divergent pathways activated for the release of progranulin and IL-1 β at the same time. Non-canonical inflammasome pathway leads to the activation of GSDMD that creates membrane pores followed by ionic efflux activating the canonical pathway^{81,98}. A similar pathway was identified for the unconventional secretion of proteins¹¹⁴. Surprisingly, our results demonstrate that the Gram-positive bacteria secrete progranulin by activating caspase-5 and being independent of caspase-1 (**Fig. 25e,g**). Previous studies show the involvement of lysosome on the secretion pathway of progranulin^{258,259}. Nonetheless, it has also been reported that the levels of cathepsin (Cat D) were elevated in progranulin knockout mice and co-localized with progranulin in neurons, while cathepsin L degraded progranulin^{260,261}. These findings prompts further investigation for the mechanism of progranulin secretion with respect to lysosomes and cathepsins.

5.7 Cytoplasmic delivery of lipoproteins induces TLR2 independent caspase-5 dependent secretion of progranulin

Gram-positive bacterial lipoproteins are involved in the activation of the innate immune system to release pro- and anti-inflammatory cytokines. Bacterial lipoproteins are the vital class of surface proteins synthesized by *S. aureus*^{192,262}. Synthetic analoges of bacterial

lipoproteins like FSL and Pam3Cys (P3C) activate the innate immune system through TLR2/1 and, TLR2/6 heterodimers respectively^{198,199}. In the current study, our results show that the cytosolic stimulation of diacylated (FSL) and triacylated lipoproteins (P3C) release progranulin while the surface stimulation and the delivery control had no effect. Moreover, cytoplasmic stimulation of FSL and P3C on caspase-1, caspase-4 and caspase-5 deficient macrophages highlighted that the release of progranulin is caspase-5 dependent (**Fig. 26a**). However, consistent with the previous literature the binding of caspase-5 and biotinylated P3C was not observed in this study's experiments. These results prompt to investigate the Gram-positive bacterial lipoproteins as a potent ligand to activate human caspase-5.

Canopy FGF Signaling Regulator 3 (CNPY3) is a protein-coding gene responsible for the translocation of surface TLRs. To validate the role of TLRs we created the CNPY3 mutant following the infection of GBS and SA. CNPY3 mutant should release progranulin independently of TLR2. Moreover, the surface stimulation of FSL and P3C abrogated the release of PGRN in CNPY3 mutant while the intracellular stimulation released abundant PGRN. These results concluded the cytoplasmic activation of caspase-5 bypasses TLR2 for the release of progranulin in human macrophages (**Fig. 26d**). In *S. aureus*, three enzymes Lgt, Lsp and Lnt located on the cytoplasmic membrane are involved in the lipidation and lipoprotein processing. Here, we validated the release of progranulin by creating an Δlgt mutant of *S. aureus*. Infecting human macrophages with Δlgt mutants abrogated the release of progranulin while it showed robust release of IL-1 β (**Fig. 26e,f**). These results conclude that the human macrophages release progranulin independent of TLR2 and signify the involvement of various pathways in inflammasome activation. Following the above results, the current study, we investigated *Galleria Mellonella* for the effect of MLBs, MVs and Group B streptococcus infection. Along with the non-mammalian model organisms such as nematode, *Caenorhabditis elegans*, and the common fruit fly *Drosophila melanogaster*, *Galleria mellonella* known as wax worm has been investigated in previous studies for bacterial and fungal pathogenesis^{264,265,266}. The foremost advantage of using wax worm is that it survives at 37 °C and shares functional homology with mammalian innate immune system by possessing both humoral and cellular immunity^{267,268}. *Galleria mellonella* has been used to investigate pathogenesis of bacteria such as Group A streptococcus, *Pseudomonas aeruginosa*, *Mycobacterium fortuitum*^{269,270,271}. Moreover, *G. mellonella* belongs to the order Lepidoptera which contains caspase gene families including caspase-4,-5, -1 and caspase-6²⁷². We observed that the high levels of Group B streptococcal infections were deleterious to the larvae with early death while the larvae survived with low levels of infection. Surprisingly,

infections with sub-lethal concentration of $\Delta cylE$ mutant of GBS showed protective effect on *Galleria mellonella* (**Fig. 27c**). These observations are consistent with previous results where $\Delta cylE$ mutant lacked the ability to trigger IL-1 β in mice dendritic cells and macrophages^{207,208}. On the contrary, $\Delta cylE$ mutant of GBS showed a robust induction of inflammasome for the release of PGRN. This is due to the lack of isoprenoid lipids in the mutant that lack the capacity to activate the inflammatory pathways. Similarly, MVs from $\Delta cylE$ mutant showed a protective effect upon GBS infections suggesting that the progranulin released can be protective in pathogenesis. A similar effect was observed in naftifine treated GBS as well as its MVs (**Fig. 27e,f**).

To validate the protective effect, we observed that MV primed worms were unaffected following GBS infections. This result suggests that the priming of MVs released granulins that triggered a strong inflammatory response, thus, protecting the worms from lethal doses of GBS. These results were similar in progranulin priming, thereby, concluding that the secretory glycoproteins protect the worm from pathogenesis. Overall, our results demonstrate that MVs from Group B streptococci activate the innate immune system of *Galleria mellonella* to release granulins that render protection to the worm upon GBS infection. Moreover, *Galleria mellonella* can serve as a model organism to investigate the pathogenesis of Group B streptococcus.

5.8 Inflammasome activation and sepsis

Sepsis is one of the prime causes of death due to altered host immune response to infections leading to organ dysfunction²⁷³. The key cause of sepsis can be microbes entering the body through minor bruises or through major health conditions such as urinary infection, pneumonia, and cellulitis. Activation of the host innate immune system correlates directly to the pathogenesis causing sepsis. Gram-positive bacteria such as *S. aureus* and GBS are a major class of pathogens causing sepsis. In the current study, we explored the pathogenesis of *S. aureus* in sepsis patients.

To complement the previous results of the inflammasome activation through small regulatory RNAIII for the release of IL-1 β , we collected fifty *S. aureus* patient isolates. Clinically, these isolates were peripheral and central venous blood culture positive and our analysis highlighted that majorly 84% of the isolates were RNAIII positive. Interestingly, the μ RNA from RNAIII positive isolates activated the inflammasome pathway while the RNAIII negative isolates failed to release IL-1 β (**Fig. 28b**). These results suggest that CDN binding RNA aptamers are

involved in the progression of sepsis. Similarly, plasma from the varied sepsis patient's cohort showed cleaved GSDMD in comparison with the control patients. GSDMD being the prime component in the release of IL-1 β and pyroptosis, our results laid the evidence for the involvement of inflammasome pathways in sepsis.

Along with the cytokines, various unconventional proteins and alarmins such as HMGB1, SH100, IL-1 α are secreted upon inflammasome activation. In our current study, a key clinical observation shows the accumulation and release of progranulin and galectin-1 in the plasma of sepsis patients (**Fig. 28f,g**). These results emphasized on the clinical relevance suggesting possible use as a biomarker for stratification of sepsis patients. The elevated levels of PGRN were consistent with the previous reports showing association with several inflammatory disorders¹²⁷. We further show that the levels of progranulin in sepsis patients correlates with the SOFA score of the patient suggesting that the levels of progranulin elevate as the sepsis progresses (**Fig. 28g**). Moreover, caspase-5 activation was observed in the sepsis patients as compared to the healthy donors indicating the activation of inflammasome for the release of progranulin. Collectively, our data demonstrate the relevance of inflammasome activation in sepsis patients suggesting therapeutic targets for Gram-positive pathogenesis.

6. CONCLUSIONS

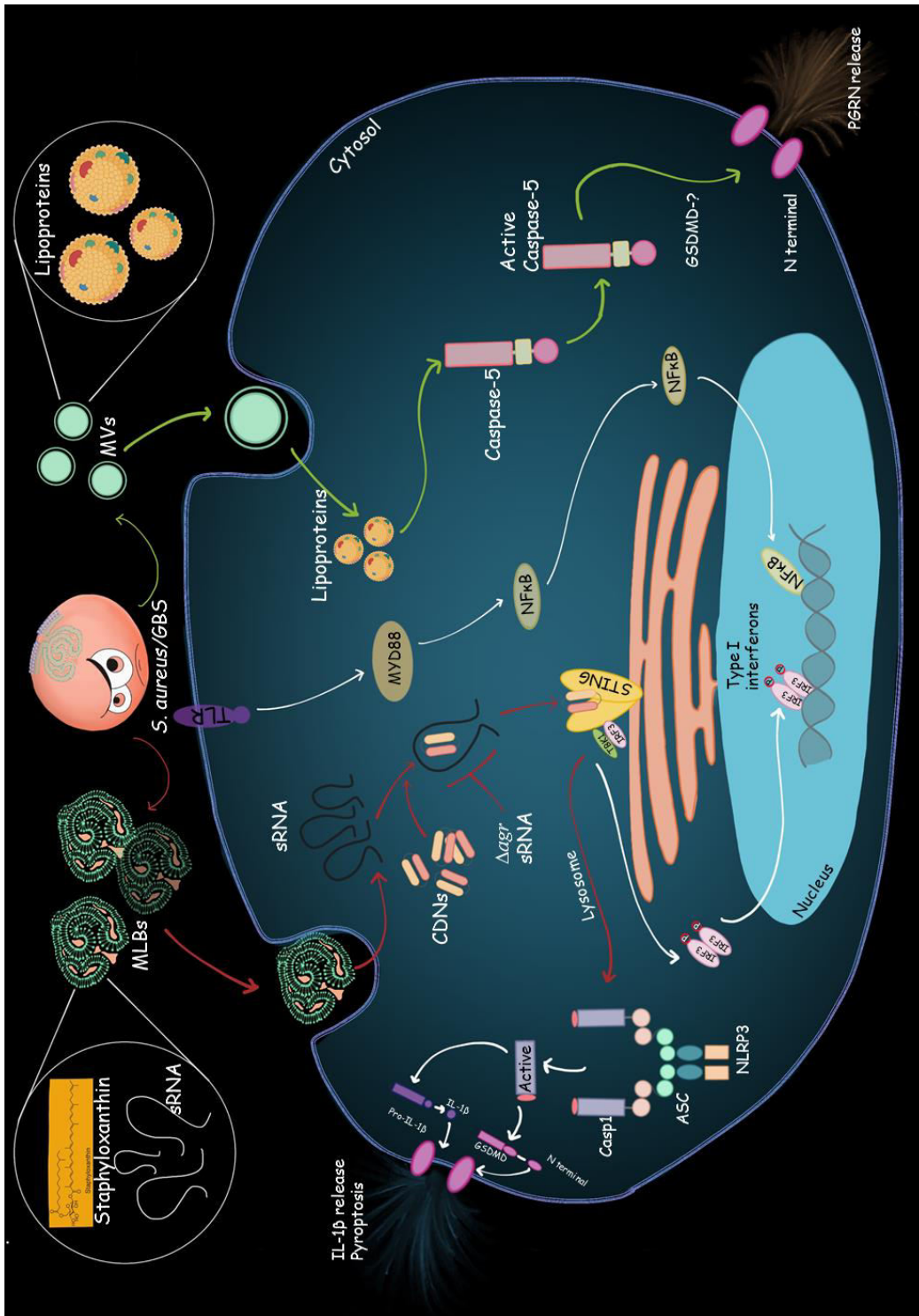


Figure 30: Diagrammatic representation of the overview of the pathways activated by MLBs and MVs: MLBs contain small RNA and staphyloxanthin type of lipids which activate the canonical inflammasome pathway via STING for the release of IL-1 β . While MVs contain lipoproteins that activate non-canonical inflammasome pathway via caspase-5 for the release of progranulin. Figure adopted from previous (38,45,81,90,100,156) and present work depicted in the thesis (The novel pathways are depicted in red and green arrows).

The data obtained in this study mainly illustrates that the Gram-positive bacteria shed unique vesicles named multilamellar lipid bodies (MLBs) along with the known membrane vesicles (MVs). Further, the inflammasome pathway was elucidated through MLBs enclosing cyclic di-nucleotide specific RNA aptamers and polyunsaturated lipids while MVs enclose lipoproteins. Based on these findings, the most important aspect of this work is STING

dependent canonical inflammasome activation for the release of IL-1 β . Interestingly, the DNA sensing nucleotidyl transferase enzyme cGAS is dispensable for the canonical inflammasome pathway emphasizing the importance of Gram-positive RNA aptamers. Scrutinizing the pathway further, we find that the accessory gene regulator (*agr*) quorum sensing system regulates the expression and release of RNA aptamers. Moreover, the polyunsaturated lipids from MLBs facilitate the small RNA to activate cytosolic inflammasome receptors in host macrophages. Another remarkable finding of the thesis is the involvement of the non-canonical inflammasome pathway for the release of progranulin in Gram-positive bacterial infections. Altogether, the data provides a new perspective for the pathogenicity of Gram-positive bacteria infections in man.

7. PROSPECTIVE

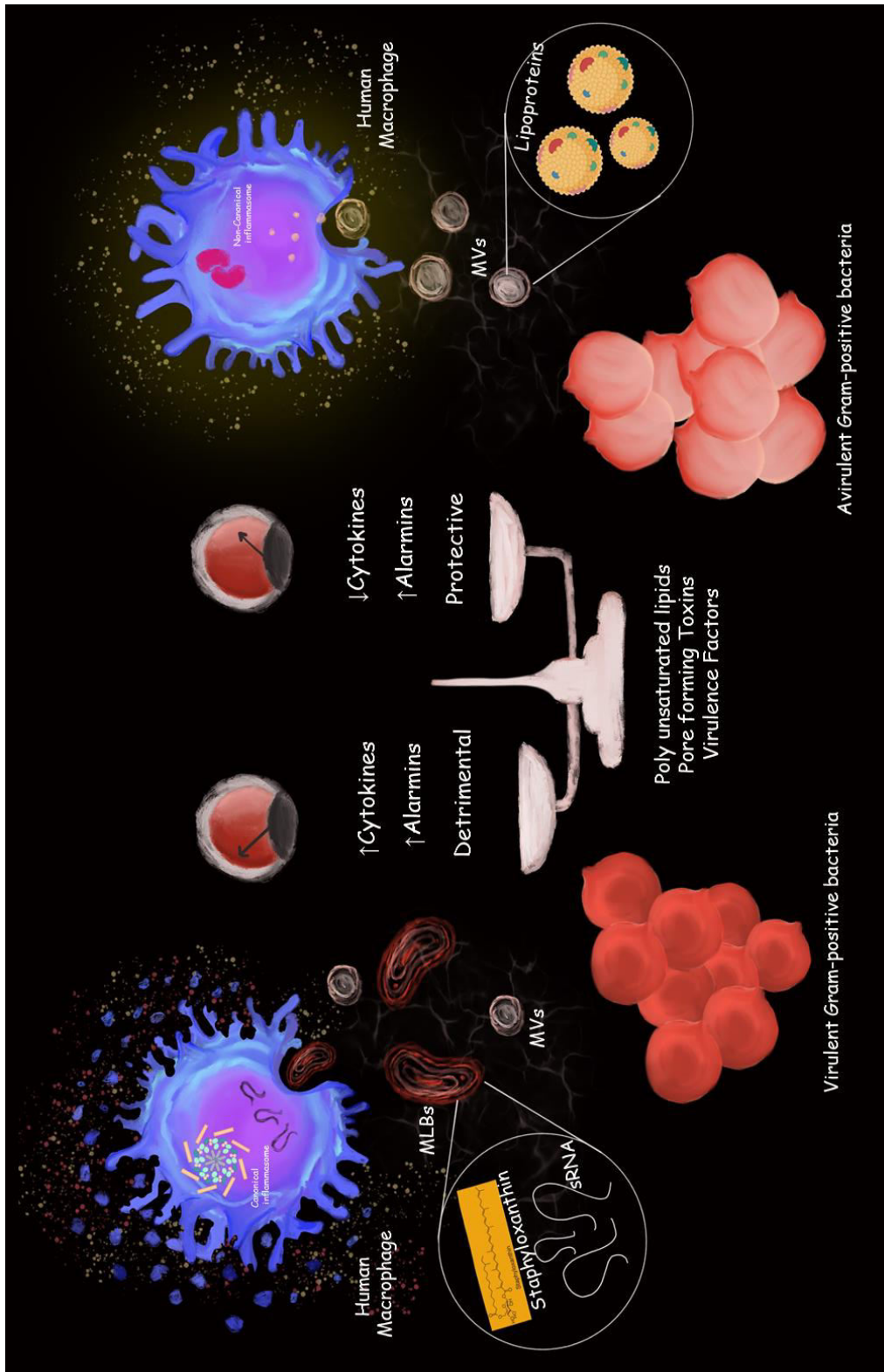


Figure 31: Figure illustrating the interplay of toxins and virulence factors activating the inflammasome pathway for production of cytokines and alarmins. Virulent Gram-positive bacteria produces polyunsaturated lipid and sRNA containing vesicles named multilamellar lipid bodies and lipoproteins containing membrane vesicles activating the inflammasome pathway for the release of cytokines and alarmins. In contrast, avirulent strains of Gram-positive bacteria secrete only membrane vesicles which activate the inflammasome pathway for the release of alarmins. Figure illustrated on the basis of the overall thesis and previous literature (206,207,208,81,100).

In less than a decade since inflammasome activation its vital physiological response, activation by Gram-positive bacteria has become one of the pillars in the field of host-pathogen interaction, and most active areas of research at the present time. The current thesis reports evident findings regarding Gram-positive bacteria activating canonical inflammasome

pathway via STING for the release of IL-1 β . As the figure illustrates, the interplay between pore forming toxins present in the Gram-positive bacteria subsequently leads to pathogenic or commensal microorganisms. We demonstrate that the bacteria consisting of higher virulence factors secrete newly discovered multi-lamellar lipid bodies (MLBs) delivering short RNA aptamers that harbour the ability to bind cyclic di-nucleotides into the host cell thereby activating STING. In contrast bacteria possessing comparatively less toxins release membrane vesicles thereby activating non-canonical inflammasome pathway for the release of PGRN.

Despite the remarkable advances, the current state of art is still primitive. One of the long standing issues in the activation of canonical inflammasome via STING for the release of IL-1 β is the source and nature of cyclic di-nucleotides (CDNs) that bind to RNA aptamer. Indeed, production of cyclic di-nucleotides in Gram-positive bacteria is complex and tightly regulated by diadenylate cyclase (DAC)^{226,227}. Till date, three mechanisms are known in bacteria to shape c-di-AMP host responses; regulating c-di-AMP metabolism, controlling c-di-AMP release and degrading extracellular c-di-AMP. This explains the complexity of the c-di-AMP synthesis in the bacteria showing secreting CDNs is not that effortless. Nonetheless, using the mass spectroscopic approaches, we show the accumulation of c-di-AMP in the MLBs and the binding to the RNA aptamers. An apparent limitation of this finding is the source of the CDN and the exact mechanism involved in the delivery through MLBs. The role of endogenous host cGAMP is ruled out as the release of IL-1 β is independent of cGAS. Recently, Andrade et al depicted the existence of an extracellular cell wall anchored enzyme CdnP in GBS which shows phosphodiesterase activity towards cyclic-di-AMP and in the absence of CdnP the host overproduced type I IFN leading to clearance of the bacteria⁴⁸. The recent review by Woodward depicts the role of CdnP in GBS and importance of cGAS and STING activation in the host against the extracellular bacteria⁵¹. Further studies are needed in this direction to evaluate the exact mechanism and enzymes involved for the delivery of CDNs in the host cytoplasm.

In addition, activation of inflammasome is triggered by pathogenic bacteria through the virulence factors such as pore-forming toxins or the bacterial secretion systems. In *S. pyogenes* the virulence factor streptolysin O leads to caspase-1 activation but is independent of P2X7 and TLR signaling²⁷⁴. Prior studies also demonstrated that β -hemolysin, a pore-forming toxin in GBS activates the NLRP3 inflammasome for the release of IL-1 β ²⁰⁸. Recently, Wang et al 2020 reported the involvement of pore forming toxins of *S. aureus* in EV cargo for the NLRP3 inflammasome activation. The major finding of the thesis is the

involvement of STING for the activation of canonical inflammasome pathway for the release of IL-1 β . We demonstrate that the small RNA released by the MLBs activates STING upstream on NLRP3 for the release of IL-1 β . Although the current thesis proposes activation of canonical inflammasome pathway it lacks the exact mechanism linking STING and NLRP3. Our results hold true to the fact that NLRP3 activation is driven through the efflux of intracellular K⁺. These results are consistent with the previous literature in which depletion of the intracellular K⁺ due to pore forming toxins inturn activates NLRP3⁸⁵. Meanwhile it was also shown that STING signaling causes lytic cell death demonstrating apoptotic like features leading to K⁺ efflux upstream of NLRP3¹⁰³. Regulation of inflammasome components such as NLRP3, ASC, caspase-1 and GSDMD through post translational modifications could play a crucial role in activation and execution of inflammasome upon bacterial infections. In human many types of post translational modifications such as phosphorylation, ubiquitination, alkylation and S-nitrosylation have been detected in NLRP3, ASC or caspase-1 which play a key role in activation of inflammasome^{275,276}. Consistently protein tyrosine phosphatase, protein phosphatase 2A, protein kinase A, Jun N-terminal kinase and protein kinase D and nitric oxide have been shown to regulate inflammasome assembly^{277,278}. Liu et al summarizes the formation of mitochondria-associated endoplasmic reticulum membranes (MAMs) through NLRP3 activators which subsequently provides a location for NLRP3 inflammasome assembly²⁷⁹. Shimada et al proposed NLRP3 activation by binding to oxidized mitochondrial DNA released from mitochondria following activation of the 'mitochondrial' apoptotic pathway⁸⁸. This explains how plethora of divergent molecules and cellular stresses engage the same signaling pathway. From the given evidences it can be postulated that various cellular factors may be responsible for the activation of NLRP3 downstream of STING which can be cell type specific in human host. Hence, it needs further evaluation with specific studies. In the current thesis, we demonstrate upstream bacterial strategy to deliver specific ligand to STING for downstream activation of inflammasome. In line with this STING has recently been shown in autophagy induction through a mechanism which is independent of interferons²⁸⁰. All these processes may be interlinked and complex which may or may not be dependent on IRFs for regulation of inflammasome genes upon bacterial infection²⁸¹.

Lastly, we report the activation of inflammatory caspase-5 through Gram-positive bacteria and its role in the release of progranulin. Overall, our study sheds new light on the involvement of non-canonical inflammasome pathway in Gram-positive bacteria induced infection. Nevertheless, further experimentation is required on how lipoproteins activate caspase-5 and the mechanism for the release PGRN. Both these mechanisms involved in

activation and release of caspase-5 in Gram-positive bacterial infections are important yet complex. PGRN contains seven and a half tandem granulin motifs separated by linker regions and proteolytic processing of PGRN results in the formation of several distinct granulin proteins^{282,122}. Predominantly extracellular proteases, as well as lysosomal PGRN proteases have been identified^{126,283}. Specifically, it points that the biological role of exocytic pathway for PGRN remains unclear. Hence, further experiments to determine functional and molecular mechanisms of pathways taking part into caspase-5 mediated release of PGRN in human macrophages are needed. A genetic approach to elucidate the processes at early and late endosomes as well as to study lysosomal homeostasis can be employed to determine the mechanism of how PGRN is differentially released from macrophages upon activation of caspase-5. Hence, it is imperative to expand future inflammasome investigations into the context of Gram-positive bacterial infection.

8. REFERENCES

- 1 Hoffmann, J. A., Kafatos, F. C., Janeway, C. A. & Ezekowitz, R. A. Phylogenetic perspectives in innate immunity. *Science* **284**, 1313-1318, doi:10.1126/science.284.5418.1313 (1999).
- 2 Akira, S., Takeda, K. & Kaisho, T. Toll-like receptors: critical proteins linking innate and acquired immunity. *Nat Immunol* **2**, 675-680, doi:10.1038/90609 (2001).
- 3 Medzhitov, R., Preston-Hurlburt, P. & Janeway, C. A., Jr. A human homologue of the Drosophila Toll protein signals activation of adaptive immunity. *Nature* **388**, 394-397, doi:10.1038/41131 (1997).
- 4 Medzhitov, R. & Janeway, C., Jr. Innate immune recognition: mechanisms and pathways. *Immunological reviews* **173**, 89-97 (2000).
- 5 Kumar, H., Kawai, T. & Akira, S. Pathogen recognition by the innate immune system. *Int Rev Immunol* **30**, 16-34, doi:10.3109/08830185.2010.529976 (2011).
- 6 Ikeda, K., Sannoh, T., Kawasaki, N., Kawasaki, T. & Yamashina, I. Serum lectin with known structure activates complement through the classical pathway. *J Biol Chem* **262**, 7451-7454 (1987).
- 7 Rathinam, V. A. *et al.* TRIF licenses caspase-11-dependent NLRP3 inflammasome activation by gram-negative bacteria. *Cell* **150**, 606-619, doi:10.1016/j.cell.2012.07.007 (2012).
- 8 Latz, E., Xiao, T. S. & Stutz, A. Activation and regulation of the inflammasomes. *Nature reviews. Immunology* **13**, 397-411, doi:10.1038/nri3452 (2013).
- 9 Anderson, K. V., Jurgens, G. & Nusslein-Volhard, C. Establishment of dorsal-ventral polarity in the Drosophila embryo: genetic studies on the role of the Toll gene product. *Cell* **42**, 779-789, doi:10.1016/0092-8674(85)90274-0 (1985).
- 10 Lemaitre, B., Nicolas, E., Michaut, L., Reichhart, J. M. & Hoffmann, J. A. The dorsoventral regulatory gene cassette spatzle/Toll/cactus controls the potent antifungal response in Drosophila adults. *Cell* **86**, 973-983, doi:10.1016/s0092-8674(00)80172-5 (1996).
- 11 Botos, I., Segal, D. M. & Davies, D. R. The structural biology of Toll-like receptors. *Structure* **19**, 447-459, doi:10.1016/j.str.2011.02.004 (2011).
- 12 Akira, S., Uematsu, S. & Takeuchi, O. Pathogen recognition and innate immunity. *Cell* **124**, 783-801, doi:10.1016/j.cell.2006.02.015 (2006).
- 13 Alexopoulou, L., Holt, A. C., Medzhitov, R. & Flavell, R. A. Recognition of double-stranded RNA and activation of NF-kappaB by Toll-like receptor 3. *Nature* **413**, 732-738, doi:10.1038/35099560 (2001).
- 14 Diebold, S. S., Kaisho, T., Hemmi, H., Akira, S. & Reis e Sousa, C. Innate antiviral responses by means of TLR7-mediated recognition of single-stranded RNA. *Science* **303**, 1529-1531, doi:10.1126/science.1093616 (2004).
- 15 Heil, F. *et al.* Species-specific recognition of single-stranded RNA via toll-like receptor 7 and 8. *Science* **303**, 1526-1529, doi:10.1126/science.1093620 (2004).
- 16 Hemmi, H. *et al.* A Toll-like receptor recognizes bacterial DNA. *Nature* **408**, 740-745, doi:10.1038/35047123 (2000).
- 17 Hidmark, A., von Saint Paul, A. & Dalpke, A. H. Cutting edge: TLR13 is a receptor for bacterial RNA. *J Immunol* **189**, 2717-2721, doi:10.4049/jimmunol.1200898 (2012).

- 18 Ozinsky, A. *et al.* The repertoire for pattern recognition of pathogens by the innate immune system is defined by cooperation between toll-like receptors. *Proc Natl Acad Sci U S A* **97**, 13766-13771, doi:10.1073/pnas.250476497 (2000).
- 19 Takada, E. *et al.* C-terminal LRRs of human Toll-like receptor 3 control receptor dimerization and signal transmission. *Mol Immunol* **44**, 3633-3640, doi:10.1016/j.molimm.2007.04.021 (2007).
- 20 Zhang, H., Tay, P. N., Cao, W., Li, W. & Lu, J. Integrin-nucleated Toll-like receptor (TLR) dimerization reveals subcellular targeting of TLRs and distinct mechanisms of TLR4 activation and signaling. *FEBS Lett* **532**, 171-176, doi:10.1016/s0014-5793(02)03669-4 (2002).
- 21 Ivicak-Kocjan, K., Panter, G., Bencina, M. & Jerala, R. Determination of the physiological 2:2 TLR5:flagellin activation stoichiometry revealed by the activity of a fusion receptor. *Biochem Biophys Res Commun* **435**, 40-45, doi:10.1016/j.bbrc.2013.04.030 (2013).
- 22 Ohto, U. *et al.* Structural basis of CpG and inhibitory DNA recognition by Toll-like receptor 9. *Nature* **520**, 702-705, doi:10.1038/nature14138 (2015).
- 23 Motshwene, P. G. *et al.* An oligomeric signaling platform formed by the Toll-like receptor signal transducers MyD88 and IRAK-4. *J Biol Chem* **284**, 25404-25411, doi:10.1074/jbc.M109.022392 (2009).
- 24 Kawasaki, T. & Kawai, T. Toll-like receptor signaling pathways. *Front Immunol* **5**, 461, doi:10.3389/fimmu.2014.00461 (2014).
- 25 Fitzgerald, K. A. *et al.* IKKepsilon and TBK1 are essential components of the IRF3 signaling pathway. *Nat Immunol* **4**, 491-496, doi:10.1038/ni921 (2003).
- 26 Cheng, Z., Taylor, B., Ourthiague, D. R. & Hoffmann, A. Distinct single-cell signaling characteristics are conferred by the MyD88 and TRIF pathways during TLR4 activation. *Sci Signal* **8**, ra69, doi:10.1126/scisignal.aaa5208 (2015).
- 27 Robinson, M. J., Sancho, D., Slack, E. C., LeibundGut-Landmann, S. & Reis e Sousa, C. Myeloid C-type lectins in innate immunity. *Nat Immunol* **7**, 1258-1265, doi:10.1038/ni1417 (2006).
- 28 Takeuchi, O. & Akira, S. Pattern recognition receptors and inflammation. *Cell* **140**, 805-820, doi:10.1016/j.cell.2010.01.022 (2010).
- 29 Yoneyama, M. *et al.* The RNA helicase RIG-I has an essential function in double-stranded RNA-induced innate antiviral responses. *Nat Immunol* **5**, 730-737, doi:10.1038/ni1087 (2004).
- 30 Kato, H. *et al.* Differential roles of MDA5 and RIG-I helicases in the recognition of RNA viruses. *Nature* **441**, 101-105, doi:10.1038/nature04734 (2006).
- 31 Binder, M. *et al.* Molecular mechanism of signal perception and integration by the innate immune sensor retinoic acid-inducible gene-I (RIG-I). *J Biol Chem* **286**, 27278-27287, doi:10.1074/jbc.M111.256974 (2011).
- 32 Hornung, V. *et al.* 5'-Triphosphate RNA is the ligand for RIG-I. *Science* **314**, 994-997, doi:10.1126/science.1132505 (2006).
- 33 Gitlin, L. *et al.* Essential role of mda-5 in type I IFN responses to polyriboinosinic:polyribocytidylic acid and encephalomyocarditis picornavirus. *Proc Natl Acad Sci U S A* **103**, 8459-8464, doi:10.1073/pnas.0603082103 (2006).
- 34 Pippig, D. A. *et al.* The regulatory domain of the RIG-I family ATPase LGP2 senses double-stranded RNA. *Nucleic Acids Res* **37**, 2014-2025, doi:10.1093/nar/gkp059 (2009).
- 35 Seth, R. B., Sun, L., Ea, C. K. & Chen, Z. J. Identification and characterization of MAVS, a mitochondrial antiviral signaling protein that activates NF-kappaB and IRF 3. *Cell* **122**, 669-682, doi:10.1016/j.cell.2005.08.012 (2005).

- 36 Liu, S. *et al.* MAVS recruits multiple ubiquitin E3 ligases to activate antiviral signaling cascades. *Elife* **2**, e00785, doi:10.7554/eLife.00785 (2013).
- 37 Ishikawa, H. & Barber, G. N. STING is an endoplasmic reticulum adaptor that facilitates innate immune signalling. *Nature* **455**, 674-678, doi:10.1038/nature07317 (2008).
- 38 Zhong, B. *et al.* The adaptor protein MITA links virus-sensing receptors to IRF3 transcription factor activation. *Immunity* **29**, 538-550, doi:10.1016/j.immuni.2008.09.003 (2008).
- 39 Sun, W. *et al.* ERIS, an endoplasmic reticulum IFN stimulator, activates innate immune signaling through dimerization. *Proc Natl Acad Sci U S A* **106**, 8653-8658, doi:10.1073/pnas.0900850106 (2009).
- 40 Wu, J. *et al.* Cyclic GMP-AMP is an endogenous second messenger in innate immune signaling by cytosolic DNA. *Science* **339**, 826-830, doi:10.1126/science.1229963 (2013).
- 41 Sun, L., Wu, J., Du, F., Chen, X. & Chen, Z. J. Cyclic GMP-AMP synthase is a cytosolic DNA sensor that activates the type I interferon pathway. *Science* **339**, 786-791, doi:10.1126/science.1232458 (2013).
- 42 Ouyang, S. *et al.* Structural analysis of the STING adaptor protein reveals a hydrophobic dimer interface and mode of cyclic di-GMP binding. *Immunity* **36**, 1073-1086, doi:10.1016/j.immuni.2012.03.019 (2012).
- 43 Gao, P. *et al.* Cyclic [G(2',5')pA(3',5')p] is the metazoan second messenger produced by DNA-activated cyclic GMP-AMP synthase. *Cell* **153**, 1094-1107, doi:10.1016/j.cell.2013.04.046 (2013).
- 44 Zhang, X. *et al.* Cyclic GMP-AMP containing mixed phosphodiester linkages is an endogenous high-affinity ligand for STING. *Mol Cell* **51**, 226-235, doi:10.1016/j.molcel.2013.05.022 (2013).
- 45 Tanaka, Y. & Chen, Z. J. STING specifies IRF3 phosphorylation by TBK1 in the cytosolic DNA signaling pathway. *Sci Signal* **5**, ra20, doi:10.1126/scisignal.2002521 (2012).
- 46 Chen, H. *et al.* Activation of STAT6 by STING is critical for antiviral innate immunity. *Cell* **147**, 436-446, doi:10.1016/j.cell.2011.09.022 (2011).
- 47 Ma, F. *et al.* Positive feedback regulation of type I IFN production by the IFN-inducible DNA sensor cGAS. *J Immunol* **194**, 1545-1554, doi:10.4049/jimmunol.1402066 (2015).
- 48 Andrade, W. A. *et al.* Group B Streptococcus Degrades Cyclic-di-AMP to Modulate STING-Dependent Type I Interferon Production. *Cell host & microbe* **20**, 49-59, doi:10.1016/j.chom.2016.06.003 (2016).
- 49 Jin, L. *et al.* MPYS is required for IFN response factor 3 activation and type I IFN production in the response of cultured phagocytes to bacterial second messengers cyclic-di-AMP and cyclic-di-GMP. *Journal of immunology* **187**, 2595-2601, doi:10.4049/jimmunol.1100088 (2011).
- 50 Sauer, J. D. *et al.* The N-ethyl-N-nitrosourea-induced Goldenticket mouse mutant reveals an essential function of Sting in the in vivo interferon response to *Listeria monocytogenes* and cyclic dinucleotides. *Infect Immun* **79**, 688-694, doi:10.1128/IAI.00999-10 (2011).
- 51 Woodward, J. J., Iavarone, A. T. & Portnoy, D. A. c-di-AMP secreted by intracellular *Listeria monocytogenes* activates a host type I interferon response. *Science* **328**, 1703-1705, doi:10.1126/science.1189801 (2010).
- 52 Dey, B. *et al.* A bacterial cyclic dinucleotide activates the cytosolic surveillance pathway and mediates innate resistance to tuberculosis. *Nat Med* **21**, 401-406, doi:10.1038/nm.3813 (2015).

- 53 Barker, J. R. *et al.* STING-dependent recognition of cyclic di-AMP mediates type I interferon responses during *Chlamydia trachomatis* infection. *MBio* **4**, e00018-00013, doi:10.1128/mBio.00018-13 (2013).
- 54 Harton, J. A., Linhoff, M. W., Zhang, J. & Ting, J. P. Cutting edge: CATERPILLER: a large family of mammalian genes containing CARD, pyrin, nucleotide-binding, and leucine-rich repeat domains. *J Immunol* **169**, 4088-4093, doi:10.4049/jimmunol.169.8.4088 (2002).
- 55 Cridland, J. A. *et al.* The mammalian PYHIN gene family: phylogeny, evolution and expression. *BMC Evol Biol* **12**, 140, doi:10.1186/1471-2148-12-140 (2012).
- 56 Martinon, F., Burns, K. & Tschopp, J. The inflammasome: a molecular platform triggering activation of inflammatory caspases and processing of proIL-beta. *Mol Cell* **10**, 417-426, doi:10.1016/s1097-2765(02)00599-3 (2002).
- 57 Cai, X. *et al.* Prion-like polymerization underlies signal transduction in antiviral immune defense and inflammasome activation. *Cell* **156**, 1207-1222, doi:10.1016/j.cell.2014.01.063 (2014).
- 58 Lu, A. *et al.* Unified polymerization mechanism for the assembly of ASC-dependent inflammasomes. *Cell* **156**, 1193-1206, doi:10.1016/j.cell.2014.02.008 (2014).
- 59 Jin, T. *et al.* Structures of the HIN domain:DNA complexes reveal ligand binding and activation mechanisms of the AIM2 inflammasome and IFI16 receptor. *Immunity* **36**, 561-571, doi:10.1016/j.immuni.2012.02.014 (2012).
- 60 Nour, A. M. *et al.* Anthrax lethal toxin triggers the formation of a membrane-associated inflammasome complex in murine macrophages. *Infect Immun* **77**, 1262-1271, doi:10.1128/IAI.01032-08 (2009).
- 61 Ponomareva, L. *et al.* AIM2, an IFN-inducible cytosolic DNA sensor, in the development of benign prostate hyperplasia and prostate cancer. *Mol Cancer Res* **11**, 1193-1202, doi:10.1158/1541-7786.MCR-13-0145 (2013).
- 62 Boyden, E. D. & Dietrich, W. F. Nalp1b controls mouse macrophage susceptibility to anthrax lethal toxin. *Nat Genet* **38**, 240-244, doi:10.1038/ng1724 (2006).
- 63 Finger, J. N. *et al.* Autolytic proteolysis within the function to find domain (FIIND) is required for NLRP1 inflammasome activity. *J Biol Chem* **287**, 25030-25037, doi:10.1074/jbc.M112.378323 (2012).
- 64 Faustin, B. *et al.* Reconstituted NALP1 inflammasome reveals two-step mechanism of caspase-1 activation. *Mol Cell* **25**, 713-724, doi:10.1016/j.molcel.2007.01.032 (2007).
- 65 Jin, Y. *et al.* NALP1 in vitiligo-associated multiple autoimmune disease. *N Engl J Med* **356**, 1216-1225, doi:10.1056/NEJMoa061592 (2007).
- 66 Magitta, N. F. *et al.* A coding polymorphism in NALP1 confers risk for autoimmune Addison's disease and type 1 diabetes. *Genes Immun* **10**, 120-124, doi:10.1038/gene.2008.85 (2009).
- 67 Poyet, J. L. *et al.* Identification of Ipaf, a human caspase-1-activating protein related to Apaf-1. *J Biol Chem* **276**, 28309-28313, doi:10.1074/jbc.C100250200 (2001).
- 68 Franchi, L. *et al.* Cytosolic flagellin requires Ipaf for activation of caspase-1 and interleukin 1beta in salmonella-infected macrophages. *Nat Immunol* **7**, 576-582, doi:10.1038/ni1346 (2006).
- 69 Yang, J., Zhao, Y., Shi, J. & Shao, F. Human NAIP and mouse NAIP1 recognize bacterial type III secretion needle protein for inflammasome activation. *Proc Natl Acad Sci U S A* **110**, 14408-14413, doi:10.1073/pnas.1306376110 (2013).
- 70 Zhao, Y. *et al.* The NLRC4 inflammasome receptors for bacterial flagellin and type III secretion apparatus. *Nature* **477**, 596-600, doi:10.1038/nature10510 (2011).
- 71 Rayamajhi, M., Zak, D. E., Chavarria-Smith, J., Vance, R. E. & Miao, E. A. Cutting edge: Mouse NAIP1 detects the type III secretion system needle protein. *J Immunol* **191**, 3986-3989, doi:10.4049/jimmunol.1301549 (2013).

- 72 Fernandes-Alnemri, T., Yu, J. W., Datta, P., Wu, J. & Alnemri, E. S. AIM2 activates the inflammasome and cell death in response to cytoplasmic DNA. *Nature* **458**, 509-513, doi:10.1038/nature07710 (2009).
- 73 Hornung, V. *et al.* AIM2 recognizes cytosolic dsDNA and forms a caspase-1-activating inflammasome with ASC. *Nature* **458**, 514-518, doi:10.1038/nature07725 (2009).
- 74 Roberts, T. L. *et al.* HIN-200 proteins regulate caspase activation in response to foreign cytoplasmic DNA. *Science* **323**, 1057-1060, doi:10.1126/science.1169841 (2009).
- 75 Hoffman, H. M., Mueller, J. L., Broide, D. H., Wanderer, A. A. & Kolodner, R. D. Mutation of a new gene encoding a putative pyrin-like protein causes familial cold autoinflammatory syndrome and Muckle-Wells syndrome. *Nat Genet* **29**, 301-305, doi:10.1038/ng756 (2001).
- 76 von Moltke, J., Ayres, J. S., Kofoed, E. M., Chavarria-Smith, J. & Vance, R. E. Recognition of bacteria by inflammasomes. *Annu Rev Immunol* **31**, 73-106, doi:10.1146/annurev-immunol-032712-095944 (2013).
- 77 Liston, A. & Masters, S. L. Homeostasis-altering molecular processes as mechanisms of inflammasome activation. *Nat Rev Immunol* **17**, 208-214, doi:10.1038/nri.2016.151 (2017).
- 78 Broz, P., von Moltke, J., Jones, J. W., Vance, R. E. & Monack, D. M. Differential requirement for Caspase-1 autoproteolysis in pathogen-induced cell death and cytokine processing. *Cell Host Microbe* **8**, 471-483, doi:10.1016/j.chom.2010.11.007 (2010).
- 79 Guey, B., Bodnar, M., Manie, S. N., Tardivel, A. & Petrilli, V. Caspase-1 autoproteolysis is differentially required for NLRP1b and NLRP3 inflammasome function. *Proc Natl Acad Sci U S A* **111**, 17254-17259, doi:10.1073/pnas.1415756111 (2014).
- 80 Dick, M. S., Sborgi, L., Ruhl, S., Hiller, S. & Broz, P. ASC filament formation serves as a signal amplification mechanism for inflammasomes. *Nat Commun* **7**, 11929, doi:10.1038/ncomms11929 (2016).
- 81 Kayagaki, N. *et al.* Caspase-11 cleaves gasdermin D for non-canonical inflammasome signalling. *Nature* **526**, 666-671, doi:10.1038/nature15541 (2015).
- 82 Shi, J. *et al.* Cleavage of GSDMD by inflammatory caspases determines pyroptotic cell death. *Nature* **526**, 660-665, doi:10.1038/nature15514 (2015).
- 83 Liu, X. *et al.* Inflammasome-activated gasdermin D causes pyroptosis by forming membrane pores. *Nature* **535**, 153-158, doi:10.1038/nature18629 (2016).
- 84 Fink, S. L. & Cookson, B. T. Caspase-1-dependent pore formation during pyroptosis leads to osmotic lysis of infected host macrophages. *Cell Microbiol* **8**, 1812-1825, doi:10.1111/j.1462-5822.2006.00751.x (2006).
- 85 Munoz-Planillo, R. *et al.* K(+) efflux is the common trigger of NLRP3 inflammasome activation by bacterial toxins and particulate matter. *Immunity* **38**, 1142-1153, doi:10.1016/j.immuni.2013.05.016 (2013).
- 86 Murakami, T. *et al.* Critical role for calcium mobilization in activation of the NLRP3 inflammasome. *Proc Natl Acad Sci U S A* **109**, 11282-11287, doi:10.1073/pnas.1117765109 (2012).
- 87 Hornung, V. *et al.* Silica crystals and aluminum salts activate the NALP3 inflammasome through phagosomal destabilization. *Nat Immunol* **9**, 847-856, doi:10.1038/ni.1631 (2008).
- 88 Shimada, K. *et al.* Oxidized mitochondrial DNA activates the NLRP3 inflammasome during apoptosis. *Immunity* **36**, 401-414, doi:10.1016/j.immuni.2012.01.009 (2012).

- 89 Gross, C. J. *et al.* K(+) Efflux-Independent NLRP3 Inflammasome Activation by Small Molecules Targeting Mitochondria. *Immunity* **45**, 761-773, doi:10.1016/j.immuni.2016.08.010 (2016).
- 90 Kayagaki, N. *et al.* Non-canonical inflammasome activation targets caspase-11. *Nature* **479**, 117-121, doi:10.1038/nature10558 (2011).
- 91 Shi, J. *et al.* Inflammatory caspases are innate immune receptors for intracellular LPS. *Nature* **514**, 187-192, doi:10.1038/nature13683 (2014).
- 92 Napier, B. A. *et al.* Complement pathway amplifies caspase-11-dependent cell death and endotoxin-induced sepsis severity. *J Exp Med* **213**, 2365-2382, doi:10.1084/jem.20160027 (2016).
- 93 Man, S. M. *et al.* IRGB10 Liberates Bacterial Ligands for Sensing by the AIM2 and Caspase-11-NLRP3 Inflammasomes. *Cell* **167**, 382-396 e317, doi:10.1016/j.cell.2016.09.012 (2016).
- 94 Meunier, E. *et al.* Caspase-11 activation requires lysis of pathogen-containing vacuoles by IFN-induced GTPases. *Nature* **509**, 366-370, doi:10.1038/nature13157 (2014).
- 95 Shi, J., Gao, W. & Shao, F. Pyroptosis: Gasdermin-Mediated Programmed Necrotic Cell Death. *Trends Biochem Sci* **42**, 245-254, doi:10.1016/j.tibs.2016.10.004 (2017).
- 96 Lee, E. Y. *et al.* Gram-positive bacteria produce membrane vesicles: proteomics-based characterization of Staphylococcus aureus-derived membrane vesicles. *Proteomics* **9**, 5425-5436, doi:10.1002/pmic.200900338 (2009).
- 97 Zanoni, I. *et al.* An endogenous caspase-11 ligand elicits interleukin-1 release from living dendritic cells. *Science* **352**, 1232-1236, doi:10.1126/science.aaf3036 (2016).
- 98 Kayagaki, N. *et al.* Noncanonical inflammasome activation by intracellular LPS independent of TLR4. *Science* **341**, 1246-1249, doi:10.1126/science.1240248 (2013).
- 99 Bian, Z. M. *et al.* Expression and functional roles of caspase-5 in inflammatory responses of human retinal pigment epithelial cells. *Invest Ophthalmol Vis Sci* **52**, 8646-8656, doi:10.1167/iovs.11-7570 (2011).
- 100 Casson, C. N. *et al.* Human caspase-4 mediates noncanonical inflammasome activation against gram-negative bacterial pathogens. *Proceedings of the National Academy of Sciences of the United States of America* **112**, 6688-6693, doi:10.1073/pnas.1421699112 (2015).
- 101 Schmid-Burgk, J. L. *et al.* Caspase-4 mediates non-canonical activation of the NLRP3 inflammasome in human myeloid cells. *European journal of immunology* **45**, 2911-2917, doi:10.1002/eji.201545523 (2015).
- 102 Baker, P. J. *et al.* NLRP3 inflammasome activation downstream of cytoplasmic LPS recognition by both caspase-4 and caspase-5. *Eur J Immunol* **45**, 2918-2926, doi:10.1002/eji.201545655 (2015).
- 103 Gaidt, M. M. *et al.* Human Monocytes Engage an Alternative Inflammasome Pathway. *Immunity* **44**, 833-846, doi:10.1016/j.immuni.2016.01.012 (2016).
- 104 Bergsbaken, T., Fink, S. L. & Cookson, B. T. Pyroptosis: host cell death and inflammation. *Nat Rev Microbiol* **7**, 99-109, doi:10.1038/nrmicro2070 (2009).
- 105 He, W. T. *et al.* Gasdermin D is an executor of pyroptosis and required for interleukin-1beta secretion. *Cell Res* **25**, 1285-1298, doi:10.1038/cr.2015.139 (2015).
- 106 Ding, J. *et al.* Pore-forming activity and structural autoinhibition of the gasdermin family. *Nature* **535**, 111-116, doi:10.1038/nature18590 (2016).
- 107 Dinarello, C. A. Immunological and inflammatory functions of the interleukin-1 family. *Annu Rev Immunol* **27**, 519-550, doi:10.1146/annurev.immunol.021908.132612 (2009).
- 108 Dinarello, C. A. Anti-inflammatory Agents: Present and Future. *Cell* **140**, 935-950, doi:10.1016/j.cell.2010.02.043 (2010).

- 109 Monteleone, M., Stow, J. L. & Schroder, K. Mechanisms of unconventional secretion of IL-1 family cytokines. *Cytokine* **74**, 213-218, doi:10.1016/j.cyto.2015.03.022 (2015).
- 110 Afonina, I. S., Muller, C., Martin, S. J. & Beyaert, R. Proteolytic Processing of Interleukin-1 Family Cytokines: Variations on a Common Theme. *Immunity* **42**, 991-1004, doi:10.1016/j.immuni.2015.06.003 (2015).
- 111 van de Veerdonk, F. L., Netea, M. G., Dinarello, C. A. & Joosten, L. A. Inflammasome activation and IL-1beta and IL-18 processing during infection. *Trends Immunol* **32**, 110-116, doi:10.1016/j.it.2011.01.003 (2011).
- 112 Kobayashi, T. *et al.* The Shigella OspC3 effector inhibits caspase-4, antagonizes inflammatory cell death, and promotes epithelial infection. *Cell Host Microbe* **13**, 570-583, doi:10.1016/j.chom.2013.04.012 (2013).
- 113 Knodler, L. A. *et al.* Noncanonical inflammasome activation of caspase-4/caspase-11 mediates epithelial defenses against enteric bacterial pathogens. *Cell Host Microbe* **16**, 249-256, doi:10.1016/j.chom.2014.07.002 (2014).
- 114 Keller, M., Ruegg, A., Werner, S. & Beer, H. D. Active caspase-1 is a regulator of unconventional protein secretion. *Cell* **132**, 818-831, doi:10.1016/j.cell.2007.12.040 (2008).
- 115 Nickel, W. & Rabouille, C. Mechanisms of regulated unconventional protein secretion. *Nat Rev Mol Cell Biol* **10**, 148-155, doi:10.1038/nrm2617 (2009).
- 116 Sundblad, V., Morosi, L. G., Geffner, J. R. & Rabinovich, G. A. Galectin-1: A Jack-of-All-Trades in the Resolution of Acute and Chronic Inflammation. *Journal of immunology* **199**, 3721-3730, doi:10.4049/jimmunol.1701172 (2017).
- 117 Di Lella, S. *et al.* When galectins recognize glycans: from biochemistry to physiology and back again. *Biochemistry* **50**, 7842-7857, doi:10.1021/bi201121m (2011).
- 118 Liu, F. T. & Rabinovich, G. A. Galectins: regulators of acute and chronic inflammation. *Ann N Y Acad Sci* **1183**, 158-182, doi:10.1111/j.1749-6632.2009.05131.x (2010).
- 119 Pace, K. E., Lee, C., Stewart, P. L. & Baum, L. G. Restricted receptor segregation into membrane microdomains occurs on human T cells during apoptosis induced by galectin-1. *Journal of immunology* **163**, 3801-3811 (1999).
- 120 Zuniga, E., Rabinovich, G. A., Iglesias, M. M. & Gruppi, A. Regulated expression of galectin-1 during B-cell activation and implications for T-cell apoptosis. *J Leukoc Biol* **70**, 73-79 (2001).
- 121 Rabinovich, G., Castagna, L., Landa, C., Riera, C. M. & Sotomayor, C. Regulated expression of a 16-kd galectin-like protein in activated rat macrophages. *J Leukoc Biol* **59**, 363-370, doi:10.1002/jlb.59.3.363 (1996).
- 122 Bateman, A. & Bennett, H. P. Granulins: the structure and function of an emerging family of growth factors. *J Endocrinol* **158**, 145-151, doi:10.1677/joe.0.1580145 (1998).
- 123 Hrabal, R., Chen, Z., James, S., Bennett, H. P. & Ni, F. The hairpin stack fold, a novel protein architecture for a new family of protein growth factors. *Nat Struct Biol* **3**, 747-752, doi:10.1038/nsb0996-747 (1996).
- 124 De Muynck, L. & Van Damme, P. Cellular effects of progranulin in health and disease. *J Mol Neurosci* **45**, 549-560, doi:10.1007/s12031-011-9553-z (2011).
- 125 Baker, M. *et al.* Mutations in progranulin cause tau-negative frontotemporal dementia linked to chromosome 17. *Nature* **442**, 916-919, doi:10.1038/nature05016 (2006).
- 126 Zhu, J. *et al.* Conversion of proepithelin to epithelins: roles of SLPI and elastase in host defense and wound repair. *Cell* **111**, 867-878, doi:10.1016/s0092-8674(02)01141-8 (2002).

- 127 Zhang, Y. J. *et al.* Progranulin mediates caspase-dependent cleavage of TAR DNA binding protein-43. *J Neurosci* **27**, 10530-10534, doi:10.1523/JNEUROSCI.3421-07.2007 (2007).
- 128 Tang, W. *et al.* The growth factor progranulin binds to TNF receptors and is therapeutic against inflammatory arthritis in mice. *Science* **332**, 478-484, doi:10.1126/science.1199214 (2011).
- 129 Yin, F. *et al.* Exaggerated inflammation, impaired host defense, and neuropathology in progranulin-deficient mice. *The Journal of experimental medicine* **207**, 117-128, doi:10.1084/jem.20091568 (2010).
- 130 Yan, W. *et al.* Progranulin Controls Sepsis via C/EBPalpha-Regulated I110 Transcription and Ubiquitin Ligase/Proteasome-Mediated Protein Degradation. *Journal of immunology* **197**, 3393-3405, doi:10.4049/jimmunol.1600862 (2016).
- 131 Doran, K. S. & Nizet, V. Molecular pathogenesis of neonatal group B streptococcal infection: no longer in its infancy. *Mol Microbiol* **54**, 23-31, doi:10.1111/j.1365-2958.2004.04266.x (2004).
- 132 Mandal, S. M., Ghosh, A. K. & Pati, B. R. Dissemination of antibiotic resistance in methicillin-resistant *Staphylococcus aureus* and vancomycin-resistant *S aureus* strains isolated from hospital effluents. *Am J Infect Control* **43**, e87-88, doi:10.1016/j.ajic.2015.08.015 (2015).
- 133 Thammavongsa, V., Kim, H. K., Missiakas, D. & Schneewind, O. Staphylococcal manipulation of host immune responses. *Nat Rev Microbiol* **13**, 529-543, doi:10.1038/nrmicro3521 (2015).
- 134 Ogston, A. Report upon Micro-Organisms in Surgical Diseases. *Br Med J* **1**, 369 b362-375, doi:10.1136/bmj.1.1054.369 (1881).
- 135 Ogston, A. Micrococcus Poisoning. *J Anat Physiol* **16**, 526-567 (1882).
- 136 Lowy, F. D. *Staphylococcus aureus* infections. *N Engl J Med* **339**, 520-532, doi:10.1056/NEJM199808203390806 (1998).
- 137 Tuchscher, L. & Loffler, B. *Staphylococcus aureus* dynamically adapts global regulators and virulence factor expression in the course from acute to chronic infection. *Curr Genet* **62**, 15-17, doi:10.1007/s00294-015-0503-0 (2016).
- 138 Ibarra, J. A., Perez-Rueda, E., Carroll, R. K. & Shaw, L. N. Global analysis of transcriptional regulators in *Staphylococcus aureus*. *BMC Genomics* **14**, 126, doi:10.1186/1471-2164-14-126 (2013).
- 139 Marshall, J. H. & Wilmoth, G. J. Pigments of *Staphylococcus aureus*, a series of triterpenoid carotenoids. *J Bacteriol* **147**, 900-913, doi:10.1128/JB.147.3.900-913.1981 (1981).
- 140 Khodade, V. S. *et al.* Bioreductively Activated Reactive Oxygen Species (ROS) Generators as MRSA Inhibitors. *ACS Med Chem Lett* **5**, 777-781, doi:10.1021/ml5001118 (2014).
- 141 Oldfield, E. & Feng, X. Resistance-resistant antibiotics. *Trends Pharmacol Sci* **35**, 664-674, doi:10.1016/j.tips.2014.10.007 (2014).
- 142 Ribeiro, D., Freitas, M., Silva, A. M. S., Carvalho, F. & Fernandes, E. Antioxidant and pro-oxidant activities of carotenoids and their oxidation products. *Food Chem Toxicol* **120**, 681-699, doi:10.1016/j.fct.2018.07.060 (2018).
- 143 Pelz, A. *et al.* Structure and biosynthesis of staphyloxanthin from *Staphylococcus aureus*. *The Journal of biological chemistry* **280**, 32493-32498, doi:10.1074/jbc.M505070200 (2005).
- 144 Bischoff, M. *et al.* Microarray-based analysis of the *Staphylococcus aureus* sigmaB regulon. *J Bacteriol* **186**, 4085-4099, doi:10.1128/JB.186.13.4085-4099.2004 (2004).

- 145 Giachino, P., Engelmann, S. & Bischoff, M. Sigma(B) activity depends on RsbU in Staphylococcus aureus. *J Bacteriol* **183**, 1843-1852, doi:10.1128/JB.183.6.1843-1852.2001 (2001).
- 146 Fang, F. C. Antimicrobial reactive oxygen and nitrogen species: concepts and controversies. *Nat Rev Microbiol* **2**, 820-832, doi:10.1038/nrmicro1004 (2004).
- 147 El-Agamey, A. *et al.* Carotenoid radical chemistry and antioxidant/pro-oxidant properties. *Arch Biochem Biophys* **430**, 37-48, doi:10.1016/j.abb.2004.03.007 (2004).
- 148 Liu, G. Y. *et al.* Staphylococcus aureus golden pigment impairs neutrophil killing and promotes virulence through its antioxidant activity. *The Journal of experimental medicine* **202**, 209-215, doi:10.1084/jem.20050846 (2005).
- 149 Xue, L. *et al.* Staphyloxanthin: a potential target for antivirulence therapy. *Infect Drug Resist* **12**, 2151-2160, doi:10.2147/IDR.S193649 (2019).
- 150 Liu, C. I. *et al.* A cholesterol biosynthesis inhibitor blocks Staphylococcus aureus virulence. *Science* **319**, 1391-1394, doi:10.1126/science.1153018 (2008).
- 151 Chen, F. *et al.* Small-molecule targeting of a diapophytoene desaturase inhibits S. aureus virulence. *Nature chemical biology* **12**, 174-179, doi:10.1038/nchembio.2003 (2016).
- 152 Recsei, P. *et al.* Regulation of exoprotein gene expression in Staphylococcus aureus by agar. *Mol Gen Genet* **202**, 58-61, doi:10.1007/BF00330517 (1986).
- 153 Roux, A., Todd, D. A., Velazquez, J. V., Cech, N. B. & Sonenshein, A. L. CodY-mediated regulation of the Staphylococcus aureus Agr system integrates nutritional and population density signals. *J Bacteriol* **196**, 1184-1196, doi:10.1128/JB.00128-13 (2014).
- 154 Cheung, A. L., Koomey, J. M., Butler, C. A., Projan, S. J. & Fischetti, V. A. Regulation of exoprotein expression in Staphylococcus aureus by a locus (sar) distinct from agr. *Proc Natl Acad Sci U S A* **89**, 6462-6466, doi:10.1073/pnas.89.14.6462 (1992).
- 155 Giraud, A. T., Cheung, A. L. & Nagel, R. The sae locus of Staphylococcus aureus controls exoprotein synthesis at the transcriptional level. *Arch Microbiol* **168**, 53-58, doi:10.1007/s002030050469 (1997).
- 156 Kleerebezem, M., Quadri, L. E., Kuipers, O. P. & de Vos, W. M. Quorum sensing by peptide pheromones and two-component signal-transduction systems in Gram-positive bacteria. *Mol Microbiol* **24**, 895-904, doi:10.1046/j.1365-2958.1997.4251782.x (1997).
- 157 Ji, G., Beavis, R. C. & Novick, R. P. Cell density control of staphylococcal virulence mediated by an octapeptide pheromone. *Proc Natl Acad Sci U S A* **92**, 12055-12059, doi:10.1073/pnas.92.26.12055 (1995).
- 158 Zhang, L., Gray, L., Novick, R. P. & Ji, G. Transmembrane topology of AgrB, the protein involved in the post-translational modification of AgrD in Staphylococcus aureus. *J Biol Chem* **277**, 34736-34742, doi:10.1074/jbc.M205367200 (2002).
- 159 Thoendel, M., Kavanaugh, J. S., Flack, C. E. & Horswill, A. R. Peptide signaling in the staphylococci. *Chem Rev* **111**, 117-151, doi:10.1021/cr100370n (2011).
- 160 Thoendel, M. & Horswill, A. R. Identification of Staphylococcus aureus AgrD residues required for autoinducing peptide biosynthesis. *J Biol Chem* **284**, 21828-21838, doi:10.1074/jbc.M109.031757 (2009).
- 161 Novick, R. P. *et al.* The agr P2 operon: an autocatalytic sensory transduction system in Staphylococcus aureus. *Mol Gen Genet* **248**, 446-458, doi:10.1007/BF02191645 (1995).
- 162 Geisinger, E., Muir, T. W. & Novick, R. P. agr receptor mutants reveal distinct modes of inhibition by staphylococcal autoinducing peptides. *Proc Natl Acad Sci U S A* **106**, 1216-1221, doi:10.1073/pnas.0807760106 (2009).

- 163 Traber, K. & Novick, R. A slipped-mispairing mutation in AgrA of laboratory strains and clinical isolates results in delayed activation of agr and failure to translate delta- and alpha-haemolysins. *Molecular microbiology* **59**, 1519-1530, doi:10.1111/j.1365-2958.2006.04986.x (2006).
- 164 Koenig, R. L., Ray, J. L., Maleki, S. J., Smeltzer, M. S. & Hurlburt, B. K. Staphylococcus aureus AgrA binding to the RNAIII-agr regulatory region. *J Bacteriol* **186**, 7549-7555, doi:10.1128/JB.186.22.7549-7555.2004 (2004).
- 165 Marchais, A., Naville, M., Bohn, C., Bouloc, P. & Gautheret, D. Single-pass classification of all noncoding sequences in a bacterial genome using phylogenetic profiles. *Genome Res* **19**, 1084-1092, doi:10.1101/gr.089714.108 (2009).
- 166 Geissmann, T. *et al.* A search for small noncoding RNAs in Staphylococcus aureus reveals a conserved sequence motif for regulation. *Nucleic Acids Res* **37**, 7239-7257, doi:10.1093/nar/gkp668 (2009).
- 167 Abu-Qatouseh, L. F. *et al.* Identification of differentially expressed small non-protein-coding RNAs in Staphylococcus aureus displaying both the normal and the small-colony variant phenotype. *J Mol Med (Berl)* **88**, 565-575, doi:10.1007/s00109-010-0597-2 (2010).
- 168 Bohn, C. *et al.* Experimental discovery of small RNAs in Staphylococcus aureus reveals a riboregulator of central metabolism. *Nucleic Acids Res* **38**, 6620-6636, doi:10.1093/nar/gkq462 (2010).
- 169 Beaume, M. *et al.* Cartography of methicillin-resistant S. aureus transcripts: detection, orientation and temporal expression during growth phase and stress conditions. *PLoS One* **5**, e10725, doi:10.1371/journal.pone.0010725 (2010).
- 170 Guillet, J., Hallier, M. & Felden, B. Emerging functions for the Staphylococcus aureus RNome. *PLoS Pathog* **9**, e1003767, doi:10.1371/journal.ppat.1003767 (2013).
- 171 Boisset, S. *et al.* Staphylococcus aureus RNAIII coordinately represses the synthesis of virulence factors and the transcription regulator Rot by an antisense mechanism. *Genes Dev* **21**, 1353-1366, doi:10.1101/gad.423507 (2007).
- 172 Benito, Y. *et al.* Probing the structure of RNAIII, the Staphylococcus aureus agr regulatory RNA, and identification of the RNA domain involved in repression of protein A expression. *RNA* **6**, 668-679, doi:10.1017/s1355838200992550 (2000).
- 173 Janzon, L., Lofdahl, S. & Arvidson, S. Identification and nucleotide sequence of the delta-lysin gene, hld, adjacent to the accessory gene regulator (agr) of Staphylococcus aureus. *Mol Gen Genet* **219**, 480-485, doi:10.1007/BF00259623 (1989).
- 174 Verdon, J., Girardin, N., Lacombe, C., Berjeaud, J. M. & Hechard, Y. delta-hemolysin, an update on a membrane-interacting peptide. *Peptides* **30**, 817-823, doi:10.1016/j.peptides.2008.12.017 (2009).
- 175 Morfeldt, E., Taylor, D., von Gabain, A. & Arvidson, S. Activation of alpha-toxin translation in Staphylococcus aureus by the trans-encoded antisense RNA, RNAIII. *EMBO J* **14**, 4569-4577 (1995).
- 176 Liu, Y. *et al.* RNAIII activates map expression by forming an RNA-RNA complex in Staphylococcus aureus. *FEBS Lett* **585**, 899-905, doi:10.1016/j.febslet.2011.02.021 (2011).
- 177 Novick, R. P. *et al.* Synthesis of staphylococcal virulence factors is controlled by a regulatory RNA molecule. *The EMBO journal* **12**, 3967-3975 (1993).
- 178 Geisinger, E., Adhikari, R. P., Jin, R., Ross, H. F. & Novick, R. P. Inhibition of rot translation by RNAIII, a key feature of agr function. *Mol Microbiol* **61**, 1038-1048, doi:10.1111/j.1365-2958.2006.05292.x (2006).
- 179 Morales-Fillooy, H. G. *et al.* The 5' NAD Cap of RNAIII Modulates Toxin Production in Staphylococcus aureus Isolates. *J Bacteriol* **202**, doi:10.1128/JB.00591-19 (2020).

- 180 Roier, S. *et al.* A novel mechanism for the biogenesis of outer membrane vesicles in Gram-negative bacteria. *Nature communications* **7**, 10515, doi:10.1038/ncomms10515 (2016).
- 181 Ellis, T. N. & Kuehn, M. J. Virulence and immunomodulatory roles of bacterial outer membrane vesicles. *Microbiology and molecular biology reviews : MMBR* **74**, 81-94, doi:10.1128/MMBR.00031-09 (2010).
- 182 Vanaja, S. K. *et al.* Bacterial Outer Membrane Vesicles Mediate Cytosolic Localization of LPS and Caspase-11 Activation. *Cell* **165**, 1106-1119, doi:10.1016/j.cell.2016.04.015 (2016).
- 183 Kim, J. H., Lee, J., Park, J. & Ghoo, Y. S. Gram-negative and Gram-positive bacterial extracellular vesicles. *Semin Cell Dev Biol* **40**, 97-104, doi:10.1016/j.semcdb.2015.02.006 (2015).
- 184 Lee, B. L. *et al.* Caspase-11 auto-proteolysis is crucial for noncanonical inflammasome activation. *J Exp Med* **215**, 2279-2288, doi:10.1084/jem.20180589 (2018).
- 185 Rivera, J. *et al.* Bacillus anthracis produces membrane-derived vesicles containing biologically active toxins. *Proc Natl Acad Sci U S A* **107**, 19002-19007, doi:10.1073/pnas.1008843107 (2010).
- 186 Olaya-Abril, A. *et al.* Characterization of protective extracellular membrane-derived vesicles produced by Streptococcus pneumoniae. *J Proteomics* **106**, 46-60, doi:10.1016/j.jprot.2014.04.023 (2014).
- 187 Resch, U. *et al.* A Two-Component Regulatory System Impacts Extracellular Membrane-Derived Vesicle Production in Group A Streptococcus. *MBio* **7**, doi:10.1128/mBio.00207-16 (2016).
- 188 Surve, M. V. *et al.* Membrane Vesicles of Group B Streptococcus Disrupt Feto-Maternal Barrier Leading to Preterm Birth. *PLoS pathogens* **12**, e1005816, doi:10.1371/journal.ppat.1005816 (2016).
- 189 Hong, S. W. *et al.* An important role of alpha-hemolysin in extracellular vesicles on the development of atopic dermatitis induced by Staphylococcus aureus. *PLoS One* **9**, e100499, doi:10.1371/journal.pone.0100499 (2014).
- 190 Jun, S. H. *et al.* Staphylococcus aureus-derived membrane vesicles exacerbate skin inflammation in atopic dermatitis. *Clin Exp Allergy* **47**, 85-96, doi:10.1111/cea.12851 (2017).
- 191 Sugimoto, S. *et al.* Imaging of bacterial multicellular behaviour in biofilms in liquid by atmospheric scanning electron microscopy. *Sci Rep* **6**, 25889, doi:10.1038/srep25889 (2016).
- 192 Hayashi, S. & Wu, H. C. Lipoproteins in bacteria. *J Bioenerg Biomembr* **22**, 451-471, doi:10.1007/BF00763177 (1990).
- 193 Gan, K., Gupta, S. D., Sankaran, K., Schmid, M. B. & Wu, H. C. Isolation and characterization of a temperature-sensitive mutant of Salmonella typhimurium defective in prolipoprotein modification. *J Biol Chem* **268**, 16544-16550 (1993).
- 194 Hussain, M., Ozawa, Y., Ichihara, S. & Mizushima, S. Signal peptide digestion in Escherichia coli. Effect of protease inhibitors on hydrolysis of the cleaved signal peptide of the major outer-membrane lipoprotein. *Eur J Biochem* **129**, 233-239, doi:10.1111/j.1432-1033.1982.tb07044.x (1982).
- 195 Sankaran, K. & Wu, H. C. Lipid modification of bacterial prolipoprotein. Transfer of diacylglycerol moiety from phosphatidylglycerol. *J Biol Chem* **269**, 19701-19706 (1994).
- 196 Romero-Steiner, S. *et al.* Inhibition of pneumococcal adherence to human nasopharyngeal epithelial cells by anti-PsaA antibodies. *Clin Diagn Lab Immunol* **10**, 246-251, doi:10.1128/cdli.10.2.246-251.2003 (2003).

- 197 Brightbill, H. D. *et al.* Host defense mechanisms triggered by microbial lipoproteins through toll-like receptors. *Science* **285**, 732-736, doi:10.1126/science.285.5428.732 (1999).
- 198 Takeuchi, O. *et al.* Discrimination of bacterial lipoproteins by Toll-like receptor 6. *Int Immunol* **13**, 933-940, doi:10.1093/intimm/13.7.933 (2001).
- 199 Takeuchi, O. *et al.* Cutting edge: role of Toll-like receptor 1 in mediating immune response to microbial lipoproteins. *Journal of immunology* **169**, 10-14, doi:10.4049/jimmunol.169.1.10 (2002).
- 200 Misawa, T. *et al.* Microtubule-driven spatial arrangement of mitochondria promotes activation of the NLRP3 inflammasome. *Nat Immunol* **14**, 454-460, doi:10.1038/ni.2550 (2013).
- 201 Zhou, R., Yazdi, A. S., Menu, P. & Tschopp, J. A role for mitochondria in NLRP3 inflammasome activation. *Nature* **469**, 221-225, doi:10.1038/nature09663 (2011).
- 202 Lamkanfi, M. & Dixit, V. M. Mechanisms and functions of inflammasomes. *Cell* **157**, 1013-1022, doi:10.1016/j.cell.2014.04.007 (2014).
- 203 Perregaux, D. & Gabel, C. A. Interleukin-1 beta maturation and release in response to ATP and nigericin. Evidence that potassium depletion mediated by these agents is a necessary and common feature of their activity. *J Biol Chem* **269**, 15195-15203 (1994).
- 204 Mariathasan, S. *et al.* Cryopyrin activates the inflammasome in response to toxins and ATP. *Nature* **440**, 228-232, doi:10.1038/nature04515 (2006).
- 205 Craven, R. R. *et al.* Staphylococcus aureus alpha-hemolysin activates the NLRP3-inflammasome in human and mouse monocytic cells. *PLoS One* **4**, e7446, doi:10.1371/journal.pone.0007446 (2009).
- 206 Whidbey, C. *et al.* A streptococcal lipid toxin induces membrane permeabilization and pyroptosis leading to fetal injury. *EMBO molecular medicine* **7**, 488-505, doi:10.15252/emmm.201404883 (2015).
- 207 Costa, A. *et al.* Activation of the NLRP3 inflammasome by group B streptococci. *Journal of immunology* **188**, 1953-1960, doi:10.4049/jimmunol.1102543 (2012).
- 208 Gupta, R. *et al.* RNA and beta-hemolysin of group B Streptococcus induce interleukin-1beta (IL-1beta) by activating NLRP3 inflammasomes in mouse macrophages. *The Journal of biological chemistry* **289**, 13701-13705, doi:10.1074/jbc.C114.548982 (2014).
- 209 Sha, W. *et al.* Human NLRP3 inflammasome senses multiple types of bacterial RNAs. *Proceedings of the National Academy of Sciences of the United States of America* **111**, 16059-16064, doi:10.1073/pnas.1412487111 (2014).
- 210 Sander, L. E. *et al.* Detection of prokaryotic mRNA signifies microbial viability and promotes immunity. *Nature* **474**, 385-389, doi:10.1038/nature10072 (2011).
- 211 Gaidt, M. M. *et al.* The DNA Inflammasome in Human Myeloid Cells Is Initiated by a STING-Cell Death Program Upstream of NLRP3. *Cell* **171**, 1110-1124 e1118, doi:10.1016/j.cell.2017.09.039 (2017).
- 212 Costa Franco, M. M. *et al.* Brucella abortus Triggers a cGAS-Independent STING Pathway To Induce Host Protection That Involves Guanylate-Binding Proteins and Inflammasome Activation. *Journal of immunology* **200**, 607-622, doi:10.4049/jimmunol.1700725 (2018).
- 213 Lee, E. Y. *et al.* Gram-positive bacteria produce membrane vesicles: Proteomics-based characterization of Staphylococcus aureus-derived membrane vesicles. *Proteomics* **9**, 5425-5436, doi:10.1002/pmic.200900338 (2009).
- 214 Gurung, M. *et al.* Staphylococcus aureus produces membrane-derived vesicles that induce host cell death. *PloS one* **6**, e27958, doi:10.1371/journal.pone.0027958 (2011).

- 215 Wang, W. *et al.* Caspase-11 Plays a Protective Role in Pulmonary *Acinetobacter*
baumannii Infection. *Infect Immun* **85**, doi:10.1128/IAI.00350-17 (2017).
- 216 Lamkanfi, M. *et al.* Inflammasome-dependent release of the alarmin HMGB1 in
endotoxemia. *J Immunol* **185**, 4385-4392, doi:10.4049/jimmunol.1000803 (2010).
- 217 Crowley, S. M., Vallance, B. A. & Knodler, L. A. Noncanonical inflammasomes:
Antimicrobial defense that does not play by the rules. *Cell Microbiol* **19**,
doi:10.1111/cmi.12730 (2017).
- 218 Wiggins, K. A. *et al.* IL-1 α cleavage by inflammatory caspases of the
noncanonical inflammasome controls the senescence-associated secretory phenotype.
Aging Cell **18**, e12946, doi:10.1111/accel.12946 (2019).
- 219 Yang, K. D., He, Y., Xiao, S., Ai, Q. & Yu, J. L. Identification of progranulin as a
novel diagnostic biomarker for early-onset sepsis in neonates. *European journal of*
clinical microbiology & infectious diseases : official publication of the European
Society of Clinical Microbiology, doi:10.1007/s10096-020-03981-x (2020).
- 220 Rao, L. *et al.* Progranulin as a novel biomarker in diagnosis of early-onset neonatal
sepsis. *Cytokine* **128**, 155000, doi:10.1016/j.cyto.2020.155000 (2020).
- 221 Paige, J. S., Nguyen-Duc, T., Song, W. & Jaffrey, S. R. Fluorescence imaging of
cellular metabolites with RNA. *Science* **335**, 1194, doi:10.1126/science.1218298
(2012).
- 222 Gu, T. *et al.* Highly efficient base editing in *Staphylococcus aureus* using an
engineered CRISPR RNA-guided cytidine deaminase. *Chem Sci* **9**, 3248-3253,
doi:10.1039/c8sc00637g (2018).
- 223 Marsollier, L. *et al.* Impact of *Mycobacterium ulcerans* biofilm on transmissibility to
ecological niches and Buruli ulcer pathogenesis. *PLoS Pathog* **3**, e62,
doi:10.1371/journal.ppat.0030062 (2007).
- 224 Deshmukh, S. D. *et al.* Macrophages recognize streptococci through bacterial single-
stranded RNA. *EMBO reports* **12**, 71-76, doi:10.1038/embor.2010.189 (2011).
- 225 Deshmukh, S. D. *et al.* NO is a macrophage autonomous modifier of the cytokine
response to streptococcal single-stranded RNA. *Journal of immunology* **188**, 774-780,
doi:10.4049/jimmunol.1101383 (2012).
- 226 Corrigan, R. M. *et al.* Systematic identification of conserved bacterial c-di-AMP
receptor proteins. *Proc Natl Acad Sci U S A* **110**, 9084-9089,
doi:10.1073/pnas.1300595110 (2013).
- 227 Romling, U., Galperin, M. Y. & Gomelsky, M. Cyclic di-GMP: the first 25 years of a
universal bacterial second messenger. *Microbiol Mol Biol Rev* **77**, 1-52,
doi:10.1128/MMBR.00043-12 (2013).
- 228 Coll, R. C. *et al.* A small-molecule inhibitor of the NLRP3 inflammasome for the
treatment of inflammatory diseases. *Nature medicine* **21**, 248-255,
doi:10.1038/nm.3806 (2015).
- 229 Haag, S. M. *et al.* Targeting STING with covalent small-molecule inhibitors. *Nature*
559, 269-273, doi:10.1038/s41586-018-0287-8 (2018).
- 230 Bronesky, D. *et al.* *Staphylococcus aureus* RNAIII and Its Regulon Link Quorum
Sensing, Stress Responses, Metabolic Adaptation, and Regulation of Virulence Gene
Expression. *Annu Rev Microbiol* **70**, 299-316, doi:10.1146/annurev-micro-102215-
095708 (2016).
- 231 Felden, B., Vandenesch, F., Boulloc, P. & Romby, P. The *Staphylococcus aureus*
RNome and its commitment to virulence. *PLoS pathogens* **7**, e1002006,
doi:10.1371/journal.ppat.1002006 (2011).
- 232 Bubeck Wardenburg, J., Williams, W. A. & Missiakas, D. Host defenses against
Staphylococcus aureus infection require recognition of bacterial lipoproteins. *Proc*
Natl Acad Sci U S A **103**, 13831-13836, doi:10.1073/pnas.0603072103 (2006).

- 234 Hanzelmann, D. *et al.* Toll-like receptor 2 activation depends on lipopeptide shedding by bacterial surfactants. *Nat Commun* **7**, 12304, doi:10.1038/ncomms12304 (2016).
- 235 Stoll, H., Dengjel, J., Nerz, C. & Gotz, F. Staphylococcus aureus deficient in lipidation of prelipoproteins is attenuated in growth and immune activation. *Infect Immun* **73**, 2411-2423, doi:10.1128/IAI.73.4.2411-2423.2005 (2005).
- 236 Raymond, S. L. *et al.* Microbial recognition and danger signals in sepsis and trauma. *Biochim Biophys Acta Mol Basis Dis* **1863**, 2564-2573, doi:10.1016/j.bbadis.2017.01.013 (2017).
- 237 Thery, C. *et al.* Minimal information for studies of extracellular vesicles 2018 (MISEV2018): a position statement of the International Society for Extracellular Vesicles and update of the MISEV2014 guidelines. *J Extracell Vesicles* **7**, 1535750, doi:10.1080/20013078.2018.1535750 (2018).
- 238 Beveridge, T. J. Structures of gram-negative cell walls and their derived membrane vesicles. *J Bacteriol* **181**, 4725-4733, doi:10.1128/JB.181.16.4725-4733.1999 (1999).
- 239 Askarian, F. *et al.* Staphylococcus aureus Membrane-Derived Vesicles Promote Bacterial Virulence and Confer Protective Immunity in Murine Infection Models. *Front Microbiol* **9**, 262, doi:10.3389/fmicb.2018.00262 (2018).
- 240 Olofsson, A. *et al.* Biochemical and functional characterization of Helicobacter pylori vesicles. *Mol Microbiol* **77**, 1539-1555, doi:10.1111/j.1365-2958.2010.07307.x (2010).
- 241 Haurat, M. F. *et al.* Selective sorting of cargo proteins into bacterial membrane vesicles. *J Biol Chem* **286**, 1269-1276, doi:10.1074/jbc.M110.185744 (2011).
- 242 Jeon, H. *et al.* Variation among Staphylococcus aureus membrane vesicle proteomes affects cytotoxicity of host cells. *Microb Pathog* **93**, 185-193, doi:10.1016/j.micpath.2016.02.014 (2016).
- 243 Albuquerque, P. C. *et al.* Vesicular transport in Histoplasma capsulatum: an effective mechanism for trans-cell wall transfer of proteins and lipids in ascomycetes. *Cell Microbiol* **10**, 1695-1710, doi:10.1111/j.1462-5822.2008.01160.x (2008).
- 244 Geissmann, T. *et al.* Regulatory RNAs as mediators of virulence gene expression in bacteria. *Handb Exp Pharmacol*, 9-43, doi:10.1007/3-540-27262-3_2 (2006).
- 245 Toledo-Arana, A., Repoila, F. & Cossart, P. Small noncoding RNAs controlling pathogenesis. *Curr Opin Microbiol* **10**, 182-188, doi:10.1016/j.mib.2007.03.004 (2007).
- 246 Koeppen, K. *et al.* A Novel Mechanism of Host-Pathogen Interaction through sRNA in Bacterial Outer Membrane Vesicles. *PLoS pathogens* **12**, e1005672, doi:10.1371/journal.ppat.1005672 (2016).
- 247 Sassi, M. *et al.* SRD: a Staphylococcus regulatory RNA database. *RNA* **21**, 1005-1017, doi:10.1261/rna.049346.114 (2015).
- 248 Queck, S. Y. *et al.* RNAlII-independent target gene control by the agr quorum-sensing system: insight into the evolution of virulence regulation in Staphylococcus aureus. *Molecular cell* **32**, 150-158, doi:10.1016/j.molcel.2008.08.005 (2008).
- 249 Pauli, N. T. *et al.* Staphylococcus aureus infection induces protein A-mediated immune evasion in humans. *The Journal of experimental medicine* **211**, 2331-2339, doi:10.1084/jem.20141404 (2014).
- 250 Clauditz, A., Resch, A., Wieland, K. P., Peschel, A. & Gotz, F. Staphyloxanthin plays a role in the fitness of Staphylococcus aureus and its ability to cope with oxidative stress. *Infect Immun* **74**, 4950-4953, doi:10.1128/IAI.00204-06 (2006).
- 251 Ayala, O. D. *et al.* Drug-Resistant Staphylococcus aureus Strains Reveal Distinct Biochemical Features with Raman Microspectroscopy. *ACS Infect Dis* **4**, 1197-1210, doi:10.1021/acsinfecdis.8b00029 (2018).

- 252 Rosa-Fraile, M., Rodriguez-Granger, J., Haidour-Benamin, A., Cuerva, J. M. & Sampedro, A. Granadaene: proposed structure of the group B Streptococcus polyenic pigment. *Applied and environmental microbiology* **72**, 6367-6370, doi:10.1128/AEM.00756-06 (2006).
- 253 Lamy, M. C. *et al.* CovS/CovR of group B streptococcus: a two-component global regulatory system involved in virulence. *Molecular microbiology* **54**, 1250-1268, doi:10.1111/j.1365-2958.2004.04365.x (2004).
- 254 Landwehr-Kenzel, S. & Henneke, P. Interaction of Streptococcus agalactiae and Cellular Innate Immunity in Colonization and Disease. *Frontiers in immunology* **5**, 519, doi:10.3389/fimmu.2014.00519 (2014).
- 255 Rathinam, V. A. K., Zhao, Y. & Shao, F. Innate immunity to intracellular LPS. *Nature immunology* **20**, 527-533, doi:10.1038/s41590-019-0368-3 (2019).
- 256 Martens, L. H. *et al.* Progranulin deficiency promotes neuroinflammation and neuron loss following toxin-induced injury. *J Clin Invest* **122**, 3955-3959, doi:10.1172/JCI63113 (2012).
- 257 Matsubara, T. *et al.* PGRN is a key adipokine mediating high fat diet-induced insulin resistance and obesity through IL-6 in adipose tissue. *Cell Metab* **15**, 38-50, doi:10.1016/j.cmet.2011.12.002 (2012).
- 258 Nathan, C. & Ding, A. Nonresolving inflammation. *Cell* **140**, 871-882, doi:10.1016/j.cell.2010.02.029 (2010).
- 259 Gowrishankar, S. *et al.* Massive accumulation of luminal protease-deficient axonal lysosomes at Alzheimer's disease amyloid plaques. *Proceedings of the National Academy of Sciences of the United States of America* **112**, E3699-3708, doi:10.1073/pnas.1510329112 (2015).
- 260 Tanaka, Y., Chambers, J. K., Matsuwaki, T., Yamanouchi, K. & Nishihara, M. Possible involvement of lysosomal dysfunction in pathological changes of the brain in aged progranulin-deficient mice. *Acta Neuropathol Commun* **2**, 78, doi:10.1186/s40478-014-0078-x (2014).
- 261 Beel, S. *et al.* Progranulin functions as a cathepsin D chaperone to stimulate axonal outgrowth in vivo. *Hum Mol Genet* **26**, 2850-2863, doi:10.1093/hmg/ddx162 (2017).
- 262 Lee, C. W. *et al.* The lysosomal protein cathepsin L is a progranulin protease. *Mol Neurodegener* **12**, 55, doi:10.1186/s13024-017-0196-6 (2017).
- 263 Nguyen, M. T. & Gotz, F. Lipoproteins of Gram-Positive Bacteria: Key Players in the Immune Response and Virulence. *Microbiology and molecular biology reviews : MMBR* **80**, 891-903, doi:10.1128/MMBR.00028-16 (2016).
- 264 Takeda, K., Takeuchi, O. & Akira, S. Recognition of lipopeptides by Toll-like receptors. *J Endotoxin Res* **8**, 459-463, doi:10.1179/096805102125001073 (2002).
- 265 Arvanitis, M., Glavis-Bloom, J. & Mylonakis, E. Invertebrate models of fungal infection. *Biochim Biophys Acta* **1832**, 1378-1383, doi:10.1016/j.bbadis.2013.03.008 (2013).
- 266 Kurz, C. L. & Ewbank, J. J. Infection in a dish: high-throughput analyses of bacterial pathogenesis. *Curr Opin Microbiol* **10**, 10-16, doi:10.1016/j.mib.2006.12.001 (2007).
- 267 Desbois, A. P. & Coote, P. J. Wax moth larva (*Galleria mellonella*): an in vivo model for assessing the efficacy of antistaphylococcal agents. *J Antimicrob Chemother* **66**, 1785-1790, doi:10.1093/jac/dkr198 (2011).
- 268 Hoffmann, J. A. Innate immunity of insects. *Current opinion in immunology* **7**, 4-10, doi:10.1016/0952-7915(95)80022-0 (1995).
- 269 Lionakis, M. S. Drosophila and Galleria insect model hosts: new tools for the study of fungal virulence, pharmacology and immunology. *Virulence* **2**, 521-527, doi:10.4161/viru.2.6.18520 (2011).

- 270 Loh, J. M., Adenwalla, N., Wiles, S. & Proft, T. *Galleria mellonella* larvae as an infection model for group A streptococcus. *Virulence* **4**, 419-428, doi:10.4161/viru.24930 (2013).
- 271 Beeton, M. L., Alves, D. R., Enright, M. C. & Jenkins, A. T. Assessing phage therapy against *Pseudomonas aeruginosa* using a *Galleria mellonella* infection model. *Int J Antimicrob Agents* **46**, 196-200, doi:10.1016/j.ijantimicag.2015.04.005 (2015).
- 272 Entwistle, F. M. & Coote, P. J. Evaluation of greater wax moth larvae, *Galleria mellonella*, as a novel in vivo model for non-tuberculosis Mycobacteria infections and antibiotic treatments. *J Med Microbiol* **67**, 585-597, doi:10.1099/jmm.0.000696 (2018).
- 273 Courtiade, J., Pauchet, Y., Vogel, H. & Heckel, D. G. A comprehensive characterization of the caspase gene family in insects from the order Lepidoptera. *BMC Genomics* **12**, 357, doi:10.1186/1471-2164-12-357 (2011).
- 274 Singer, M. *et al.* The Third International Consensus Definitions for Sepsis and Septic Shock (Sepsis-3). *Jama* **315**, 801-810, doi:10.1001/jama.2016.0287 (2016).
- 275 Harder, J. *et al.* Activation of the Nlrp3 inflammasome by *Streptococcus pyogenes* requires streptolysin O and NF-kappa B activation but proceeds independently of TLR signaling and P2X7 receptor. *J Immunol* **183**, 5823-5829, doi:10.4049/jimmunol.0900444 (2009).
- 276 Shim, D. W. & Lee, K. H. Posttranslational Regulation of the NLR Family Pyrin Domain-Containing 3 Inflammasome. *Frontiers in immunology* **9**, 1054, doi:10.3389/fimmu.2018.01054 (2018).
- 277 Song, N. & Li, T. Regulation of NLRP3 Inflammasome by Phosphorylation. *Frontiers in immunology* **9**, 2305, doi:10.3389/fimmu.2018.02305 (2018).
- 278 Py, B. F., Kim, M. S., Vakifahmetoglu-Norberg, H. & Yuan, J. Deubiquitination of NLRP3 by BRCC3 critically regulates inflammasome activity. *Molecular cell* **49**, 331-338, doi:10.1016/j.molcel.2012.11.009 (2013).
- 279 Juliana, C. *et al.* Non-transcriptional priming and deubiquitination regulate NLRP3 inflammasome activation. *The Journal of biological chemistry* **287**, 36617-36622, doi:10.1074/jbc.M112.407130 (2012).
- 280 Liu, Q., Zhang, D., Hu, D., Zhou, X. & Zhou, Y. The role of mitochondria in NLRP3 inflammasome activation. *Mol Immunol* **103**, 115-124, doi:10.1016/j.molimm.2018.09.010 (2018).
- 281 Gui, X. *et al.* Autophagy induction via STING trafficking is a primordial function of the cGAS pathway. *Nature* **567**, 262-266, doi:10.1038/s41586-019-1006-9 (2019).
- 282 Benaoudia, S. *et al.* A genome-wide screen identifies IRF2 as a key regulator of caspase-4 in human cells. *EMBO reports* **20**, e48235, doi:10.15252/embr.201948235 (2019).
- 283 Holler, C. J., Taylor, G., Deng, Q. & Kukar, T. Intracellular Proteolysis of Progranulin Generates Stable, Lysosomal Granulins that Are Haploinsufficient in Patients with Frontotemporal Dementia Caused by GRN Mutations. *eNeuro* **4**, doi:10.1523/ENEURO.0100-17.2017 (2017).
- 284 Suh, H. S., Choi, N., Tarassishin, L. & Lee, S. C. Regulation of progranulin expression in human microglia and proteolysis of progranulin by matrix metalloproteinase-12 (MMP-12). *PloS one* **7**, e35115, doi:10.1371/journal.pone.0035115 (2012).

9. APPENDIX

METHODS

Raman Measurement

MLBs washed with Millipore water were subjected to Raman analysis. MLBs and a single colony from freshly streaked SA and GBS blood agar plate were smeared onto a calcium fluoride slide. Raman spectra were recorded with a upright micro-Raman set up (CRM 300, WITec GmbH, Germany) equipped with a 600 g/mm grating and a deep depletion CCD camera (DU401A BV-532, ANDOR, 1024 x 127 pixels) cooled down to -60 °C. Samples dried on the calcium fluoride slide were excited through a Nikon 100X objective (NA 0.8) using an excitation wavelength of 532 nm Nd-YAG laser (20 mW of laser power and exposure time of 1s per spectrum). Single Raman spectra were collected from 300 different sample positions either in time series mode or single accumulation.

Fluorescence background was subtracted prior to analysis and spectral regions, fingerprint (600 to 1800 cm^{-1}) and C-H stretching (2750 to 3100 cm^{-1}) was further used for analysis. The collected data was pre-processed and statistical analysis was carried out. Raman spectra were background corrected using the sensitive non-linear iterative peak (SNIP) clipping algorithm and vector normalized. Further the pre-processed Raman spectra were carefully sorted as per dominating bio-molecules to generate the vibration signatures and average Raman spectra of proteins, lipids and nucleic acids. The prominent vibrations at 1009, 1163 and 1528 cm^{-1} indicate microbial polyene-type lipids whereas 1580, 1335 and 787 cm^{-1} Raman bands indicated the ribose type of nucleic acid.

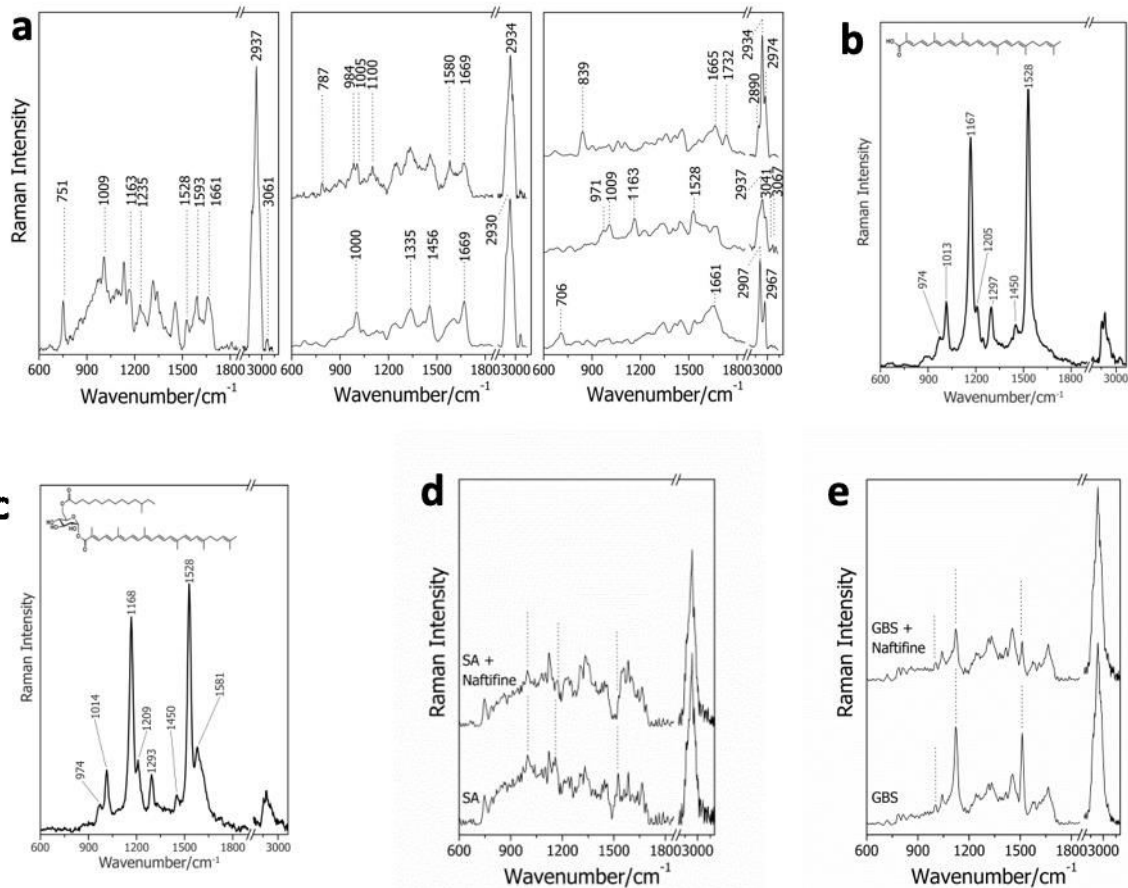


Figure 32: RAMAN spectroscopy data obtained for the study

(a) Raman spectra of SA and MLBs isolated from *S. aureus* showing prominent Raman peaks of lipids. (b,c) 4,4'-diaponeurosporenoic acid and staphyloxanthin were HPLC purified from SA followed by fingerprint LC-MS spectral analysis and confirmed by Raman spectra analysis. The prominent Raman peaks are marked with dotted lines. (d,e) Raman spectra of SA and SA treated with naftifine (SA+Naftifine) and GBS and GBS treated with naftifine (GBS+Naftifine). The fingerprint Raman peaks are marked by dotted lines.

Electron Microscopy

For Negative staining electron microscopy (TEM) carbon-coated EM-grids (400 meshes, quantifoil, Großlobichau, Germany) were used. The grids were hydrophilized by glow discharging at low pressure in air. 20 μ l of the isolated MLBs and MVs were absorbed on to the hydrophilic grids for 2 min. Further, the grids were washed twice with drops of distilled water and stained with a drop of 2 % uranyl acetate in distilled water. The stained grid is subjected to transmission electron microscope.

Freeze fracture transmission electron microscopy (FEM) was performed on GBS and SA bacteria. The aliquoted of the bacterial suspension were enclosed between two 0.1 mm thick copper profiles similar to the sandwich double replica technique. The sandwich prepared was

physically fixed by rapid plunge freezing in a liquid ethane/propane mixture and further cooled by liquid nitrogen. Freeze fracturing was performed at -150 °C in a BAF400T freeze fracture unit (BAL-TEC, Lichtenstein) using a double replica stage. The fractured samples were further shadowed with 2 nm platinum/carbon (Pt/C) at an angle of 35°, followed by perpendicular evaporation of a 15-20 nm thick carbon layer. The evaporation of the Pt/C was controlled by a thin-layer quartz crystal monitor; the thickness of the carbon layer was controlled optically. The obtained freeze fracture replicas were further transferred to a cleaning solution (Commercial sodium hypochlorite containing 12 % active Cl₂) for 30 min at 45 °C. Finally the replicas were washed four times in distilled water and transferred onto Formvar-coated grids for examination under the transmission electron microscope.

The negative staining and freeze fracture samples were imaged under Zeiss EM902A electron microscope (Carl Zeiss AG, Oberkochen, Germany). Operated at 80 kV accelerating voltage, and images were recorded with 1k (1024 x 1024) FastScan-CCD-camera (CCD camera and acquisition software EMMANU4 v 4.00.9.17, TVIPS, Munich, Germany).

The bacterial suspension of GBS and SA were subjected to scanning electron microscopy. The grown culture was washed with PBS and fixed in 2.5 % glutaraldehyde in cacodylic acid buffer (100 mM, pH 7.2) for 1 h. To avoid lipid extraction, dehydration by ethanol series and critical drying steps were omitted. The fixed cells were air dried on the glass cover slips. Further, the glass cover slips were mounted on aluminum sample holders and gold sputter coated (layer thickness 20 nm) in a compact Coating Unit CCU-010 (Savematic GmbH, Bad Ragaz, Switzerland). The cover slips were examined under a Zeiss LEO 1530 SEM (Carl Zeiss AG, Oberkochen, Germany) at 8 kV acceleration voltages with a working distance of 3 mm using an InLense secondary electron detector.

LC-MS for lipids

LC-MS was performed on MLBs and MVs isolated from *S. aureus* for the detection of staphyloxanthin type of lipids. The extraction process was carried in dark condition or under the protection of aluminium foil due to the light sensitivity of staphyloxanthin derivatives.

As a positive control, staphyloxanthin derivatives were isolated from wild type *S. aureus* bacteria. Wild type strain LS1 was grown until the late logarithmic phase and the pellet was processed for the isolation of lipids. *S. aureus* bacterial pellet was mixed with 50 ml EtOH followed by ultra-sonication for 20 min. The pigments are extracted in the EtOH as the pellet turns colorless. The mixture was further centrifuged at 8000 rpm for 10 mins and the EtOH

extract was collected, filtered and finally concentrated under reduced vacuum until completely dried. The EtOH extract was further separated by solvent extraction with CHCl₃: MeOH: H₂O (2:2:1) v/v/v and through mixing by vortex. Following centrifugation two layers were clearly separated and the bottom layer was collected and concentrated under reduced vacuum for lipid extraction. The lipid extract was suspended into MeCN to a concentration of 1mg/ml. Finally, after centrifugation the clear suspension was submitted to Shimadzu UHPLC-MS with the linear gradient: 0-1 min, 10% B; 1-7 min, 10%-100% B; 7-10 min, 100% B (A: dd H₂O with 0.1% formic acid; B: MeCN with 0.1% formic acid) with a flow rate of 0.7 mL/min. 5µl sample solution was injected into UHPLC-MS for analysis.

Similarly, isolated MLBs and MVs were suspended with 25 µl H₂O followed by adding 25 µl MeOH, and ultrasonicated for 10 min. This solution was further centrifuged at room temperature at 13000 rpm for 10 min and the supernatant was transferred into brown HPLC vials and directly underwent Shimadzu UHPLC-MS following the same procedure as for the bacteria. Simultaneously, the metabolite analysis was carried out on ThermoQExactive Plus HESI-HRMS equipped with a Luna Omega C18 column (100 x 2.1 mm, particle size 1.6 µm, pore diameter 100Å, Phenomenex) preceded by a Security GuardTM ULTRA guard cartridge (2 x 2.1 mm, Phenomenex) with the linear gradient: 0-0.5 min, 70% B; 0.5-17 min, 70%-97% B; 17-22 min 97% B (A: dd H₂O with 0.1 % formic acid; B: MeCN with 0.1% formic acid) with a flow rate of 0.3 ml/min. The column oven was set to 40 °C. 5 µl of the sample were submitted for analysis and metabolite separation was followed by a data-dependent MS/MS analysis in positive (MS1 and MS2) ionization mode. The gas flow rates were set to 35 and 10 for the sheath and auxiliary gases, respectively. The capillary and the probe heater temperatures were 340 °C and 200 °C, respectively. The spray voltages were 4 kV for the positive ionization modes. S-lens RF level was set to 50. MS1 had the resolving power set to 70,000 FWHM at *m/z* 200, scan range to *m/z* 150 – 2,000; injection time to 100 ms; and AGC to 3e6. The ten most intense ions were selected for MS2 with a scan rate of 12 Hz. Resolving power was 17,500 FWHM at *m/z* 200, AGC target was 1e5, and injection time was 50 ms. Fragmentations were performed at 28 NCE (normalized collision energy). Data analysis was performed with ThermoXCalibur software (Thermo Scientific).

Isolation of Staphyloxanthin and its precursor from *S. aureus*

NMR measurements were performed on a Bruker AVANCE III 600 MHz spectrometer, equipped with a Bruker Cryoplatfom. Chemical shifts are reported in parts per million (ppm) relative to the solvent residual peak of CDCl₃ (¹H: 7.26 ppm, singlet; ¹³C: 77.16 ppm, triplet).

LC-ESI-HRMS measurements were carried out on an Accela UPLC system (Thermo Scientific) coupled with a Accucore C18 column (100 x 2.1 mm, particle size 2.6 μm) combined with a Q-Exactive mass spectrometer (Thermo Scientific) equipped with an electrospray ion (ESI) source. UHPLC-MS measurements were performed on a Shimadzu LCMS-2020 system equipped with single quadrupole mass spectrometer using a Phenomenex Kinetex C18 column (50 x 2.1 mm, particle size 1.7 μm , pore diameter 100 \AA). The column oven was set to 40 $^{\circ}\text{C}$; scan range of MS was set to m/z 150 to 2,000 with a scan speed of 10,000 u/s and event time of 0.25 s under positive and negative mode. DL temperature was set to 250 $^{\circ}\text{C}$ with an interface temperature of 350 $^{\circ}\text{C}$ and a heat block of 400 $^{\circ}\text{C}$. The nebulizing gas flow was set to 1.5 L/min and dry gas flow to 15 L/min. Semi-preparative HPLC was performed on a Shimadzu HPLC system using a Phenomenex Luna Phenyl Hexyl 250 x 10 mm column (particle size 5 μm , pore diameter 100 \AA). Solid phase extraction was carried out using ChromabondSiOH cartridges filled with 2 g of unmodified silica gel (Macherey-Nagel, Germany). Chemicals: Methanol (VWR, Germany); water for analytical and preparative HPLC (Millipore, Germany), formic acid (Carl Roth, Germany); acetonitrile (VWR as LC-MS grade), media ingredients (Carl Roth, Germany).

SA was cultured overnight in THY medium (37 $^{\circ}\text{C}$, 160 rpm). The cell pellet was separated from the supernatant by centrifugation at 4000 rpm at 4 $^{\circ}\text{C}$. The cell pellet was extracted twice using 100 mL ethanol at 37 $^{\circ}\text{C}$ for 2 h. The EtOH extract was combined and concentrated under reduced pressure. The dried extract was partitioned using 100 mL 1.7 M NaCl and 100 mL ethyl acetate three times. The EtOAc phase was combined, dried over MgSO_4 and concentrated under reduced pressure conditions. In total, 189 mg crude extract was obtained from 10 L liquid culture. The crude extract was separated using a SiOH cartridge (2 g, twice) and eluted by a step gradient of cyclohexane and EtOAc (100% cyclohexane, 5:1, 2:1, 1:1, 1:2, 100 % EtOAc and 100 % MeOH). The fraction resulting in an orange band was collected from the elution of cyclohexane: EtOAc 5:1 (v/v) (Fraction 2, 36.22 mg) and 1:1 (v/v) (Fraction 5, 4.58 mg).

Fr. 2 was further separated on RP-C18 F254s preparative TLC plates (Merck) using a methanol-acetonitrile (1:1, v/v) mixture. The pigment band with R_f value of 0.61 was scratched from the preparative TLC plates, extracted by 1 x 3 mL EtOAc, and concentrated under reduced pressure to yield (Fr. 2.1, 4.29 mg). Similarly, Fr. 5 was further separated with pigment band with R_f value of 0.55 scratched from the preparative TLC plates and extracted three times with 1 mL EtOAc. The EtOAc extract of pigment band (Fr. 5.1, 1.6 mg) was concentrated under reduced pressure and subjected to the purification by semi preparative

HPLC on Phenomenex Phenyl-Hexyl column 250 x 10 mm, 100 Å. Staphyloxanthin (**2**, 0.1 mg, $t_R = 19.54$ min) was obtained by semi-preparative HPLC under the gradient of 0–5 min, 90 % MeCN/10 % H₂O containing 0.1% formic acid; 5–10 min, 90 %–100 % MeCN; 10–20 min, 100 % MeCN, under the flow rate of 2.0 mL/min.

The sample was analysed using a Shimadzu UHPLC-MS (gradient: 0–1 min, 70 % B; 1–5 min, 70 %–100 % B; 5–7 min, 100 % B (A: dd H₂O with 0.1 % formic acid; B: MeCN with 0.1 % formic acid) with a flow rate of 1.0 mL/min. 1 µL sample solution was injected into UHPLC-MS for analysis.

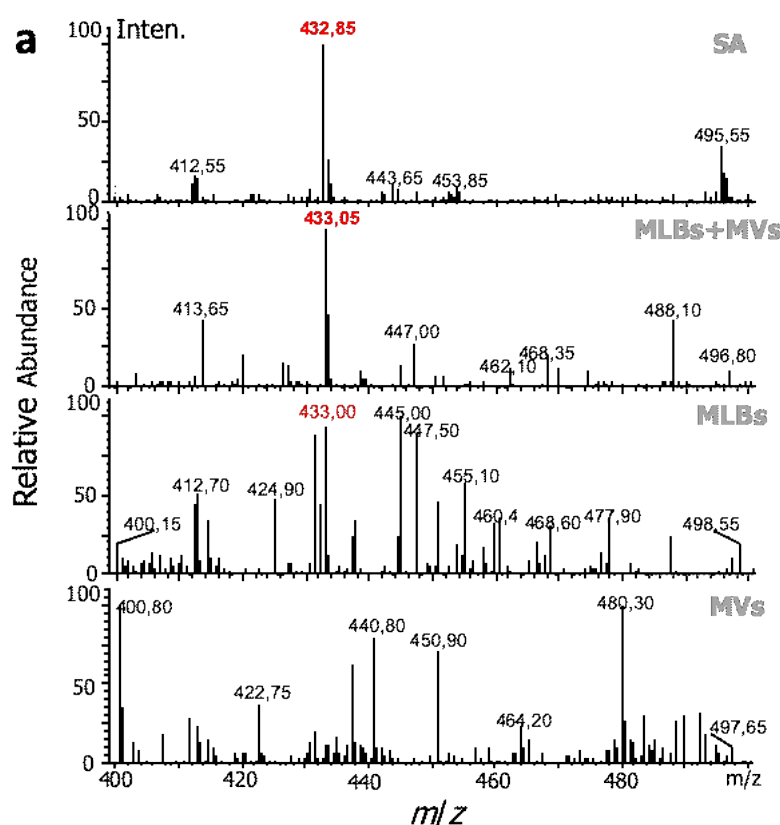


Figure 33: LC-MS analysis for the detection of staphyloxanthin

(a) EIC chromatogram showing comparative LCMS analysis of 4,4'-diaponeurosporenoic acid (St1) m/z 433.3 at $t^R=7.625$ min I) SA lipid extract II vesicle mixture (MLBs+MVs) III) multilamellar vesicular bodies (MLBs) IV) membrane vesicles (MVs).

LC-MS for c di-AMP and it's derivatives in MLBs

LC-MS was also performed for the detection of cyclic di-nucleotides and its derivatives in the *S. aureus* MLBs. Ultra high performance liquid chromatography coupled with high resolution mass spectrometry was carried out using a THERMO (Bremen, Germany) UltiMate HPG-3400 RS binary pump, WPS-3000 auto sampler which was set to 10 °C and which was equipped with a 25 µL injection syringe and a 100 µL sample loop. The column was kept at 25 °C

within the column compartment TCC-3200. Chromatography column was used PHENOMENEX® (Aschaffenburg, Germany) Hydro-RP (80 Å pore size, 150 × 2 mm; 4 μm particle size) using the gradient inat a constant flow rate of 0.4 mL/min. Eluent A was water, with 2 % acetonitrile and 0.1 % formic acid. Eluent B was pure acetonitrile. For each sample 5 μL were injected prior to dilution with 10 μL UPLC-grade water.

Mass spectra were recorded with THERMOQExactive plus orbitrap mass spectrometer coupled to a heated electrospray source (HESI). Column flow was switched at 0.5 min from waste to the MS and at 11.5 min again back to the waste, to prevent source contamination. For monitoring two full scan modes were selected with the following parameters. Polarity: positive; scan range: 100 to 1500 m/z ; resolution: 70,000; AGC target: 3×10^6 ; maximum IT: 200 ms. General settings: sheath gas flow rate: 60; auxiliary gas flow rate 20; sweep gas flow rate: 5; spray voltage: 3.0 kV; capillary temperature: 360 °C; S-lens RF level: 50; auxiliary gas heater temperature: 400 °C; acquisition time frame: 0.5 - 11.5 min. For negative mode all values were kept instead of the spray voltage which was set to 3.3 kV.

Presence of pApA was confirmed based on their $[M-2H+Na]^-$ and c-di-AMP based on $[M-H]^-$; respectively using their exact masses and a 10 ppm mass window. Presence was further verified by at least two of additionally occurring ions ($[M-2H+Na]^-$; $[M-H]^-$; $[M+H]^+$; $[M+Na]^+$; $[M-H+2Na]^+$) within a retention time range of ± 0.2 min comparing to the authentic standards. Peak detection and integration were carried out using the THERMOXcalibur™ 3.0.63 software.

RNA Sequencing

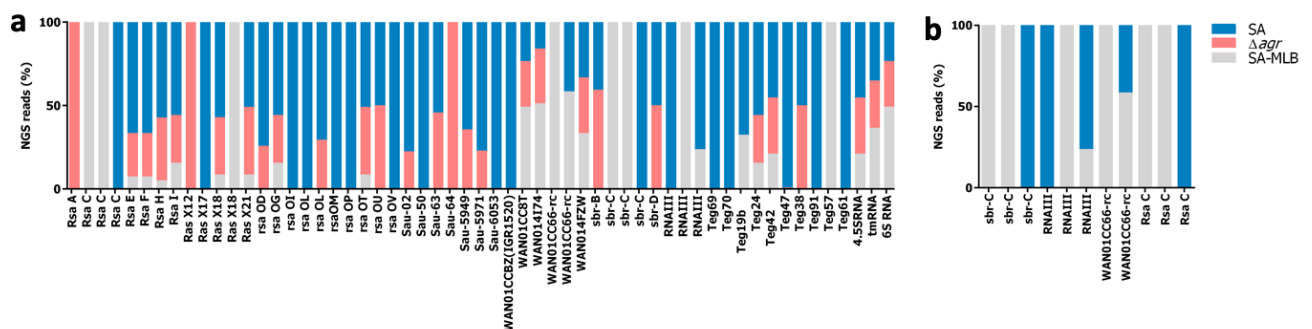


Figure 34: RNA seq data obtained from μRNA of SA, Δagr and SA-MLB

(a) Comparative percent abundance sequencing read profiles of different sRNA quantified from *S. aureus* MLB (SA-MLB) (Grey), *S. aureus* (SA) (blue), and *S. aureus* Δagr (SA-Δagr) (Pink). (b) Comparative percent abundance sequencing read profile of sbr-C, Rsa C, RNAIII,

and WAN01CC66-rc in wild type *S. aureus* (SA) (Blue) and *S. aureus* MLBs (SA-MLB) (Grey).

Patient Characteristics

The *S. aureus* patient isolates were isolated from the patients in the age group 4-90 years and 64 % of the patients were male. The other characteristics are as follows:

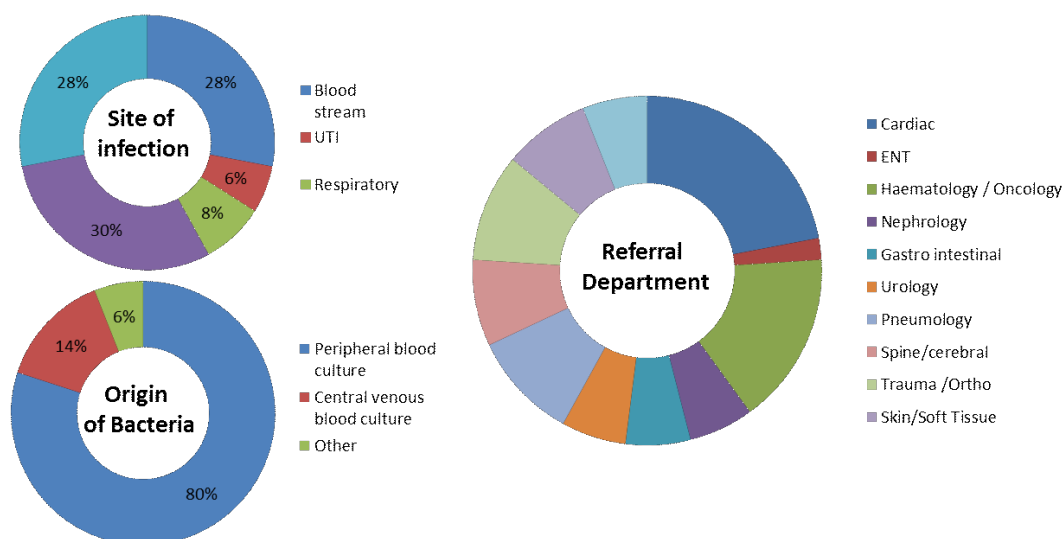


Figure 35: Characteristics of *S. aureus* patient isolate mentioning the site of infection, origin of bacteria and the referral department.

Table 21: Characteristics of *S. aureus* infected patients screened for inflammasome activation

Patient No	1	2	3	4
Age (years)	53	71	74	60
Gender	F	M	M	M
28 day mortality	Survived	Survived	Died	Survived
APACHE-II on admission	23	33	26	10
SAPS-II on admission	49	71	70	23
Site of infection	Endocarditis	Abdomen	Wound	Catheter
SOFA	13	14	11	5

Table 22: Characteristics of sepsis patients screened for galectin-1 release

Age (years)	64	[35.0 - 81.0]
Gender, male	19	76%
APACHE-II on admission	26	[13.0 - 49.0]
SAPS-II on admission	55	[13.0 – 91.0]
28 day mortality	4	16%
Site of infection		
Abdominal/Peritonitis	12	48%

Pneumonia/lung	7	20%
other	6	24%

Table 23: Characteristics of sepsis patients screened for PGRN release

Age (years)	68	[51.0 - 74.0]
Gender, male	16	(64 %)
APACHE-II on admission	23	[16.0 - 27.0]
SAPS-II on admission	49	[35.0 - 63.0]
28 day mortality	5	(20 %)
Site of infection		
Abdominal	10	(40 %)
Pneumonia	5	(20 %)
Primary bacteremia	5	(20 %)
Soft tissue	3	(12 %)
Urogenital	1	(4 %)
Endocarditis	1	(4 %)

Curriculum vitae

Shivalee Duduskar

Ph.D. Student, Friedrich Schiller University, Jena, Germany

Ph.: +49015731164848 Email: s.duduskar@gmail.com

Date of Birth: 4th May, 1992



Summary

To build a career with dynamic and well managed research institute, to reflect high standards of performance in research and in any assignment given, thereby ensuring institutional and personal growth.

Education

- Ph.D. Candidate- Center for Sepsis Care and Control Jan 2016-Oct 2020
Friedrich Schiller University, Jena, Germany
- M.Sc. in Biotechnology 2012-2014
Shivaji University, Kolhapur, India
- B.Sc. in Biotechnology 2009-2012
Yashwantrao Chavan Institute of Science, Satara, India

Research Techniques

- **Biochemical techniques:** Gel electrophoresis (SDS PAGE, agarose, and capillary electrophoreses), protein purification from bacterial culture, chromatography techniques (ion exchange, size exclusion, Affinity), ELISA, MALDI, Immuno-precipitation.
- **Microbial techniques:** Staining techniques, pure culture methods, and Isolation and screening methods, gated cloning, infection and cell culture, isolation of vesicles from Gram-positive and Gram-negative.
- **Molecular biology and recombinant DNA techniques:** DNA isolation, RNA isolation, plasmid isolation, blotting techniques, restriction digestion, transformation, PCR, real time PCR, RAPD, RFLP, sanger sequencing, next generation sequencing (NGS), CRISPR knockout cell lines.
- **Other:** X-ray crystallography and bioinformatics, confocal microscopy, electron microscopy, Raman spectroscopy.

Research Experience

1. Friedrich Schiller University, Center for Sepsis Care and Control, Jena, Germany
Ph.D. research under the guidance of Dr. Sachin D.Deshmukh on the topic “Initiation and regulation of cytosolic innate immunity during Sepsis”.
2. Advanced Centre for Treatment, Research and Education in Cancer, Structural biology Department
Junior Research Fellow under the guidance of Dr. M. V. Hosur on the topic “Protein Purification and X-ray Crystallization of HIV1 protease”
3. Advanced Centre for Treatment, Research and Education in Cancer, Hematology Department
Trainee in Department Of Biotechnology, Government of India funded project “Evaluation of various prognostic markers and minimal residual Disease (MRD) to

potentiate therapy for Acute Myeloid Leukemia (AML) patients: A two-step molecular-clinical investigation” led by Dr. S. Hasan

4. Shivaji University, Kolhapur, India
M.Sc. dissertation on “Isolation and characterization of Halotolerant bacteria”
5. Yashwantrao Chavan Institute of Science, Satara, India
B.Sc. dissertation on “In vitro Propagation of the *Passiflora.edulis*: An underutilized native of Brazil”

Conferences and Workshops

- Poster presentation: Cytosolic innate immune pathway activation during sepsis, Weimar Sepsis update 2016-2018
- Poster presentation at EMBO|EMBL Symposium: Innate Immunity in Host-Pathogen Interactions, Heidelberg, Germany
- AVISHKAR 2009-2010 - “Protein Synthesis of the Cell” the paper received Second prize at University level held at Yashwantrao Chavan Institute of Science, Karad.
- Paper presented on “Activity guided fraction approach for isolation of pharamatecually active constituents from root of *Acorus.calamus*” in one day National seminar on “Future Perspectives of Biological Sciences” on 4th March 2014 in association with Microbiologist Society, India.
- Attended practical workshop on “DNA barcoding” held at Shivaji University, Kolhapur.
- Attended hands on workshop in BIORAD, on “Digital droplet PCR”.
- Worked as a demonstrator in workshop on “Advanced techniques for drug development in Cancer”

Extra-curriculum activities and achievements

- DAAD fellowship for summer school of molecular medicine, Jena, Germany (2015).
- Volunteering as a scientific writer and illustrator for ScienTerrific and Neucrad.
- First Prize in Science Slam conducted by Friedrich Schiller University, Center for Sepsis Care and Control, Jena, Germany
- Cultural representative of Youth festival Yashwantrao Chavan Institute of Science, Satara.

Peer-reviewed publications

- "Gram-positive bacteria secrete RNA aptamers to activate human STING for IL-1 β release"(In submission) First author, 2019
- “Gram positive bacteria activates CASPASE 5 for the release of Progranulin during sepsis” (In review) First author, 2020
- “Loss-of-Function Variant in CNPY3 Gene impairs Caspase-1 Activation and IL-1 Processing in Human Macrophages”
(In submission) Third author, 2020
- Intracellular LPS sensing promotes inflammation via gasdermin D-driven galectin-1 release (Accepted- Nature immunology) Sixth author, 2020
- “Noncanonical Inflammasome-Induced release of Alarmins during Sepsis”
Ashley Jean Russo, Antoine Menoret, Shivelee Duduskar, Gabriel Rabinovich, Sachin D Deshmukh, Anthony T Vella and Vijay Rathinam J Immunol May 1, 2019, 202 (1 Supplement) 126.36
- “Alarmin(g) outcomes of intracellular LPS sensing”
Vijay Rathinam, Ashley Russo, Antoine Menoret, Gabriel Rabinovich, Shivelee Duduskar, Sachin Deshmukh and Anthony T Vella J Immunol May 1, 2019, 202 (1 Supplement) 63.14

Acknowledgement

First and foremost, I express my heartfelt gratitude to Junior group leader Dr. Sachin D. Deshmukh for having given me an opportunity to showcase my knowledge. I would also like to sincerely thank him for his supervision, support, critique, guidance and valuable advices throughout the professional and personal aspects. I am also grateful for enlightening me in this field of inflammasome research. `Attention to small details´ was the key learning from him throughout my doctoral studies.

I convey my grateful thanks to Prof. Micheal Bauer for giving me opportunity to undergo my research. I thank Prof. Dr. med. Regine Heller for accepting me for the summer school program. Her guidance and the program were instrumental in pursuing my research career in Jena.

I also owe my indebtedness to my group members and the collaborators for their unending support, encouragement and valuable insights that made the work environment so ebullient in order to reach the pinnacle. Also, I thank them for their assistance with all the German bureaucratic works during my project without them it would have been a difficult time for the progress of work.

I would like to sincerely acknowledge the motivation and support rendered by my best friends professionally and personally.

It's also my privilege to thank Dr. Katja Lehmann-Pohl and her group for their help and guidance throughout the visa process during the last year of work.

Last but not the least I am grateful to my family who had always been my pillar of support to make this project a success. Finally, I would also like to thank everyone who provided me with all the facilities at the division throughout my project.

Ehrenwörtliche Erklärung

Hiermit erkläre ich, dass mir die Promotionsordnung der Medizinischen Fakultät der Friedrich Schiller-Universität bekannt ist,

ich die Dissertation selbst angefertigt habe und alle von mir benutzten Hilfsmittel, persönlichen Mitteilungen und Quellen in meiner Arbeit angegeben sind,

dass die Personen, die mich bei der Auswahl und Auswertung des Materials sowie bei der Herstellung des Manuskripts unterstützt haben, vollständig genannt sind: Dr. Sachin D. Deshmukh, Prof. Dr. Micheal Bauer.

die Hilfe eines Promotionsberaters nicht in Anspruch genommen wurde und dass Dritte weder unmittelbar noch mittelbar geldwerte Leistungen von mir für Arbeiten erhalten haben, die im Zusammenhang mit dem Inhalt der vorgelegten Dissertation stehen,

dass ich die Dissertation noch nicht als Prüfungsarbeit für eine staatliche oder andere wissenschaftliche Prüfung eingereicht habe und dass ich die gleiche, eine in wesentlichen Teilen ähnliche oder eine andere Abhandlung nicht bei einer anderen Hochschule als Dissertation eingereicht habe.

Jena,

Shivalee Nilesh Duduskar